07

Final

III

AN INTERDISCIPLINARY STUDY OF THE ESTUARINE AND COASTAL OCEANOGRAPHY OF BLOCK ISLAND SOUND AND ADJACENT NEW YORK COASTAL WATERS

Principal Investigator:

Edward F. Yost
Science Engineering Research Group
C.W. Post Center-Long Island University
Greenvale, New York 11548

Co-Investigators:

Rudolph Hollman
James Alexander
Robert Nuzzi
New York Ocean Science Laboratory
Montauk, New York 11958

April 1974
Final Report under Contract NAS5-21792

Prepared for:

Goddard Space Flight Center
Greenbelt, Maryland 20771

TECHNICAL REPORT STANDARD TITLE PAGE

1. Report No.	2. Gov. Accession No.	3. Recipient's Catalog No.
4. Title and Subtitle "An Interdisciplinary Study of the Estuarine and Coastal Oceanography of Block Island Sound and Adjacent New York Coastal Waters"		5. Report Date April 1974 6. Performing Organization Code
7. Author(s) Edward F. Yost, Rudolph Hollman, Robert Nuzzi, James Alexander		8. Performing Organization Report No. TR-20
9. Performing Organization Name & Address Science Engineering Research Group C.W. Post Center Long Island University Greenvale, New York 11548		10. Work Unit No. 11. Contract or Grant No. NAS5-21792
12. Sponsoring Agency Name & Address Mr. Edmund F. Szajna Goddard Space Flight Center Greenbelt, Maryland 20771		13. Type of Report and Period Covered Type III, July 1972 - January 1974 14. Sponsoring Agency Code

15. Supplementary Notes

Prepared in cooperation with the New York Ocean Science Laboratory, Montauk, New York.

16. Abstract

Photo-optical additive color quantitative measurements were made of ERTS-1 reprocessed positives of New York Bight and Block Island Sound. Regression of these data on almost simultaneous ship sample data of water's physical, chemical, biological, and optical properties showed that ERTS bands 5 and 6 can be used to predict the absolute value of the total number of particles and bands 4 and 5 to predict the relative extinction coefficient ($-\overline{k}$) in New York Bight. Water masses and mixing patterns in Block Island Sound heretofore considered transient were found to be persistent phenomena requiring revision of existing mathematical and hydraulic models.

17. Key Words (selected by Author)		18. Distribution Statement	
Coastal remote sensing			
19. Sec. Classif. (of this report) U	20. Sec. Classif. (of this report) U	21. No. of Pages 178	22. Price

PREFACE

The main objective of this interdisciplinary research project was to develop data processing techniques for analyzing ERTS photographic data products which would provide quantitative surface water data useful to oceanographers. Block Island Sound and New York Bight were the coastal areas studied.

Twenty-four cruises were made to collect water samples at twelve stations in Block Island Sound, eight stations along the coast of Long Island and nine stations in New York Bight. Analysis of these samples included physical, chemical, organic, and optical properties of the water near the time of the ERTS overpasses.

Photo-optical analysis of the imagery incorporated precision reprocessing of the negatives supplied by NASA (to emphasize water detail), additive color viewing, and electronic density slicing of the composite image. Quantitative measurements of the image characteristics were made and correlated with the ship sampling data.

The results of this research show that the greatest value of ERTS-1 imagery is in identifying and locating water masses in coastal waters from their color differences. In order to bring out such differences in the ERTS photographs, the negatives were reprocessed to compensate for water attenuation and atmospheric effects on the imagery. It was possible to establish the absolute value of the number of total particles in New York Bight using ERTS-1 bands 5 and 6 and the relative extinction coefficient using bands 4 and 5.

Conceptual models of Block Island Sound and Long Island Sound were found to be simplified idealizations. Anomalous findings in physical and chemical parameters which had been disregarded were shown by ERTS imagery to be areas where color differences were persistent, in particular off Montauk Point on Long Island and the shores of Rhode Island. These areas are where more concentrated investigations of physical, chemical, and biological processes will be conducted. These studies will provide the needed input to environmental models both mathematical and hydraulic whose framework will now involve a more realistic conceptual model.

TABLE OF CONTENTS

LIST OF TABLES

Section I

Introduction

This report represents the results of an interdisciplinary project to demonstrate the feasibility of utilizing satellite imagery for oceanographic studies. The project was undertaken jointly by Long Island University and the New York Ocean Science Laboratory as a continuing effort related to an on-going program to study Block Island Sound and adjacent New York coastal waters. Specifically, the objectives were to study the characteristics of Block Island Sound and New York Bight as they may relate to ERTS-I imagery and to develop techniques for analyzing ERTS photographic data products which would provide quantitative surface water data of use to oceanographers.

The fundamental problem in oceanography is sampling and, in particular, synoptic sampling analogous to the sampling programs in meteorology. It is, however, economically impossible to operate ships on an adequate scale to cover the needs of not only the oceans, but more importantly, the coastal zones and estuaries. Currently, the placing of buoys equipped with adequate transducers to provide the required information is also problematical from both an engineering and economic standpoint. Satellite imagery, however, provides the synoptic over-view of an area that forms the basis for further monitoring.

The program to acquire oceanographic "ground truth" in Block Island Sound and New York Bight areas was conducted by the New York Ocean Science Laboratory. Twenty-four cruises were made to collect water samples at different stations for temperature, salinity, nutrients, oxygen, pigments, organics, phytoplankton, and particle size determinations. Oceanographic data reduction was also done to provide the critical surface parameters to be used for correlation with the satellite imagery.

Earth Resources Technology Satellite (ERTS) was launched on 23 July 1972 and placed into a nominal orbit by a Delta launch vehicle. Adjustment was done to correct the orbit to the eighteen day repeat cycle. Multispectral scanners (MSS) imagery was supplied by the Goddard Space Flight Center of NASA, Greenbelt, Maryland over the two test sites. This repetitive imagery was received in both positive and negative form on 70mm transparencies. The spectral bands included the 500-600 nm, 600-700 nm, 700-800 nm, and 800-1100 nm portions of the spectrum.

Photographic reprocessing techniques were developed which, when applied to any of the NASA multispectral imagery supplied to investigators, will yield greatly improved detectability of subtle water and land phenomena. These techniques have been related to the gray scale supplied with each of the four multispectral images in order to provide quantified data on the photographic transformations applied to the imagery. Application of these techniques to the MSS imagery over the test sites in Block Island Sound and New York Bight formed the basis for subsequent additive color analysis and the correlation of water parameters with the imagery.

The ERTS imagery which was of sufficient quality and free of clouds so as to be useable was analyzed by using an additive color viewer. Additive color and density slicing analyses were performed to extract the maximum information regarding the spatial location and probable composition of the water masses.

New York Bight

New York Bight covers approximately $48_6 \times 10^3$ square kilometers with an average depth of about 60 meters. Long Island bounds the area to the north and the New Jersey coast to the west. The entrance to New York Harbor is at the apex of the northern and western boundaries and is the major outfall for the area. The outer boundary is approximately defined by the 100 fathom curve.

Figure 1 shows a chart of New York Bight and the locations of stations at which the water samples were collected. A variety of municipal and industrial wastes are disposed of by barge dumping in the waters of the Bight, including sewage sludge and acid wastes. The flow and fate of these inputs into the area is not yet completely known.

The total volume of New York Bight is approximately 29×10^9 cubic meters. The general topography is broad and almost flat with the exception of Hudson Canyon, which runs generally NW-SE and cleaves the shelf from the 1000 fathom curve to the entrance to New York Harbor at the apex of the Bight. A general review of the oceanography of the New York Bight can be found in a publication by Hollman (1971). Figure 2 shows a typical set of positive photographs in the four bands imaged by ERTS over New York Bight.

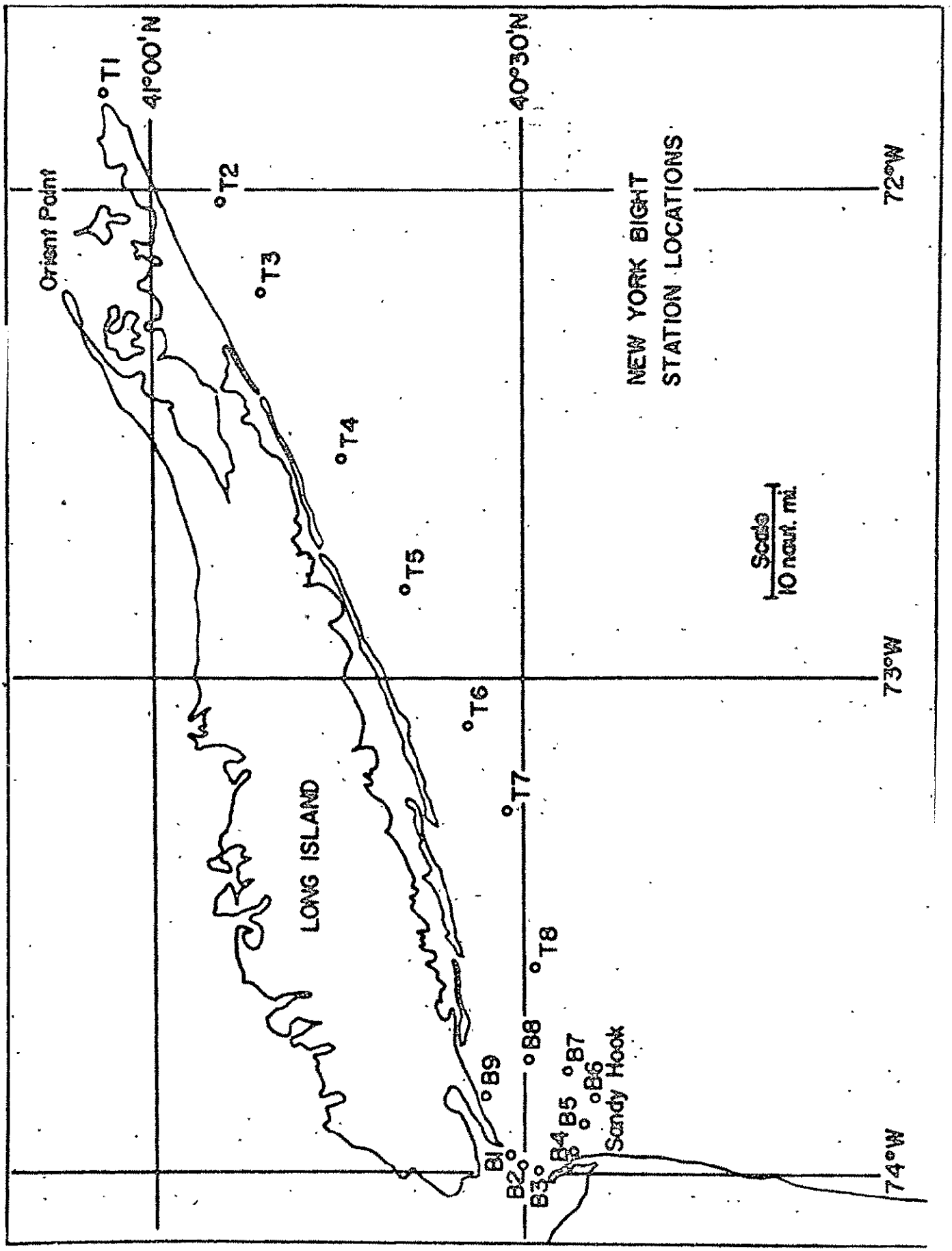

Figure 1. Chart of New York Bight showing station locations.

Band 4 (500-600 nm)

Band 5 (600-700 nm)

Band 6 (700-800 nm)

Band 7 (800-1100 nm)

Figure 2. A typical set of repetitive MSS imagery over the New York Bight area.

Block Island Sound

Block Island Sound is a partly enclosed body of water between Rhode Island and Long Island, New York, that separates the waters of Long Island Sound (and also the Peconic Bay System) from the coastal waters of the Atlantic Ocean. Figure 3 shows the chart of Block Island Sound and station locations where the water samples were collected. Block Island Sound has a surface area of approximately 1350 square kilometers and is bounded on the north by Rhode Island and by Long Island, New York, to the south. The mean depth in Block Island Sound is approximately 40 meters and has a total volume in excess of 54 x 10^3 cubic meters (1.9 million gallons).

The deepest depression in the Sound is close to 100 meters. The head of Block Canyon intrudes into Block Island Sound between Montauk Point on Long Island and Block Island, and has a maximum depth in this area of approximately 70 meters. An excellent review of the oceanography of Block Island Sound was presented by Williams (1967). A typical set of four positive MSS images over Block Island Sound is shown in Figure 4.

Water Sampling Program

Two transects were followed in the New York Bight. The first transect runs parallel to the shore of Long Island from Montauk Point to Rockaway Inlet and comprises eight stations as shown in Figure 1. These stations are sampled once on the day spent in transect from Montauk to Rockaway and are repeated two days later on the return transect. The second transect is a large arc sweeping through the apex of the New York Bight and comprises nine stations, so that all

Figure 3. Chart of Block Island Sound showing transects and station locations.

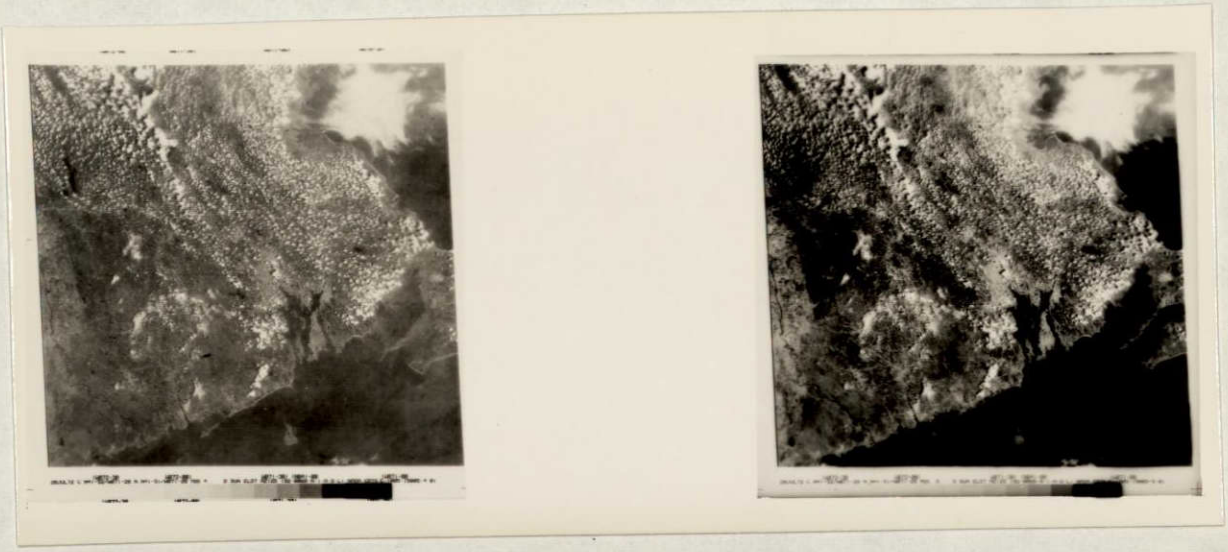

Band 4 (500-600 nm)

Band 5 (600-700 nm)

Band 6 (700-800 nm)

Band 7 (800-1100 nm)

Figure 4. Positive photographs in four MSS bands representing a typical set of repetitive coverage over Block Island Sound.

of the various dump-site positions (as provided by the U.S. Army Corps of Engineers, personal communications) are included in the transect (Table 1). These stations were all sampled during the day of ERTS transit.

Continuous surface profiles of temperature and pigments were obtained whenever the vessel was underway between the stations.

Three transects of Block Island Sound were selected, as shown in Figure 3, where large color differences in water masses were expected. The exact locations of the stations that each transect comprises are tabulated in Table 2. Each transect was occupied by continually sailing back and forth during a tidal cycle and sampling at up to 6 depths at each station. The water was collected in 5-liter Niskin bottles for chemical and biological analysis.

This general sampling program was later modified slightly to allow for continuous surface temperature and continuous flow fluorometer profiling throughout Block Island Sound on the day prior to the satellite overpass. Surface samples were also drawn for chemical and biological analysis. With this modified program, one in-depth sampling of the "H" transect was conducted during the day of surface profiling and the other two transects sampled in depth on the following days.

Parameters Sampled

The parameters sampled for include temperature, salinity, nutrients, oxygen, pigments, organics, phytoplankton, light attenuation, particle size determinations, and fluorometer readings.

Temperatures were measured with bathythermographs and thermometers.

Transect	Station	Latitude	Longitude
TR	TR 1 (E/W)	41°04.6'N	71°49.0'W
	" 2 "	40°54.5'N	72°01.5'W
	" 3 "	40°49.0'N	72°18.5'W
	" 4 "	40°44.0'N	72°33.6'W
	" 5 "	40°39.2'N	72°48.5'W
	" 6 "	40°34.4'N	73°04.0'W
	" 7 "	40°31.0'N	73°13.5'W
	" 8 "	40°29.5'N	73°34.5'W
New York Bight	NYB 1	40°32.4'N	73°56.6'W
	" 2	40°30.5'N	73°58.0'W
	" 3	40°29.2'N	73°59.6'W
	" 4	40°25.1'N	73°56.0'W
	" 5	40°24.4'N	73°51.3'W
	" 6	40°23.0'N	73°48.2'W
	" 7	40°25.5'N	73°45.0'W
	" 8	40°30.0'N	73°44.0'W
	" 9	40°33.8'N	73°48.6'N

Table 1. Station locations in New York Bight.

Transect	Station	Latitude (North)	Longitude (West)	Mean Depth (meters)
"H"	H1	41°06.8'	71°51.5'	12.2
	H2	41°10.4'	"	41.1
	H3	41°13.8'	"	51.8
	H4	41°16.5'	"	38.1
"HB"	HB1	41°04.8'	71°49.4'	13.4
	HB2	41°05.8'	71°46.3'	12.5
	HB3	41°06.7'	71°43.3'	34.7
	HB4	41°07.5'	71°40.2'	18.3
	HB5	41°08.4'	71°37.3'	13.1
"BR"	BR1	41°15.7'	71°34.8'	36.6
	BR2	41°18.0'	71°33.0'	36.6
	BR3	41°20.8'	71°30.5'	9.1

Table 2. Station locations in Block Island Sound.

Light attenuation values were obtained with an irradiance meter consisting of a photocell and various glass filters. Fluorometer readings were obtained with a Turner fluorometer using a continuous flow door. These three parameters were measured in situ.

Water samples for chemical and biological analysis were collected in 5-liter Niskin bottles.

Salinities were obtained using a laboratory conductivity cell (Beckman Model RS-7), oxygen, chlorophylls, and nutrients, using the methods as described in Strickland and Parsons (1968).

Particle size determinations were performed with a Coulter Counter Model B.

Sampling Schedule

The ground truth program was designed with the intention of sampling in the areas of Block Island Sound and the New York Bight during every other ERTS overpass. This would allow for rescheduling due to weather problems and the like.

In general, this schedule was followed. Table 3 contains the tabulated cruises in Block Island Sound (20) and the New York Bight cruises (4) are tabulated in Table 4. The dates by area for the ERTS overpass are listed in Table 5.

Photometric and Additive Color Analysis of ERTS Imagery

Underflight and ERTS imagery were analyzed in order to determine the hydrologic features of the water mass, including current patterns, particulant in suspension, and the contacts between water masses.

A preliminary examination of the ERTS imagery was made and candidate frames were selected for reprocessing. This is usually required due to the low scene brightness range of the water masses. Also the extent of the cloud coverage over the area of interest was taken into consideration in such a selection. The imagery was placed into an additive color viewer for interpretation and colorimetric analysis. The first sets of ERTS images were interpreted both in color and black-and-white with specific areas of interest receiving the most attention. The results of the analysis showed that a time sequential multispectral color presentation relates color to environmental changes as a function of time, rather than spectral changes for any single date. This mode of data reduction was employed further, in conjunction with the conventional techniques.

ERTS photographic data products were also analyzed using electronic image analysis techniques. Satellite data were compared to water sample data collected simultaneously with the data of ERTS coverage in New York Bight. Four critical surface parameters were selected for correlation with the ERTS imagery:

-- Average extinction coefficient ($-\bar{K}$)

-- Total suspended particles (particles/liter)

-- Total cell counts (particles/liter)

-- Chlorophyll a (mg/liter)

These data, along with temperature (°C) and salinity (0/00), were collected during the satellite day for subsequent correlation with the ERTS imagery. Since each sampling station could not be occupied at the exact instant of the satellite overpass, the data were adjusted to the

tidal cycle which existed at the time of the ERTS satellite pass.

The reprocessed positives for a particular sampling day were placed in a Spectral Data Model 64 additive color viewer. Three brightness readings were made of the image of each sampling station using a Photo Science Spot Brightness meter. The black-and-white image brightness of MSS bands 4, 5, 6, and 7 was thus obtained and a regression analysis performed with respect to: average extinction coefficient, total suspended particles, total cell counts, and chlorophyll a.

Transect	Date	Assigned Cruise No.
H	24 Aug 1972	K7217
HB	29 Aug 1972	K7218
BR	5 Sep 1972	K7219
H	10 Oct 1972	K7225
BR	12 Oct 1972	K7226
HB	10 Nov 1972	K7230
H	14 Nov 1972	K7231
BR	16 Nov 1972	K7232
H	4 Dec 1972	K7236
HB	6 Dec 1972	K7237
BR	8 Dec 1972	K7238
H	13 Feb 1973	K7303
HB	14 Feb 1973	K7304
H, BR, HB	20 Mar 1973	K7310
BR	21 Mar 1973	K7311
H, BR, HB	24 Apr 1973	K7318
HB	25 Apr 1973	K7319
BR	26 Apr 1973	K7320
H, BR	18 Jun 1973	K7335
HB	19 Jun 1973	K7336

Table 3. List of cruises in Block Island Sound.

Date	Assigned Cruise No.
21 Sep 1972	K7222
19, 20, 21 Dec 1972	K7239
24, 25, 26 Jan 1973	K7302
30, 31, May 1973 1 Jun	K7327

Table 4. List of cruises in the New York Bight.

Year	BIS	NY Bight
1972	Aug 15	Aug 16
	Sep 2	Sep 3
	Sep 20	Sep 21
	Oct 8	Oct 9
	Oct 26	Oct 27
	Nov 13	Nov 14
	Dec 1	Dec 2
	Dec 19	Dec 20
1973	Jan 6	Jan 7
	Jan 24	Jan 25
	Feb 11	Feb 12
	Mar 1	Mar 2
	Mar 19	Mar 20
	Apr 6	Apr 7
	Apr 24	Apr 25
Power Squadrons →	May 12	May 13
	May 30	May 31
	Jun 17	Jun 18

Table 5. Schedule of satellite overpasses by area.

Section 2

Techniques and Equipment for Multispectral Additive Color Analysis

Multispectral Scanner (MSS) imagery exposed on different dates was received from the Goddard Space Flight Center in both positive and negative form. The spectral bands included the 500-600 nm, 600-700 nm, 700-800 nm, and 800-1100 nm spectral bands. Candidate frames from these ERTS photographic products were selected, taking into consideration the extent of cloud coverage and the coinciding of ERTS overpass dates with the days on which the cruises were conducted to acquire the oceanographic "ground truth". The selected frames were employed for colorimetric and additive color analysis and correlation with the coastal parameters obtained from the oceanographic data reduction.

Quick-Look Analysis and the Need for Multispectral Reprocessing

Quick-look analysis of the NASA second-generation negatives indicated that in most of the selected frames:

-- The green spectral band lacked contrast, owing perhaps to the presence of some haze; it was also overexposed.

-- Red spectral band was of acceptable contrast, although somewhat overexposed.

-- The infrared bands were overexposed for the land areas, but the exposure was good for the water.

Generally, the released ERTS images were not suitable for analysis of water mass characteristics using additive color techniques. This can be explained as follows.

In an additive color projection system, the color of an image appearing on the screen depends upon the image densities of the positives which are projected. When densities are equal in three positive images, and each is illuminated by an equal energy primary light source (blue, green, red), the screen image will be a shade of gray. This is due to the fact that the human eye sees equal amounts of blue, green, and red light which are combined in the image as white. The brightness of this achromatic (colorless) image is dependent upon the magnitude of the three densities and the brightness level of the projection system.

When the densities in the three black-and-white images are unequal, the eye sees the composite screen image as a color. This color is a function of the ratio of the three densities. The hue, or dominant wavelength, is determined by the two lesser densities and its saturation is therefore increased by increasing the density differences existing between the black-and-white images which are projected.

The greatest possible color discrimination is achieved by expanding the density range of the areas of interest in each black-and-white image to correspond to the density range accommodated by the projection system. Investigation has shown that, in general, densities over approximately 1.0 in one image will have no perceptible effect upon the color of the composite screen image which is produced by the lower densities in the other images (Anderson, 1968). This does not mean that all areas of interest in all three bands must have a density of less than 1.0. For example, in a photograph that includes both land and a water mass, the infrared negative will generally have very low density in the image of water, due to the absorption of infrared radiation by water. The density

range in the land image of well-processed green, red, and infrared positives will result in a water image density of over 1.0 in the infrared positive. In this case, any detail in the water image, as it appears on the screen, will come from the green and red positives. The color of a water image with no suspended organic material will generally be unaffected by either of the infrared positives.

While it is true that faithful color reproduction in an additive color projection system requires the gamma and density range of the three positives match each other, equal log exposure ranges in the three positives are usually assumed. Analysis of the Apollo IX S065 multispectral photography has shown that this assumption does not necessarily hold true in multispectral photography taken from orbit (Yost et al., 1970). The absorption of infrared radiation by water, when combined with the large amount of infrared radiation reflected by most vegetation, results in a greater log exposure range in the infrared than either the green or red bands. The green band, on the other hand, typically has a shorter log exposure range than the red band. The probable explanation for this experimental fact is the increased atmospheric scattering of shorter wavelength radiation which is recorded in the green band.

In view of the foregoing facts, the general requirements for multispectral positive imagery to be used for additive color projection are as follows:

1. A low base plus fog density and the lowest possible minimum image density is necessary for the greatest possible screen brightness.

2. The density range of areas of interest within the image area must be relatively high within the limitations of the projection system for full color discrimination and saturation.

3. The overall image density, density range, and gamma of the three positives should be matched to each other as closely as possible subject to the constraint imposed by log exposure range of each band. The best possible compromise should be achieved in view of the interpretive purpose of the additive color image.

Frequently general purpose release positives are not suitable for additive color projection because:

1. The image densities may be too high, being usually above the usable range of an additive color system.

2. The image densities may not be matched to each other in magnitude.

3. The density ranges may be too small for full color discrimination and saturation.

Multispectral Reprocessing

The general procedure used in the reprocessing of each MSS frame is illustrated by employing ERTS imagery data collected over Block Island Sound on 28 July 1972. NASA-processed ERTS frame E-1005-15005 was used to generate a set of characteristic curves as shown in Figure 5. The slopes of the multispectral records are well matched, although the minimum density of both the green and far-infrared images is excessive. These curves were generated plotting the gray scale step number which

appears at the bottom of the ERTS chips on the x axis with its density plotted on the y axis. Unfortunately, all the highlights of the scene fall along the toe portion of the curves where the density differences are relatively small for a large change in gray scale number. The darker regions of the imagery lie between the toe and the straight line portion of the curve where the density-brightness gradient is less than optimal.

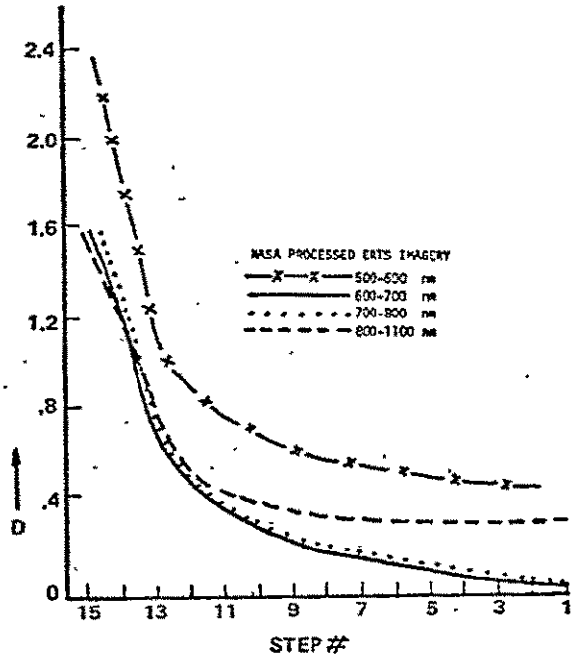

Figure 5. Curve of gray scale number vs. density of the positives supplied by NASA.

A visual analysis of the NASA positives indicated the following:

1. The green spectral band was extremely flat with a high D_{min} due to overexposure.
2. The red spectral band was of acceptable contrast.

3. The infrared bands lacked detail in both the water and land areas.

The NASA-supplied positive imagery was placed into the Spectral Data Model 66 viewer and the spectral records were projected as follows:

500-600 - Blue	700-800 - Red
600-700 - Green	800-1100 - Red

Only one of the infrared records was projected at a time with the two visible bands. The large urban areas were apparent, although most detail in the land was missing because of the heavy infrared exposure. Of all the records, the red had the most detail in both land and water. No obvious differences in water mass were apparent in this color composite image. Because of the non-optimal development of the MSS data for either the highlights (land) or the shadows (water) the NASA imagery was re-processed at Long Island University.

The negatives supplied by NASA were used to generate a second set of positives which would enhance any small detail in the water mass. Both the exposure and processing were altered to place the low brightness regions on the straight line portion of the characteristic curve shown in Figure 6. Notice that those regions which existed between the toe and straight line of Figure 5 are now imaged along the straight line portions of Figure 6. The minimum density has also been reduced on the red and near infrared bands. Due to the poor exposure of the green band, little could be done to create any significant change in the high minimum density without losing the little detail which the image contained. Contrast increased by using EK 2420 duplicating film and processing in D-19. The scene brightness range for both water and land is small so

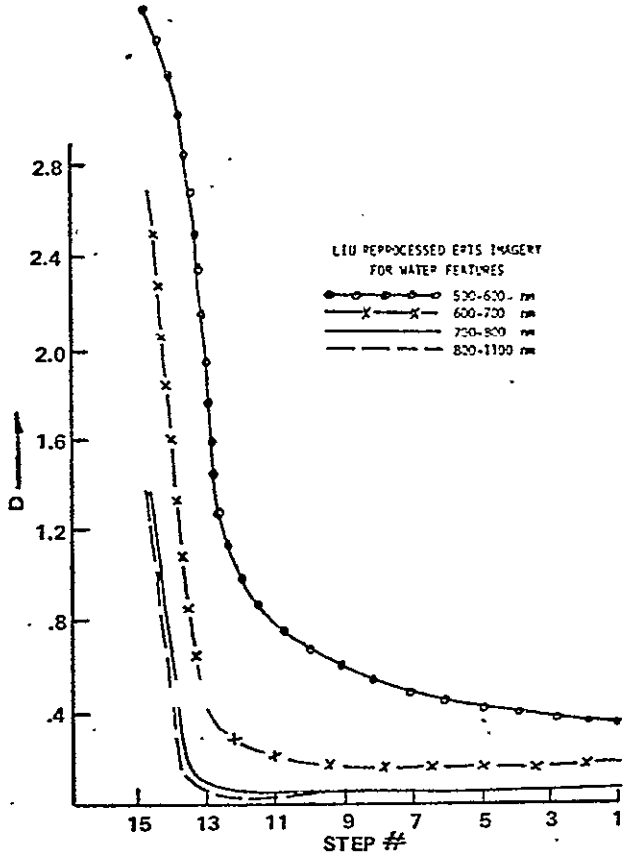

Figure 6. Curve of gray scale number vs. density for positives reprocessed to enhance water detail.

that a single reproduction of the green record has been used for the enhancement of both water and land areas. A more accurate comparison of the effects of reprocessing can be made by noting the density differences in the water between NASA and Long Island University processing. The water mass is represented by step wedge steps #14-16. The Δ density between these steps for NASA processed infrared positives is .7, while the Δ density of the water for the reprocessed infrared positives is 1.35. The Δ density in the red region is .6 for NASA processed film and .8 for Long Island University reprocessed images. It should be also noted that the lower D_{min} makes the water differences

more obvious when projected by increasing the brightness level on the viewer screen.

The NASA negatives were also reprocessed in order to enhance the land areas, the results of which are shown in Figure 7. The infrared bands

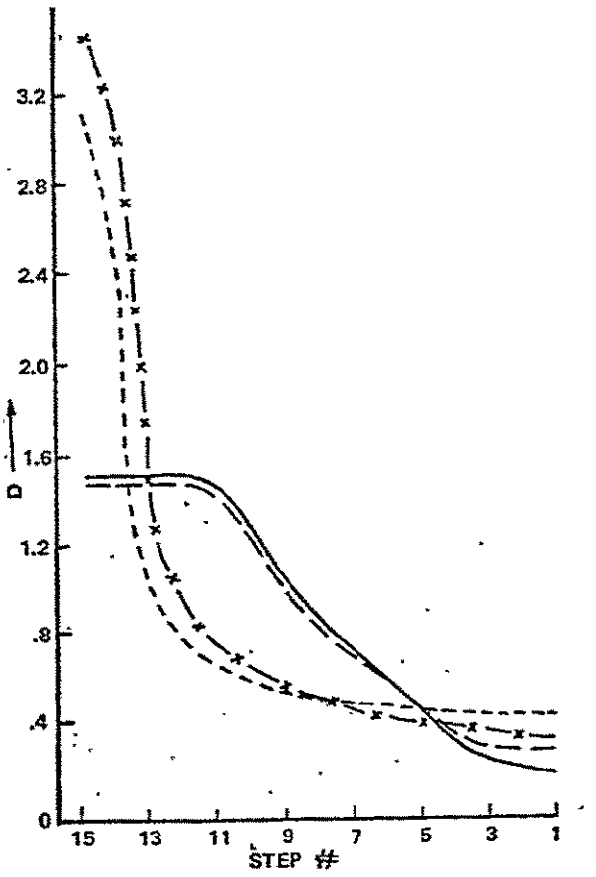

Figure 7. Curve of gray scale number vs. density of positives reprocessed to enhance land features.

required making an interpositive, an internegative, and finally the projection positive. This procedure was done in order to build-up the contrast without losing too much land detail. It was not possible to obtain sufficient contrast using a single step. The characteristic

curves of the final reprocessed positives are shown in Figure 7. Most of the information for the land areas was contained in the infrared records. Notice that the long toe region for the infrared bands shown in Figures 5 and 6 have been picked up and now exist on the straight line portion of Figure 7. Those land regions for which only small density differences existed previously have been greatly enhanced. The Δ density of the land improved from .1 (NASA processed) to .7 (Long Island University reprocessed) in the infrared regions and the minimum density of all records was decreased considerably for projection.

To summarize, the general procedure used in the reprocessing of each frame was as follows:

-- The master positive of each band was contact printed along with the calibration step wedge beneath the data block, Exposure and development were controlled to increase the density range of the areas of interest. The fifteen-step neutral density wedge was included as a processing control.

-- The internegative, including the negative image of the calibration step wedge, was contact printed to produce a final positive transparency. Again, exposure and development were controlled to produce a transparency meeting the previously listed requirements and a wedge was included as a process control. In some of the cases, internegatives and/or final positives could be enlarged rather than contact printed.

Additive Color Analysis of ERTS MSS Imagery

ERTS photographic data products were analyzed using additive color viewing and electronic image analysis techniques. The procedures used, with appropriate instrumentation and significant theories, are described in the subsequent paragraphs.

Additive Color Viewing: Spectral Data Model 64 viewer was an essential instrument for use in the interpretation and analysis of ERTS MSS imagery. The device produces a single color presentation for the spatially calibrated photos by projecting the image of one photo on top of the other using different color light sources. This technique of analysis permits a scientist to select a set of bands and to interpret within results from a single color presentation. In addition, a multispectral viewer provides the scientist with the capability of altering the color of the presentation in order to enhance the particular relationships he may be seeking. Fundamentally, the multispectral technique allows the scientist to create a color presentation specifically for the purpose of his discipline and interests.

In order to quantitatively evaluate multispectral color images, color must be colorimetrically defined as that conscious sensation which is exhibited when light of a specific spectral energy distribution enters the eye. It has been experimentally shown that differences in this energy distribution cause variations in the observed response of the eye and may be described in terms of three distinct psychophysical variables. The first is hue which is basically that quality of color which leads to the definition of an object as being red, green, yellow, etc. Saturation, the second quality of color, is described as the amount

of white in a given hue. It may be also considered as the concentration of the color. For instance, it is the difference between red and pink. As the amount of saturation in a color decreases, it approaches pure white. Brightness, which is the third variable of color, is described as the amount of visible energy contained in a certain hue which is saturated to a specific value.

Brightness Measurement: Positive images were made from ERTS MSS negatives to bring out maximum water detail. These positives were placed in Spectral Data Model 64 additive color viewer. Each MSS band was then projected individually onto the viewer screen without using any filter. An overlay was made for the projected image to give precise locations of the stations at which water samples were collected in the New York Bight and Block Island Sound. The projection lamp intensity was set at maximum for the four MSS bands. At each station location in a particular band, two brightness readings were made using a Photo Science Spot Brightness Meter - the first reading was taken with the image on the viewer screen, the second without the image. This was done to cancel out any light intensity difference on the viewer screen and thus preserve the accuracy for comparative analysis of the data at different sampling stations. The black-and-white image brightness of MSS bands 4, 5, 6, and 7 was thus obtained and a regression analysis performed with respect to surface parameters.

Density Slicing: Semi-automatic classification of water characteristics was achieved by interface of a Spatial Data Model 703 density slicer with the Spectral Data Model 64 viewer. Figure 8 shows the arrangement of the instrumentation used for such an analysis of ERTS imagery.

Figure 8. Spectral Data additive color viewer and Spatial Data density slicer used together to analyze ERTS imagery.

The composite screen image was "sliced" and the video display used to construct a chart of the water characteristics being analyzed.

Collection of Oceanographic Data in Block Island Sound and New York Bight

Twenty-four cruises were conducted in Block Island Sound and New York Bight areas to collect and analyze water samples at different stations. Three transects with twelve stations were covered in Block Island Sound and nine stations in New York Bight. Some of the analysis was done on board the research vessel KYMA immediately after collecting the water samples. The data was acquired for: (1) physical oceanography, (2) chemical oceanography, and (3) biological oceanography.

Physical Oceanography: Temperature, salinity, and calculated density values were obtained at multidepths for most stations sampled in Block Island Sound. Only surface salinity samples were taken on the New York Bight cruises.

When stations were sampled more than once per cruise, averages of temperature, salinity, and density (δ_t) were calculated at standard depths of 0, 10, 20, 30, 35, and 40 meters. Flood and ebb averages of these parameters were also calculated over each cruise. Horizontal profiles (contours of t°C, S°/$_{oo}$, and δ_t in depth versus distance) were made for each crossing of a transect.

The downwelling irradiance of the visible spectrum was measured at each station in Block Island Sound using an upward-facing irradiance meter (submarine photometer), comprising a photocell and cosine collector equipped with glass filters.

The extinction coefficient, $\bar{k}$, for these light values is defined by the equation:

$$I(z) = I(z=0)\exp - \bar{k}z$$

where I(z=0) is the total visible light energy in a particular wavelength band that is incident upon the naviface, I(z) is the remaining light energy at the depth z(m), and $\bar{k}$ is the total "extinction" coefficient for the particular wavelength band in units of m^{-1}.

On most cruises, irradiance measurements were taken as near to noon as possible at each station. Linear regression analyses were performed and correlation coefficients calculated for data sets using total particle counts and average extinction coefficients for each of the Block Island Sound and New York Bight stations.

Regression analysis and correlations were also calculated between monthly freshwater discharge into Long Island Sound and the monthly surface and bottom salinity values at the Block Island Sound stations. Dilution factors, D, defined by:

$$D = (\Delta S/\bar{S}) \times 100\%$$

where ΔS is the annual range and $\bar{S}$ the mean salinity at a station, were also calculated.

Chemical Oceanography: At each station, the locations of which have been previously described, samples were collected from selected depths with 5-liter Niskin bottles. Once on board, samples for the measurement of salinity, oxygen, and phytoplankton analyses were removed. The remainder of the sample was then filtered through Whatman GF/C filters in an all glass filtrations system. The filter pads were then placed in individual vials and frozen for later analysis of chlorophyll and particulate phosphorus. Samples of the filtrate were removed for the measurement of reactive and total soluble phosphorus, nitrite, and nitrate nitrogen, and silica.

Salinity was determined with a conductivity system (Beckman RS7-B) and oxygen was determined by the method described by Carpenter (1966). Reactive, total soluble and particulate phosphorus, silica, and chlorophyll were determined according to the methods described by Strickland and Parsons (1968). Nitrite and nitrate nitrogen were determined by the method described by Wood et al (1967).

On 12 May 1973, through the cooperation of the local power squadrons and other private yachts, a synoptic sampling of the surface waters was conducted. Salinity and suspended solids samples were collected at 0900

1200, and 1500 hours. The method described by Strickland and Parsons (1968) was used for these analyses.

Biological Oceanography: Samples for the analysis of phytoplankton and suspended particles were collected from the surface at each station in 5-liter Niskin bottles, concurrently with the chemical samples. One liter of water was removed from the bottle, immediately concentrated in a continuous plankton centrifuge to less than 10 mℓ, and brought to a final volume of 10 mℓ with filtered (0.45u) seawater and neutral buffered formalin (a final concentration of 3%). This concentrated sample was returned to the laboratory for microscopic analysis of the phytoplankton population.

An additional 50-mℓ aliquot was withdrawn from the Niskin bottle and placed in a 50-mℓ glass vial. This sample was refrigerated until return to the laboratory, when it was immediately analyzed for suspended particles with a Coulter Counter, Model B.

Aliquots of the concentrated sample were placed in a nannoplankton-counting chamber (Palmer and Maloney, 1954) and various types of microscopic counts, depending on cell size and number, were performed under 100X and 400X magnification. At least 10 field counts (a wide field being delineated by the microscopic field and a narrow field by a whipple disc placed in one eyepiece) were performed under each magnification, and three survey counts (a scan of the entire counting chamber) were performed under 100X magnification. The average counts were multiplied by the appropriate factors to yield results as cells per liter.

Immediately upon return to the laboratory, the refrigerated 50-mℓ sample was analyzed for suspended particles with a Coulter Counter, Model

B. Two aperture tubes (30μ and 100μ) were employed so that particles between $0.16\mu^3$ and $635\mu^3$ (equivalent diameter of 0.68u to 10.67μ) could be counted. Particles between 1 and 10μ equivalent diameter were counted at 1 micron intervals. Particles above 10.67μ equivalent diameter were also counted for most of the samples.

Section 3

Oceanographic Results

Presented in this section is a description of the oceanographic results obtained from the analysis of data collected under the sampling program for Block Island Sound and New York Bight. A detailed narrative of these results, along with the summary and methods of data reduction, is included in the appendices of this report: Appendix A - Physical Oceanography, Appendix B - Chemical Oceanography, and Appendix C - Phytoplankton and Suspended Particles. Also contained in these appendices are the graphs, tables, and oceanographic charts describing the specific characteristics of Block Island Sound and New York Bight water masses.

Physical Oceanography

The annual temperature regime within Block Island Sound and New York Bight is largely governed by solar radiation and correlates with the mean month temperatures in the atmosphere, lagged one month. For these waters, the maximum temperatures occur in August, the minimum in February. Vertical temperature gradients are largely governed by vertical mixing and diffusion between a surface layer composed of largely harbor and sound water and a bottom layer of coastal water.

The annual salinity regime is mainly regulated by the stream discharge entering Long Island Sound and New York Harbor. The two major sources of this stream discharge are the Connecticut River for the Sound and the Hudson River for the Harbor. There is also approximately a one-month lag between maximum stream discharge and the corresponding salinity minimums.

Linear correlations at a one-month lag and dilution factors, D, were calculated for Block Island Sound. The highest correlations occur at the center stations of the H and HB transects and the weakest correlation occurs at Station BR3 (55%). Weak correlations at depth (30m) imply a two-layered system, with a surface layer that is composed of less saline Long Island Sound waters and a bottom layer of saline coastal waters. Vertical mixing and diffusion is relatively weak in Block Island Sound, as indicated by these high correlations and dilution factors.

The average extinction coefficient for Block Island Sound in the visible spectral band was 0.335, as compared to a mean value for the New York Bight of 0.663, almost a factor of 2 greater. The mean value for the blue band is 0.400 in Block Island Sound and 1.048 in the New York Bight; for the red band, the value is 0.554 and 0.876 in the Sound and Bight respectively. The disparity in these two wavelength bands dramatizes the shift of the peak of maximum transmissivity from shorter to higher wavelengths with increasing turbidity.

The average extinction coefficients for each transect in Block Island Sound were correlated with total particle counts as determined with a Coulter Counter and for particle counts greater than 5μ in equivalent diameter. Highest correlations occur with particles greater than 5μ, but less than 10μ in size. Similar results were obtained for the New York Bight stations. These results reflect nonselective attenuation, particularly absorption, since the lower limit of the total particle count is approximately 0.7μ in equivalent size so that selective or Raleigh scattering is not included in these calculations. The correlations would be significantly improved if the resolving power of the Coulter Counter

could be increased; however, this is an engineering design problem that hopefully will be resolved in the future.

Chemical Oceanography

In Block Island Sound, the nutrients (phosphates, nitrates, and silicates) showed the seasonal variations typical of temperate waters. Indications are that the supply of nitrogen to these waters is limited and that, under the appropriate conditions, the nutrients are utilized by the phytoplankton rather quickly. Although relatively large seasonal changes in concentration were noted, the correlations between these parameters and chlorophyll a were not considered significant.

In early October 1972 what appeared to be the remnants of an algae bloom were found at those stations occupied along the H transect. Little evidence of such conditions was found for the other transects. Chlorophyll a concentrations generally remained low (0.5-1.0 mg/m^3) through the remainder of the fall and winter. A spring flowering of relatively short duration was present in March. Peak chlorophyll a concentrations of 9.4 mg/m^3 were present at Station H1. The amount of chlorophyll a present in the surface waters of this transect gradually decreased from the high value noted at Station 7 to 2.1 mg/m^3 at Station 4. No evidence of a spring outburst of similar magnitude was found in the waters of the other transects. The reasons for this may be that the frequency of sampling was such that the bloom was missed along the other transects, or the data reduction techniques affected the graphical presentation. In respect to the latter, the range of chlorophyll a at BR1 was 1.69-3.39; at BR2 a range of 2.01-2.60 mg/m^3, and at BR3 a range of 0.85 to 3.04 mg/m^3. Along the HB transect,

inclement weather prevented our sampling from 14 February until 25 April and, undoubtedly, the spring bloom was missed.

This study was designed to determine the relationship between ERTS-1 imagery and the characteristics of surface waters in this area. It was also necessary to determine how representative any of these data were for that day since in the present ERTS-1 program an image of an area represents the conditions for that moment in time only. The sampling program was designed to collect data on the effect of both tidal and non-tidal forces upon a given parameter and, consequently, to yield information pertinent to the above. ERTS time was at approximately 1100 hours and at that time higher concentrations of both particulate phosphorus and the pigmented population were present at Station H1 than at the remaining stations. This station also showed the greatest range of concentration for both of these parameters. Since this range of variation is typical of the variability to be expected for most parameters, it is particularly important that additional information be gathered relevant to the variability of all parameters in both short- and long-term space and time.

With respect to the former, an experiment was conducted on 12 May 1973, with the help of the local power squadrons and private yachts, to collect synoptic samples for the measurement of suspended material, salinity, and temperature in the surface waters of Block Island Sound and adjacent waters. In this preliminary experiment, logistics prevented the collection of samples for chlorophyll. The location of each of the sampling vessels is shown in Appendix B. The sampling times were 0900, 1200, and 1500 hours. It should also be noted that, although care was exercised in the storage of the samples, certain of those collected early

in the day remained in the plastic containers for more than ten hours prior to filtration.

The synoptic distribution of temperature, salinity, and suspended solvents is shown in Appendix B. For each of the three parameters observed large ranges in values and concentrations were noted. The effect of the tidal forces upon the distribution of these parameters was apparent.

In New York Bight, the concentration of nutrients and chlorophyll was generally higher along the New York Harbor transect than along the TR transect. This was especially apparent in the nitrate concentrations. Evidences for seasonal trends were particularly evident in the nitrate and silicate data.

No significant correlation between the nutrients, particulate phosphate, and chlorophyll a was found for the TR transect at any time. Along the NYB transect, however, strong correlations were found between the concentration of chlorophyll a and soluble organic phosphorus. It was also noted that the correlation was strongest in May. For example, the overall correlation of soluble organic phosphorus with chlorophyll a for the NYB transect was 0.88. In December and January, the correlations were not significant (r=0.01 and 0.12 respectively), while in May the correlation was 0.95.

Phytoplankton and Suspended Particles

The high correlation between phytoplankton and suspended particles >10.7μ equivalent diameter in Block Island Sound (0.858) indicates that the phytoplankton may contribute largely to the suspended material in this region. In contrast, the lower correlation between these parameters in the New York Bight (0.586) indicates that other factors are adding to the

suspended load in this area. Suspended materials are being brought into the area by the Hudson River outflow, as evidenced by the high total particle counts and lowered salinity values (see Appendix A) at Station NYB3.

The phytoplankton population was highest at the New York Bight and Block Island Sound stations, with the TR stations having the lowest number of cells. There are indications that the organic enrichment caused by the disposal of sewage sludge in the New York Bight may play a role in maintaining the relatively high phytoplankton population in this region.

In Block Island Sound, the stations around Montauk Point generally exhibited the largest phytoplankton populations, these populations probably originating in the waters of the Peconic Bay-Gardiners Bay system.

Block Island Sound can be divided into three regions: (1) northern Block Island Sound, influenced by the coastal waters of Connecticut, Rhode Island, and the Cape Cod region; (2) southern Block Island Sound, influenced by the waters of the Peconic Bay-Gardiners Bay system; and (3) central Block Island Sound, influenced by the waters of Long Island to the west and the Atlantic Ocean to the east.

In the experiment, conducted on 12 May 1973, the largest population occurred in the Peconic Bay-Gardiners Bay region, with a smaller population found in northern Long Island and Block Island Sound waters. These populations were separated by the sparsely populated waters apparently originating in central and southern Long Island Sound, passing through central Block Island Sound, and meeting the waters of the Atlantic Ocean between Montauk Point and Block Island. This type of circulation of the surface waters was shown previously by Nuzzi (1973) and Austin (1973).

Section 4

Photometric and Additive Color Analysis of ERTS Imagery

Underflight and ERTS imagery were analyzed in order to determine the hydrologic features of the water mass in New York Bight and Block Island Sound areas. These features included current patterns, particulant in suspension, and the contacts between water masses. Quick-look analysis of the ERTS MSS imagery, as discussed in Section 2, was used to determine whether reprocessing of the negatives would be necessary. All four spectral bands of MSS data were employed for both quantitative and visual additive color analysis. These bands included the 500-600 nm, 600-700 nm, 700-800 nm, and 800-1100 nm regions of the spectrum. The ERTS imagery exposed on 28 July 1972 for Block Island Sound indicated that photographic reprocessing of the negatives received from NASA was necessary in order to enhance the water detail and bring out the subtle spectral differences.

Six candidate frames over the New York Bight area were selected for multispectral photo analysis from the MSS imagery received from Goddard Space Flight Center. The extent of the cloud coverage over the test area was taken into consideration in such a selection. In addition, the availability of oceanographic ground truth and a representation of three differen seasons, fall, winter, and spring, was also taken into account.

Multispectral Additive Color Analysis

Additive color analysis was performed using four different frames from the six frames selected over the New York Bight area. The image

identification numbers are as follows:

16 August 1972	E-1024-15071
9 October 1972	E-1078-15072
25 January 1973	E-1186-15075
7 April 1973	E-1258-15082

The general region covered by these frames is shown in Figure 2 in Section 1.

The negatives supplied by Goddard Space Flight Center were used to generate a second set of positives which would enhance any detail in the water. The second generation set of these reprocessed positives was used to produce the additive color composites shown in Figures 9, 10, 11, and 12. Only one of the infrared bands was used in each multispectral rendition. This was achieved by placing the imagery into the Spectral Data Model 64 viewer and projecting the spectral records with different colors. The results were viewed by the Science Engineering Research Group, together with oceanographers from the New York Ocean Science Laboratory. The multispectral renditions were viewed on the Model 64 screen for the subtle spectral differences in the water masssin the New York Bight area. The viewer screen was photographed and positive prints were made.

Additive color presentations in this report show only the part of ERTS MSS frame which covers the study area. Certain features are observed in these photographs relating to colored water masses off Long Island and visible signs of pollution in the dump areas. Multispectral rendition shown in Figure 9 is a color composite of MSS bands 4 and 6 imaged on 16 August 1972 (E-1024-15071). Band 4 was projected as red and band 6 as green. Notice that all detail in the land area has been lost since

Figure 9. Additive color composite made from ERTS MSS bands 4 and 6 of frame E-1024-15071 taken on 16 August 1972.

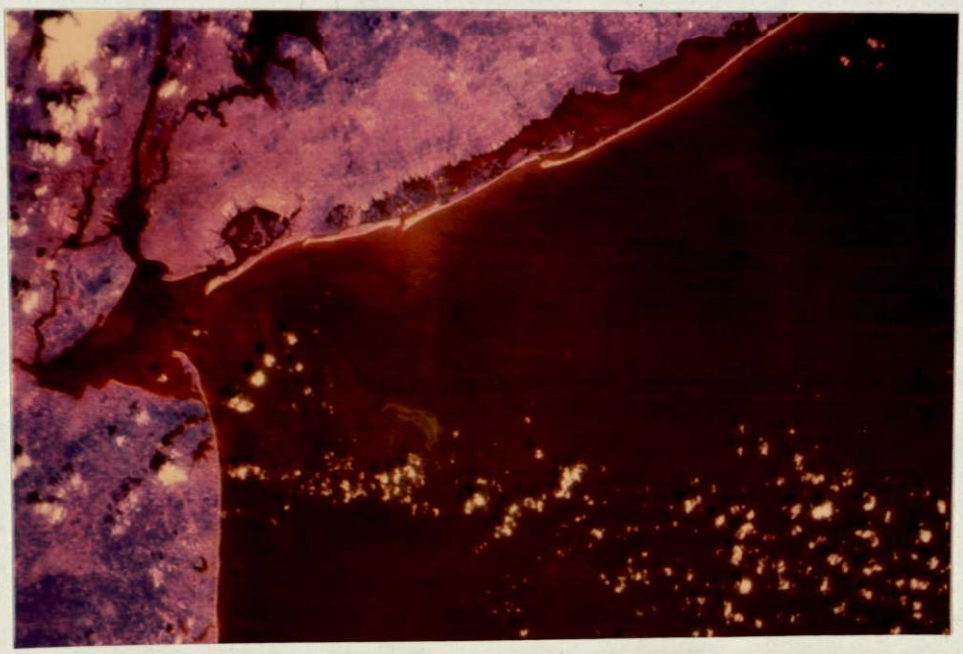

Figure 10 Additive color image of the New York Bight area from ERTS frame E-1078-15072 photographed on 9 October 1972.

the reprocessing to obtain a second generation set of positives was done to enhance water detail. The analysis of this figure and the subsequent color presentations clearly show the distribution of an acid-waste discharge, sewage dump, and major suspended sediment inputs into the New York Bight area. The area is approximately 10 kilometers east of the New Jersey shore and 20 kilometers south of Long Island's south shore.

Figure 10 shows an additive color composite of MSS bands 4, 5, and 6 of ERTS frame E-1078-15072, photographed on 9 October 1972. The spectral records were projected as follows:

Band 4 (500-600 nm) as Green

Band 5 (600-700 nm) as Red

Band 6 (700-800 nm) as Blue

The water area appears as dark green and the land area covered with vegetation appears as blue since the infrared band was projected as blue. The extent of the urbanization in the land area is indicated by the loss of blue color in different parts of the image. The dump area is clearly shown at approximately the same location as in Figure 9, but the shape has a different pattern. Concentration of suspended particulant is evident in different parts shown as a reddish-orange color, especially over the Fire Island Inlet where it appears most vividly.

Additive color presentation for the ERTS frame (E-1186-15075) imaged on 25 January 1973 is shown in Figure 11. In this multispectral rendition, MSS bands 4, 5, and 6 were used and were projected as follows in the additive color viewer:

Band 4 9500-600 nm) as Red

Band 5 (600-700 nm) as Green

Band 6 (700-800 nm) as Blue

A comparison of the color composite shown in Figure II was also made using the ERTS photographs taken on 16 August and 9 October 1972.

Although there was not any significant change in the color for New York Bight dump area in this comparison, it is interesting to notice the change in shape and size. Discussion on this feature with oceanographers from New York Ocean Science Laboratory indicated that this change in the shape and size as compared to previous visual detection could be attributed to the change in the method of dumping the sewage or it could be due to the high velocity winds in the northeast direction.

The yellowish-red color of the water mass along the south shore of Long Island is evident in the color composite as compared to the dark greenish color of water in the lower right-hand portion of this photograph. The water samples were collected on 25 January 1973 along the south shore and the dump area at the different locations shown in Figure I in Section I. The analysis of the oceanographic data showed that the yellowish-red color off the south shore was due to the heavy suspended particulant with an increase in particle count at the Fire Island Inlet. This increase in suspended material at different locations in the photograph is also responsible for the turbidity as evident in Figure II. The fluorometric data shows evidence of large-scale geographic changes in background fluorescence, as well as depicting the "patchings of chlorophyll".

Attention is also drawn to the appearance of light greenish color for water in the Hudson River as compared with ocean water mass and concentration of suspended material near the outlet appearing as patches of turbid water. The extinction coefficient, an index of turbidity, was calculated and, as such, relates to the suspended and dissolved material

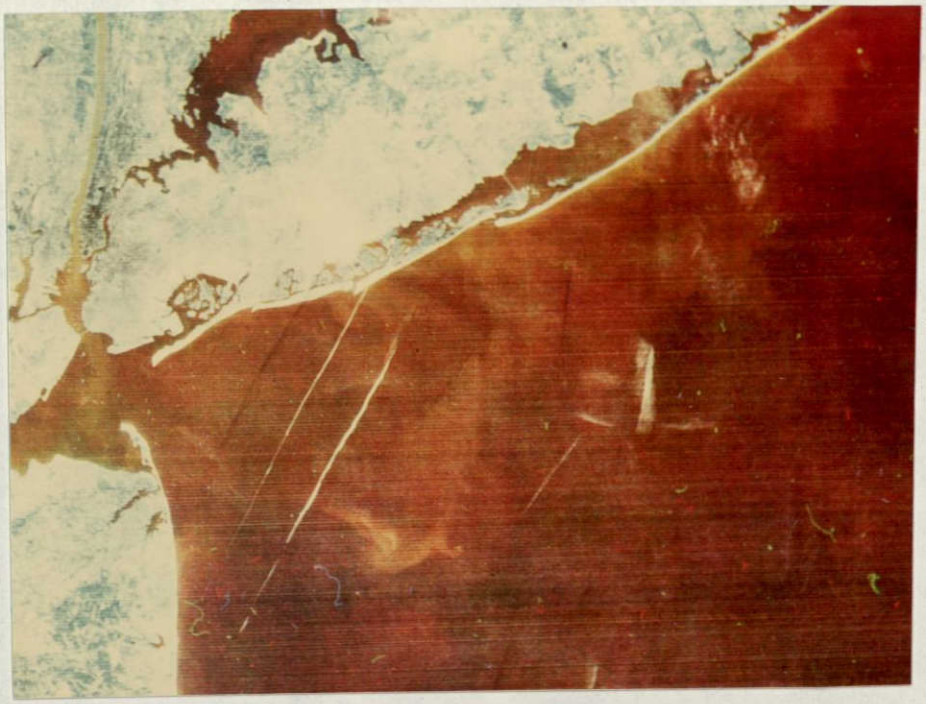

Figure 11. Additive color composite made from ERTS MSS bands 4, 5, and 6 of frame 1186-15075 taken on 25 January 1973.

Figure 12. Multispectral rendition of ERTS MSS bands 4, 5, and 6 taken on 7 April 1973. Band 4 projected as red, band 5 as green, and band 6 as blue.

in the water. The sampling stations closest to shore generally show the highest extinction values as would be expected. It is also estimated that these stations also contain the largest number of particles per liter and phytoplankton in the water.

Figure 12 is a composite additive color image of ERTS MSS bands 4, 5, and 6 (E-1258-15082) photographed on 7 April 1973. The green band (500-600 nm) was projected as red, the red band (600-700 nm) was projected as green, and one of the two infrared bands, band 6 (700-800 nm) was projected as blue. The clear ocean water in this rendition appears as dark green, while the turbid water areas near the Hudson River outlet, New Jersey coast, and New York Bight area appear as light green. The dump area is clearly shown at approximately the same location as it was in the previous color composite presentations, except for its shape which suggests barge dumping in a straight line manner. A patch of light green color appearing just southwest of this pattern probably indicates the surface spread and movement of wastes.

Time-Sequence Multispectral Color Analysis of ERTS Data

Figure 13 is a sequential multispectral color presentation of two ERTS images taken on two different dates, but of the same area. This type of presentation is useful for monitoring and detecting changes over time by showing them as colors. The analysis showed that time sequential multispectral color presentations relate color to environmental changes as a function of time, rather than spectral changes for any single date. This mode of data reduction was found useful in conjunction with the conventional techniques, especially for indication regarding the surface spread and movement of wastes discharged by barge dumping in the New York Bight area.

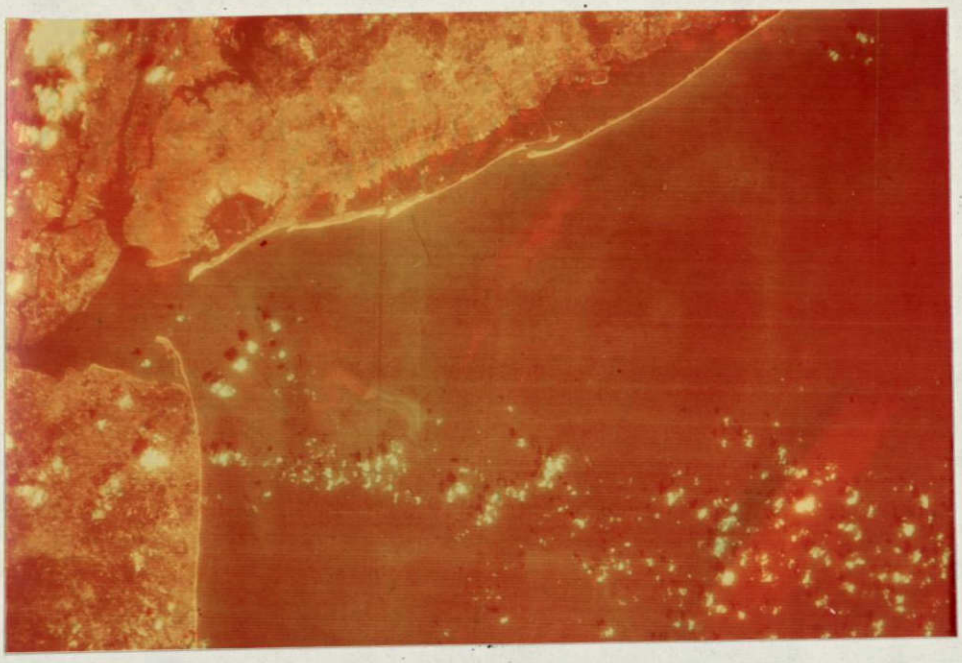

Figure 13. Time-sequential color presentation for New York Bight area.

ERTS frames E-1024-15071 (16 August 1972) and E-1078-15072 (9 October 1972) were used for the additive color presentation shown in Figure 13. Band 4 of 16 August 1972 data was projected as green and the same band for 9 October 1972 was projected as red. The color of the image tends to yellow because of the additive combination of red and green light. The suspended particulant concentration on 9 October 1972 appears as light greenish color in this presentation and the distribution of sewage sludge dump and major wastes clearly appears as a pattern light green in color. Right next to this pattern, towards the New Jersey coast, the barge dumping of industrial and municipal wastes is shown as S-shaped and red in color representing the ERTS observation on 16 August 1972. The oceanographic data indicates that under the sea-state conditions existing at the time of observation, the disposal of acid wastes and other dumping materials produces a suspension which remains in a unique pattern for

extended periods of time. Since the time-differential of the two ERTS images used in the presentation shown in Figure 13 is approximately two months, it is suggested that the movement of the distinct pattern in the east direction represents the change in the method of barge dumping. However, a more frequent monitoring system over the study area could provide accurate data regarding the surface spread and movement of the wastes and their effects on the environment.

Correlation of Oceanographic Parameters with ERTS MSS Data

ERTS imagery acquired over the New York Bight area on 25 Januarv 1972 and 31 May 1973 was analyzed using density slicing and electronic image analysis techniques. The ERTS frames E-1186-15075 and E-1312-15080 were employed for correlation with the oceanographic data collected under the water-sampling program. Two successful cruises, K7302 and K7327, were conducted in the New York Bight on 25 January and 31 May 1973 to collect water samples at different stations. Physical parameters of salinity, temperature, and extinction were measured at each station. A detailed discussion of the oceanographic results is presented in the appendices to this report.

Four critical surface parameters were selected for correlation with the ERTS-1 imagery:

-- Average extinction coefficient ($-\overline{k}$)

-- Total suspended particles (particles/litre)

-- Total cell counts (particles/litre)

-- Chlorophyll a (mg/litre)

These data, along with temperature (°C) and salinity (0/00), were collected during the satellite day for subsequent correlation with the

ERTS-1 imagery. Since each sampling station could not be occupied at the exact instant of the satellite overpass, the data were adjusted to the tidal cycle which existed at the time of the ERTS-1 satellite pass.

Image Analysis Procedures

The approach used for analysis of the ERTS-1 imagery with respect to water characteristics was:

1. Use water sample data to develop image analysis procedure for each pair of image water sample data.
2. Use the techniques thus developed on a second ERTS-1 date and compare the results with the water sample data with this second date.

Positive images were made from the ERTS-1 31 May 1973 negatives to bring out maximum water detail. These positives were placed in a Spectral Data Model 64 additive color viewer. Three brightness readings were made of the image of each sampling station using a Photo Science Spot Brightness meter. The black-and-white image brightness of MSS bands 4, 5, 6, and 7 was thus obtained and a regression analysis performed with respect to: average extinction coefficient, total suspended particles, total cell counts, and chlorophyll a.

On the basis of this analysis, composite bands were selected for subsequent analysis. In the New York Bight, combined positive images of MSS bands 4 and 5 were found to be best for the measurement of extinction coefficient and positive images of bands 5 and 6 best for the measurement of total suspended particles.

Semi-automatic classification of water characteristics was achieved by interface of a Spatial Data Model 703 density slicer with the Spectral

Data Model 64 viewer. The composite screen image was "sliced" and the video display used to construct a chart of the water characteristics being analyzed. Figure 8 in Section 2 shows the arrangement of the instrumentation used for analysis of the ERTS imagery.

Total Suspended Particles

ERTS-1 imagery acquired over New York Bight on 31 May 1973 was analyzed. A portion of this image is shown in Figure 14 on the following page.

The brightness of the projected reprocessed positive image was measured at each of the nine New York Bight sampling stations on each of the four individual MSS bands. The table below shows the image brightness and associated water data.

Table 6

Sta. No.	North Latitude	West Longitude	Image Brightness ft. lamb. MSS Bands 4	5	6	7	Av. $\bar{K}$	Surface Total part./ litre x 10^6	Total cell ct./ litre x 10^3	Chl. a mg/l
1	40°32.4'	73°56.6'	3.9	3.5	5.9	8.7	.14	274	149	4.1
2	40°32.4'	73°58.0'	4.0	2.9	5.0	7.9	.67	1665	1738	14.8
3	40°29.2'	73°59.6'	4.1	3.6	5.8	8.1	.93	2677	1134	17.2
4	40°25.1'	73°56.0'	3.4	2.2	4.8	8.6	.44	1119	1997	19.7
5	40°24.4'	73°51.3'	3.7	2.3	4.0	7.5	.30	939	865	8.9
6	40°23.0'	73°48.2'	2.9	1.5	3.3	5.6	.43	609	724	20.1
7	40°25.5'	73°45.0'	3.0	1.5	3.2	5.6	.50	923	1063	6.4
8	40°30.0'	73°44.0'	3.4	1.9	3.9	7.3	.54	561	1138	14.9
9	40°33.8'	73°48.6'	4.2	2.3	4.9	8.9	.53	478	280	5.5

New York Bight - 31 May 1973
ERTS-1 Image Brightness and Water Sample Data at Nine Stations

The relation of screen brightness in each band and total suspended particles was plotted and a linear regression line plotted for each. These relationships are shown in Figure 15 on the following page.

Figure 14. ERTS-1 MSS band 5 of New York Bight, 31 May 1973.

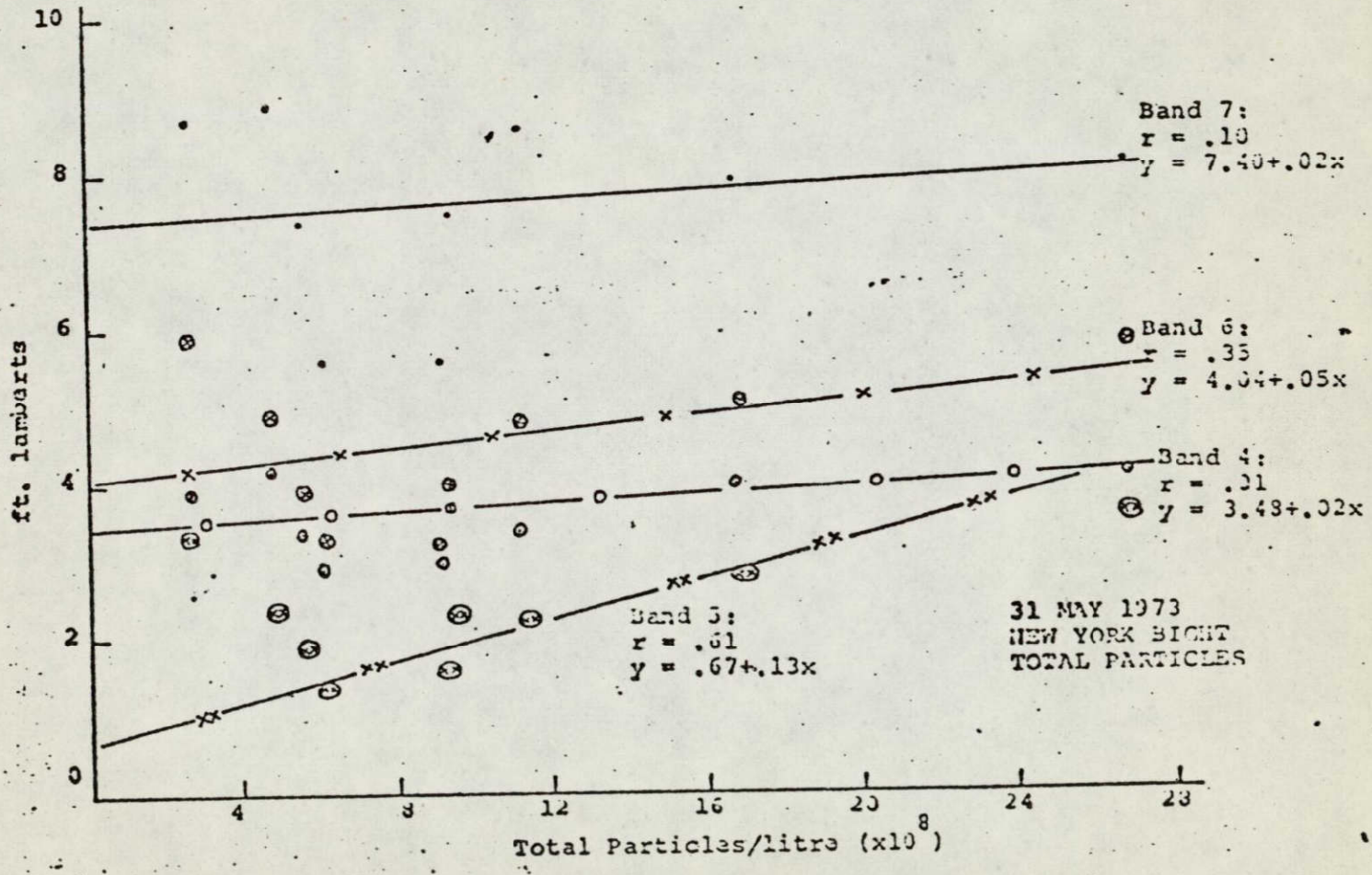

Figure 15. 31 May 1973 - New York Bight. The relationship of total particles and brightness of four ERTS-1 MSS bands.

Single band images show little relationship between total particles and image brightness, although band 5 is the best of the four bands. However, when positive images of bands 5 and 6 are combined, a significant relationship between image brightness and total particles is achieved as shown in Figure 16.

A comparison of the regression lines for the individual ERTS-1 MSS bands and the composite MSS bands 5 and 6 for 31 May 1973 is shown below:

Band	Wavelength	Regression Line	Correlation Coefficient
4	.5 - .6μ	$y = 3.48 + .02x$	.01
5	.6 - .7μ	$y = .67 + .13x$	.61
6	.7 - .8μ	$y = 4.04 + .05x$	.35
7	.8 - 1.1μ	$y = 7.40 + .02x$	.10
5&6	.6 - .8μ	$y = 4.45 + .18x$	.92

In computing the above regression lines, y (the dependent variable) is image brightness and x (the independent variable) is total suspended particles (particles per litre x 10^8).

The validity of using an additive color combination of reprocessed positive images of ERTS bands 5 and 6 for obtaining quantitative measurement of total suspended particles was evaluated by using the same image analysis techniques on the 25 January 1973 ERTS images of New York Bight. After performing the analysis, a regression of the image data on the water sample data obtained on that date was made. These results are shown in Figure16 on the following page.

By using more precise controls on the reprocessing of the positive imagery from the ERTS negatives through utilization of the step wedge calibration provided, a general relationship between image brightness and

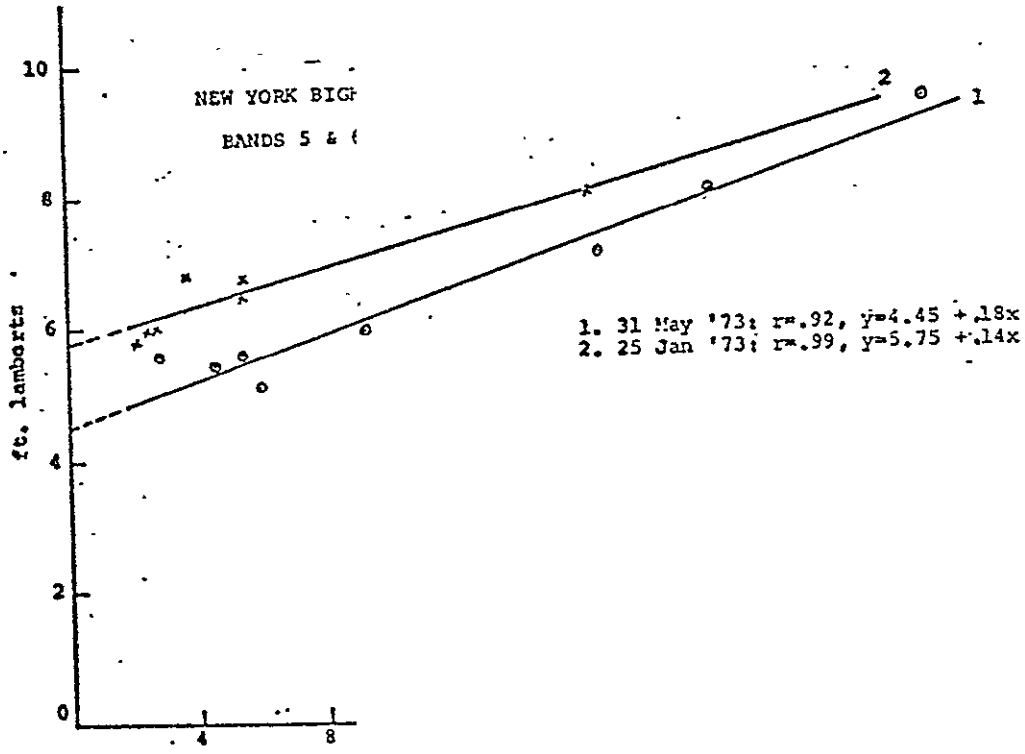

Figure 16. 25 January 1973 and 31 May 1973 - New York Bight. The relationship of total particles and image brightness of composite of ERTS-1 MSS bands 5 and 6.

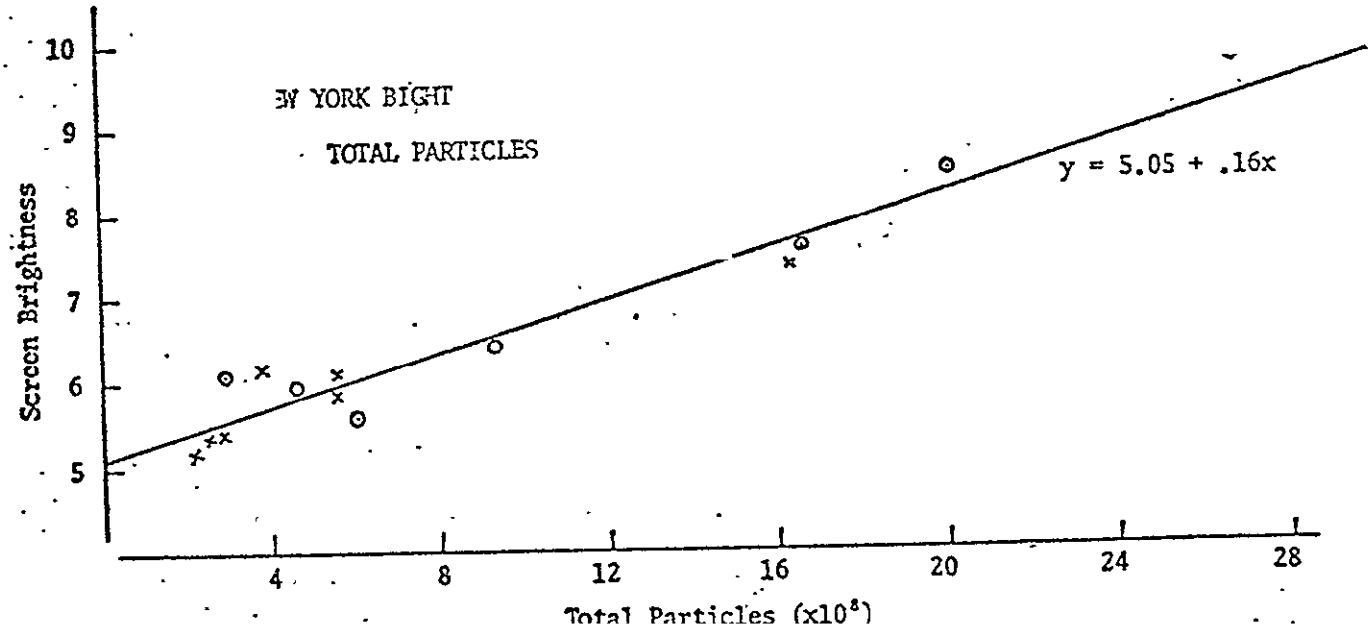

Figure 17. 25 January 1973 and 31 May 1973 - New York Bight. The relationship of total particles with image brightness of accurately processed positive composites of ERTS MSS bands 5 and 6.

total particles exists which can be used for quantitative measurement. This relationship is shown in Figure 17.

Figure 18 shows the predicted value of total particles using a composite of ERTS MSS bands 5 and 6 which have been carefully reprocessed as positives and the actual values measured by ship sampling.

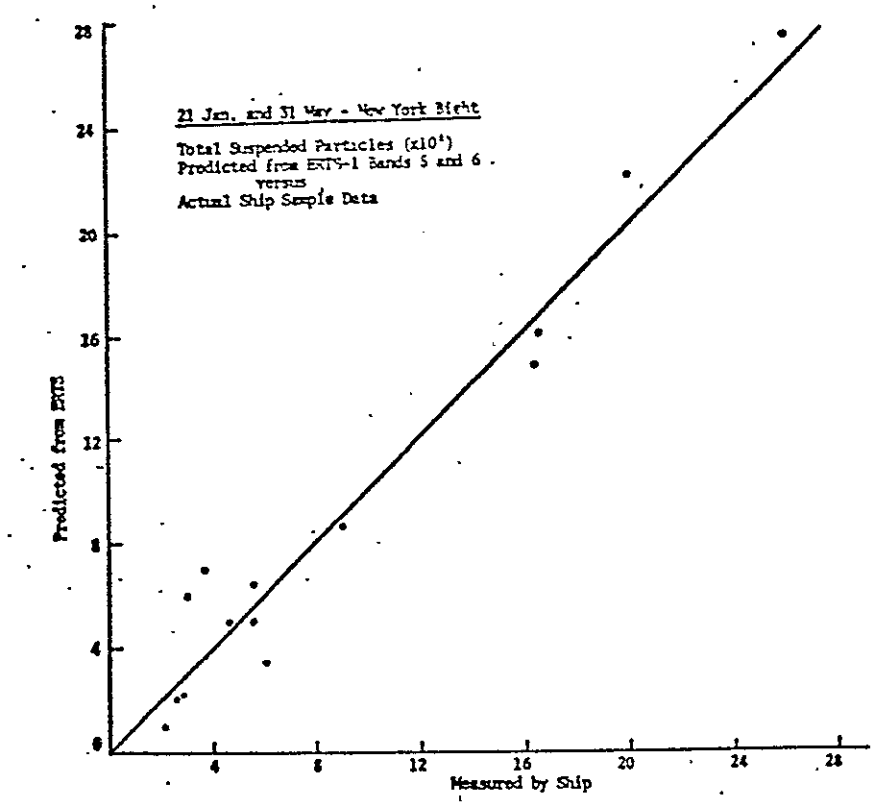

Figure 18. Total suspended particles predicted by ERTS measurements versus actually measured particles.

It should be emphasized that the above is a prediction of the absolute value of total suspended particles, not the relative value

ORIGINAL PAGE IS
OF POOR QUALITY

Extinction Coefficient

An analysis similar to that discussed was performed for determining the extinction coefficient ($-\overline{K}$) from the ERTS-1 imagery. A statistical

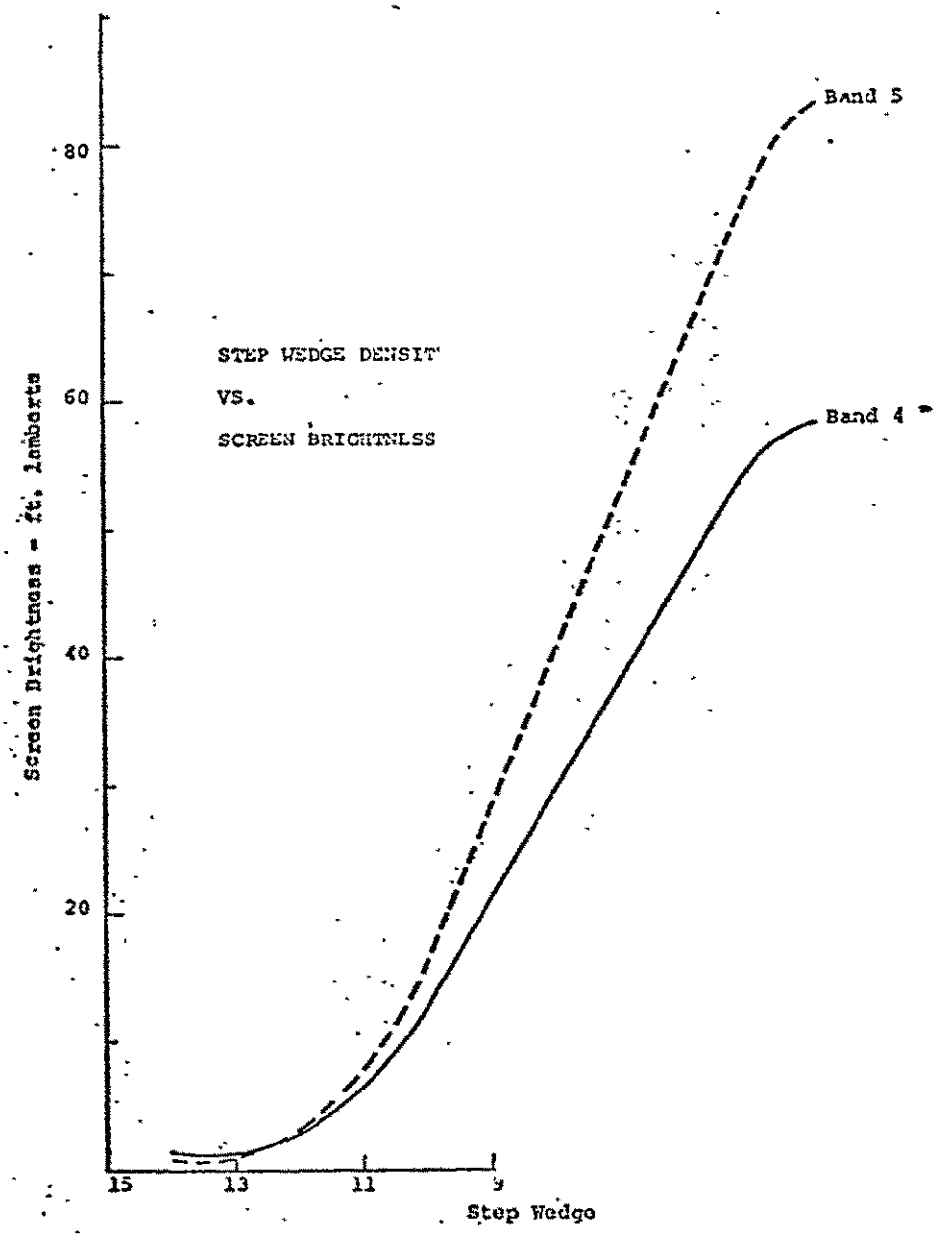

Figure 19 Step wedge density vs. screen brightness of bands 4 and 5 used to determine extinction coefficient for 31 May 1973.

analysis of the individual bands showed that positives of bands 4 and 5 could be used to predict relative values of the extinction coefficient. Figure 20 shows the results for 25 January and 31 May 1973; variability

in the slope of the regression line is believed to be due to atmospheric effects. Figure 19 shows the step wedge density versus the brightness of the 31 May 1973 positives used.

The relationship between screen brightness and extinction coefficient measured by ship sampling is shown in Figure 20 below.

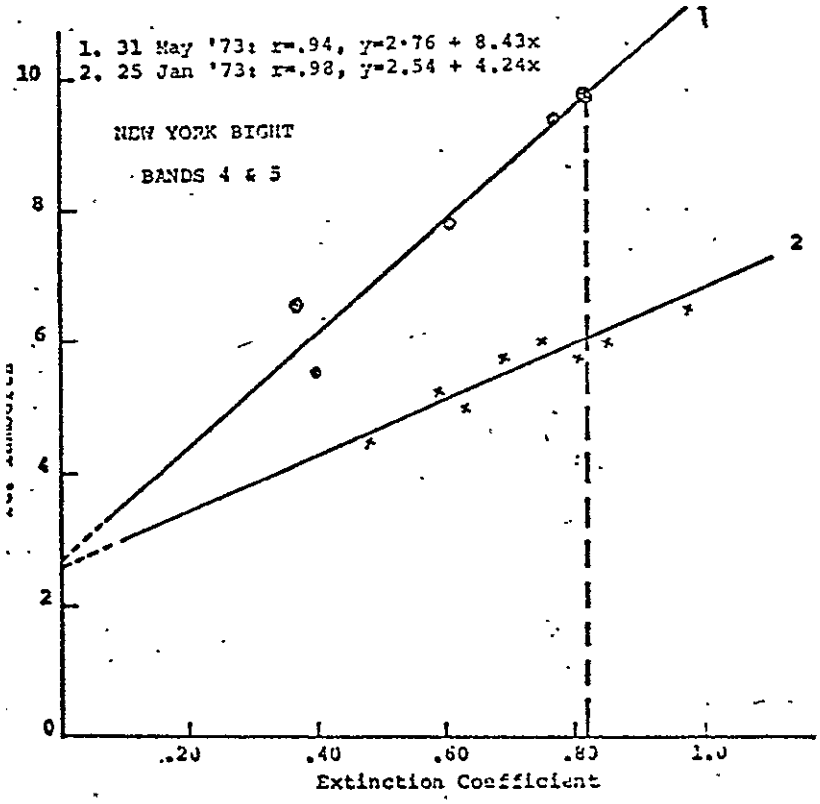

Figure 20. 25 January and 31 May 1973 - New York Bight. Screen brightness of bands 4 and 5 versus extinction coefficient measured by ship sampling.

By using the density slice attached to the additive color viewer, a visual display of the relative extinction coefficient was made. This technique is used for the analysis of all ERTS data of New York Bight and Block Island Sound. Figure 21, on the following page, is a black-and-white reproduction of the screen image and Figure 22 , the thematic chart made for the image.

Figure 21. Electronic density analysis of extinction coefficient: ERTS-1 bands 4 and 5, 31 May 1973-New York Bight.

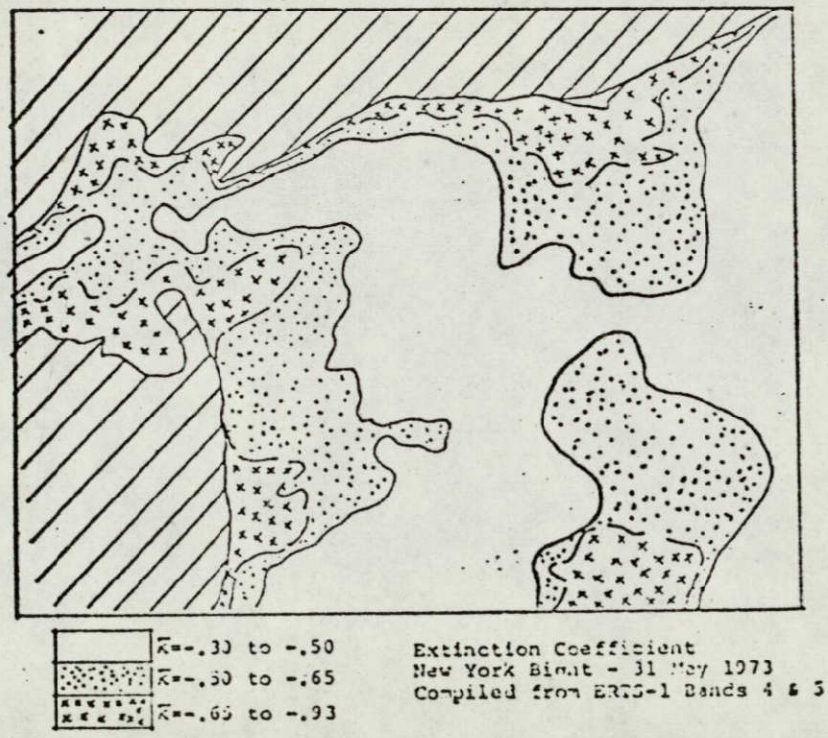

Figure 22. Thematic chart of extinction coefficient made from ERTS-1 bands 4 and 5 of New York Bight, 31 May 1973.

Total Cell Counts and Chlorophyll A

An analysis of ERTS-1 imagery and ship sampling shows that only gross approximations of total cell counts and chlorophyll a are possible in New York Bight waters. Figure 23 below shows the typical relationship of image brightness and chlorophyll a.

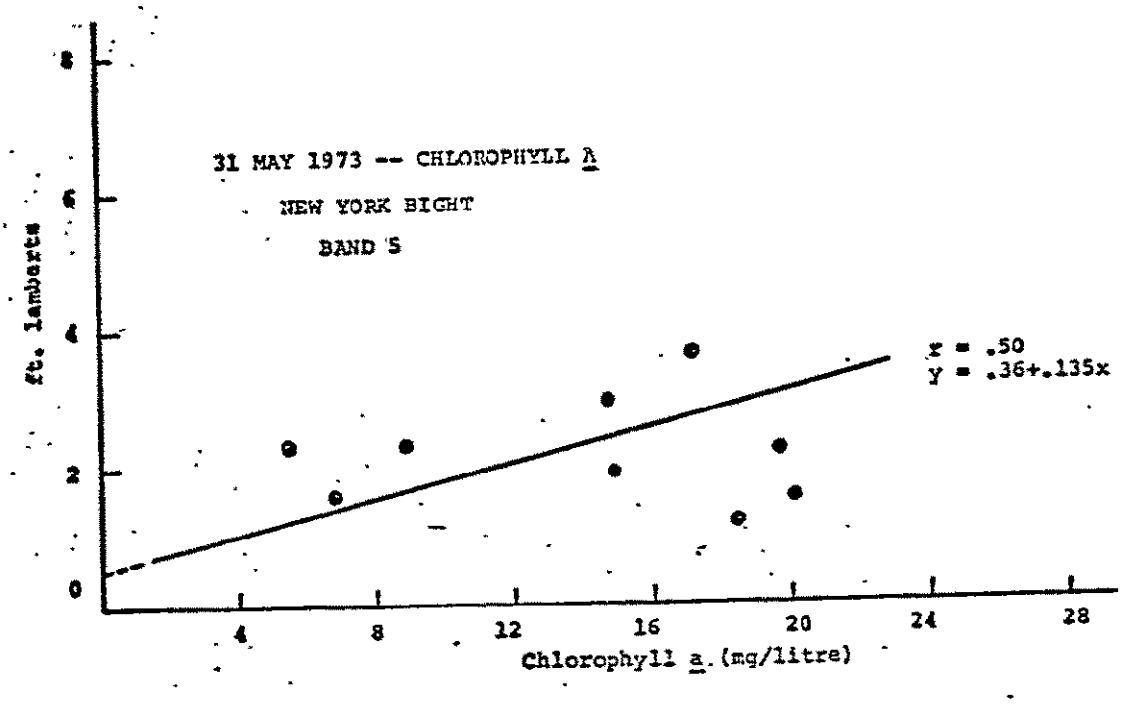

Figure 23. 31 May 1973 - New York Bight. ERTS-1 band 5 image brightness versus chlorophyll a.

Photographic Analysis of ERTS Data for Block Island Sound

Four candidate frames from the ERTS imagery over the Block Island Sound area were selected for multispectral photo analysis. All four spectral bands of MSS data were employed for both quantitative and visual additive color analysis. The image analysis procedures and the techniques

used have been described in the previous sections. The image identification numbers for the five frames are as follows:

8 October 1972 ..... E-1077-15011

19 March 1973 ..... E-1239-15021

24 April 1973 ..... E-1275-15021

17 June 1973 ..... E-1329-15014

Additive color presentations in this section show only the part of the ERTS MSS frame which covers the study area.

Interpolated Parameters

Surface values of density, chlorophyll a, total particle count, and extinction coefficients were interpolated to coincide with the time of the ERTS overpasses on 8 October 1972 and on 19 March, 24 April, and 17 June 1973. The phases of the tidal cycle at the time of the overpass were used to find the corresponding interpolated times from data obtained from cruises closest in time to the overpass. This is possible since the data acquired on each transect generally cover a tidal excursion during each season of the year. The results of such interpolations are presented in Table 7. In the case of the extinction coefficients, $\bar{k}$, the ratio of particle counts to extinction coefficients for the preceding cruises was employed to calculate the values found in Table 7.

Radiometric Measurements

Attempts were made to measure the upwelling radiance of the water in the visible portion of the spectrum. Two spectroradiometers were used - one for the incident sunlight and the other for upwelling radiance of the water. The measurements obtained could not be utilized for a scientific

Date	Station	Chlorophyll a (mg/m^3)	Density (σ_t)	Particle Count (1/liter)	$-\bar{k}$ (1/m)
8 Oct. 1972	H1	2.85	22.94	-	-
	H2	1.46	22.48	-	-
	H3	2.28	22.53	-	-
	H4	3.00	22.89	-	-
19 March 1973	BR1	1.00	24.65	140×10^5	.22
	BR2	2.20	24.92	155×10^5	.38
	BR3	2.79	24.99	270×10^5	.49
24 April 1973	HB1	.75	22.55	177×10^6	.40
	HB2	1.14	22.82	219×10^6	.44
	HB3	.75	22.90	164×10^6	.23
	HB4	.51	22.85	163×10^6	.22
	HB5	1.10	22.40	163×10^6	.53
	BR1	2.30	23.90	175×10^6	.39
	BR2	.80	24.29	111×10^6	.22
	BR3	.84	24.01	240×10^6	.34
17 June 1973	HB1	3.11	21.46	175×10^6	.34
	HB2	4.08	22.09	240×10^6	.71
	HB3	3.58	22.11	285×10^6	.34
	HB4	2.15	22.90	200×10^6	.37
	HB5	2.00	23.20	175×10^6	.44
	BR1	2.26	22.60	197×10^6	.24
	BR2	2.05	22.53	238×10^6	.30
	BR3	1.98	22.52	250×10^6	.43

Table 7. Interpolated values for chlorophyll a, density, particle count, and extinction coefficient to coincide with ERTS overflights.

analysis due to the inaccuracy and large variations in the data. These inconsistencies in the data were caused by the vibrations in the measuring instruments due to the rocking of the research vessel even on a fairly calm sea surface.

However, the downwelling irradiance of the total visible spectrum, together with spectral bands in the red, blue, and green regions, were measured during the cruises using an upward-facing irradiance meter. On most cruises, irradiance measurements were taken as near to noon as possible at each sampling station. No measurements were attempted under overcast skies. Extinction coefficients, k, were calculated from these data. The magnitude of the coefficients is related to the amount of suspended particles and dissolved materials in the water column and is, in effect, a measure of the turbidity of the water. Values for the extinction coefficients over a wavelength band comprising the visible spectrum are presented in Table 8 for each station in Block Island Sound.

As can readily be seen in this table, particularly from the averages for each station, the highest extinction values and, consequently, the waters with the greatest turbidity are those stations by Montauk Point (H1 and HB1), Block Island (HB5 and BR1), and Rhode Island (H4 and BR3). These areas with high extinction coefficients coincide with areas of high turbidity, particularly around Montauk Point and Point Judith, as determined from additive color analysis of ERTS imagery which is discussed in the subsequent paragraphs. The clearest waters are generally found near the center of each transect.

Additive Color Analysis

NASA-supplied negatives for the four selected MSS frames were reprocessed to generate a set of positives which would enhance any detail in the water. This set of positives was used to produce the additive color composites shown in Figures 24, 26, and 28.

a) H Transect

Date	Cruise	Station H1	H2	H3	H4
20 Mar. 73	K7310	0.42*	0.35	0.29	0.24
24 Apr. 73	K7318	0.35*	0.25	0.21	0.27
	Averages:	0.38	0.30	0.25	0.26

*Extrapolated

b) HB Transect

Date	Cruise	HB1	HB2	Station HB3	HB4	HB5
29 Aug. 72	K7218	0.39	0.29	0.31	0.29	0.34
24 Apr. 73	K7318	0.36	0.30	0.23	0.19	0.44
25 Apr. 73	K7319	0.35	0.31	0.37	0.36	0.27
19 June 73	K7336	0.33	0.39	0.34	0.31	0.44
	Averages:	0.36	0.32	0.31	0.29	0.37

c) BR Transect

Date	Cruise	Station BR1	BR2	BR3	
5 Sep. 72	K7219	0.35	0.37	0.50	
16 Nov. 72	K7232	0.40	0.42	0.52	
19 Mar. 73	K7310	0.32	0.42	0.59	
20 Mar. 73	K7311	0.54	0.38	0.46	
24 Apr. 73	K7318	0.32	0.28	0.31	
18 June 73	K7335	0.31	0.28	0.37	
	Averages:	0.37	0.35	0.46	

Table 8. Average extinction coefficients ($-\overline{k}$) in Block Island Sound.

Most of the photographic information concerning the water mass is contained in bands 4 (500-600 nm) and 5 (600-700 nm). Since water is highly absorbent in the infra-red region, there is little useful information in bands 6 (700-800 nm) and 7 (800-1100). These bands (6 and 7) are useful in clearly differentiating land mass from water mass, however. In both additive color synthesis and density analysis techniques used here, band 7 was used for this purpose.

A Spatial Data Model 703 density slicer was used for the density analysis. A Spectral Data Model 64 additive color viewer was used for both the additive color images and to project the black-and-white images, in register, for density analysis. In the additive color techniques, several false color modes were examined, and the one that best brought out water detail was reproduced by photographing the screen.

Figure 24 shows an additive color composite of MSS bands 4, 5, and 7 of ERTS Frame E-1077-15011, acquired on 8 October 1972 over the Block Island Sound area. The spectral bands were projected as follows:

Band 4 (500 - 600 nm) as Red
Band 5 (600 - 700 nm) as Green
Band 7 (800 -1100 nm) as Blue

The land areas covered with vegetation in this rendition appear as blue since the infra-red band was projected as blue. Urban areas are shown as light yellow in color due to the loss of infra-red reflection and their higher reflectance in the visible bands relative to the water areas. The extent of turbidity in the water area is represented mainly by three colors - yellow, orange-red, and black. The areas with greatest turbidity, related to the amount of suspended particles and dissolved materials in the water column, are those areas near Montauk Point and Rhode Island.

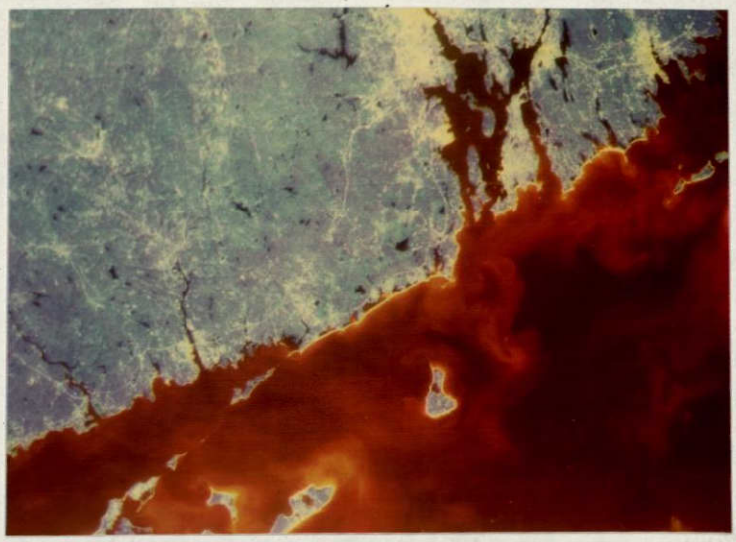

Figure 24. Additive color composite made from ERTS MSS bands 4, 5, and 7 of Frame E-1077-15011 taken on 8 October 1972.

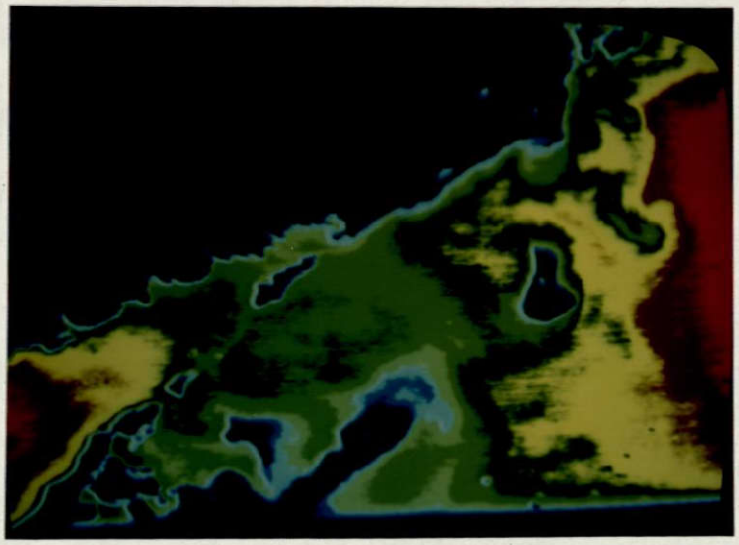

Figure 25. Electronic density analysis of ERTS Frame E-1077-15011.

These areas appear as yellow in color in the additive color presentation due to relatively higher reflectance in bands 4 and 5 of MSS data.

The water areas shown as orange-red in color are those areas with higher reflectance in MSS band 4 as compared to that of band 5. This difference in reflection by the water masses is dependent on the amount of material in suspension and their chemical and physical composition. As seen in Figure 24, large plumes near the outlet of the Connecticut River appear as an orange-red color. Such large plumes are developed during the mixing of ocean and estuarine waters and these plumes can be delineated by using multispectral techniques.

For density analysis, bands 4 and 5 were projected, in register, using white light. The brightness settings were left unchanged from the additive color mode. Band 7 was added, also in register, and the brightness was set to the point that all land masses were out of the brightness range being sliced. The land masses (and clouds) were therefore reproduced on the video screen in black. The controls of the density slicer were then set so that the brightest areas of the water mass (usually shallow coastal waters and areas of high turbidity) were reproduced on the video screen as dark blue. The less bright areas therefore are shown, in order of decreasing brightness, as light blue, light green, medium green, dark green, yellow, brown, and light red. In this way, areas of equal brightness are both differentiated from other brightnesses and classified in terms of their brightness wherever they occur in the scene.

Figure 25 is a color reproduction of the density slicer's screen image obtained by using the MSS data for 8 October 1972. Notice that all brightness differences are now represented as different colors. The water areas with the greatest amount of suspended material appear as light blue in color since these areas would have higher reflectance in comparison to other areas which are less turbulent. The water areas with less turbidity appear as yellow in color.

Similar analysis was performed for ERTS frames E-1239-15021 and E-1329-15014. Figure 26 is a color composite of MSS bands 4, 5, and 6 acquired over Block Island Sound on 19 March 1973. In this rendition, band 4 was projected as blue, band 5 as green, and band 6 as red. As shown in Figure 26, there are no apparent significant color differences in the water mass except for the area near Montauk Point where a large yellowish plume exists. This plume is associated with upwelling process, i.e., the advection of bottom materials and organisms into the surface layer. A density analysis of MSS bands for 19 March 1973 data was performed. The results are presented in Figure 27. The large plume near Montauk Point is shown as light green in color and can be completely delineated from other water masses. The other water areas which have less brightness appear as medium green, dark green, and yellow.

Figure 28 is an additive color presentation of ERTS frame E-1329-15014 (17 June 1973). In this multispectral rendition, band 4 was projected as blue, band 5 as green, and band 6 as red. The water areas are shown as yellowish-green in color and wherever the differences in water mass exist they are represented by a yellowish-red color. Notice that band 4 was projected as blue, but since the reflection in this

Figure 26. Additive color photograph of MSS bands 4, 5, and 6 for 19 March 1973.

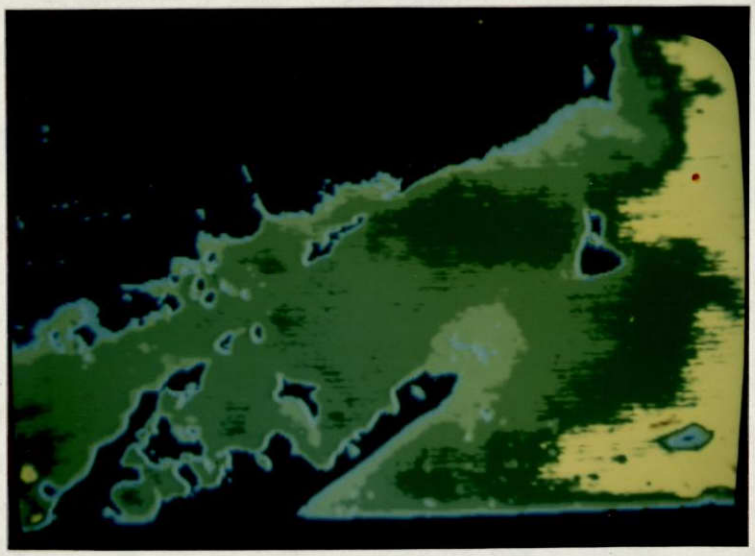

Figure 27. Reproduction of the density slicer's video screen by using MSS data for 19 March 1973.

particular band is not significant in differentiating the water mass, only bands 5 and 6 are useful in bringing out water detail.

Density analysis for 17 June 1973 data is shown in Figure 29. The mixing of Connecticut River water with the ocean water appears as yellow since this water mass would have lower reflectance than that of the water mass in Block Island Sound. The water mass which appears as medium-green in color has relatively more suspended material than that appearing as dark green. With the availability of appropriate oceanographic data, these color differences can be quantitatively correlated.

An examination of the two techniques, as illustrated by the preceding photographs of Block Island Sound, shows the superiority of the density analysis technique in differentiation and classification of water masses when the brightness differences are very subtle, as they are on the ERTS images for 17 June 1973 and 19 March 1973. When the brightness differences are greater, as they are on 8 October 1972, the color differences produced by the photographic process used in additive color synthesis yields information that cannot be obtained by density analysis alone. However, both techniques, used in conjunction, yield more information than can be obtained by one method alone. With the availability of appropriate ground truth data, these techniques can be used to provide semi-automatic thematic charts of critical oceanographic parameters. Charts of these basic water characteristics derived from satellite data should be incorporated in any ship sampling program to establish ship sampling stations, periodicity of sampling, and extend ship sampling data on a continuous basis.

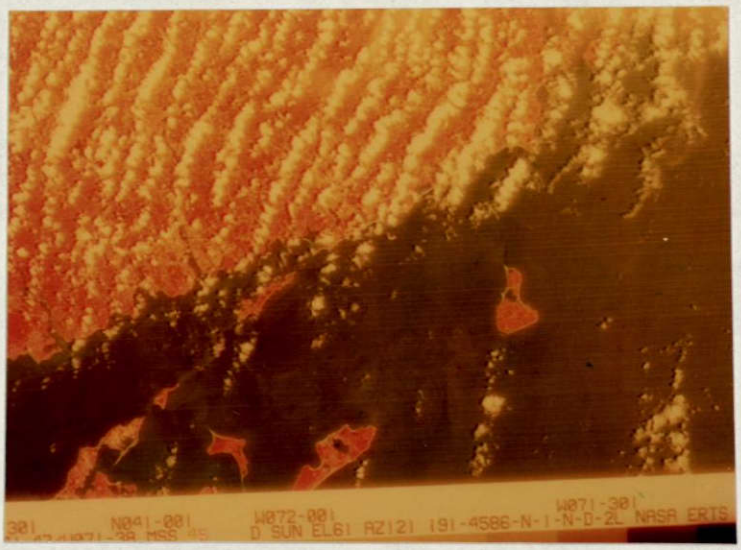

Figure 28. Multispectral rendition of MSS bands 4, 5, and 7 for ERTS data acquired over Block Island Sound on 17 June 1973.

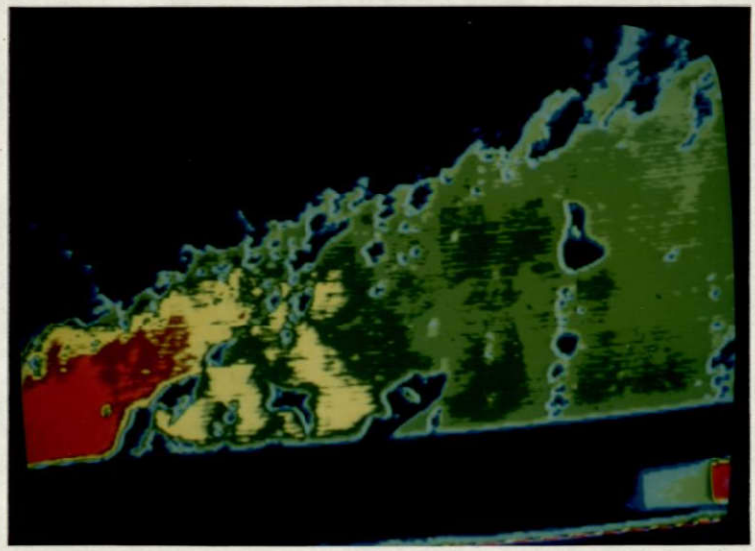

Figure 29. Electronic density analysis of MSS data obtained on 17 June 1973 over Block Island Sound.

Image Brightness Measurements

The ERTS frames E-1077-15011, E-1275-15021, and E-1329-15014 were employed for correlation with the oceanographic data collected under the water sampling program. These frames were acquired over Block Island Sound on 8 October 1972, 24 April 1973, and 17 June 1973 respectively. Values of surface parameters such as average extinction coefficient, total particles, and chlorophyll were interpolated to coincide with the time of the ERTS overpass. These values are presented in Table 8.

Positive images were made from the ERTS 8 October 1972, 24 April 1973, and 17 June 1973 negatives to bring out maximum water detail. These positives were placed in a Spectral Data Model 64 additive color viewer. The three black-and-white images for bands 4, 5, and 6 were optically registered on the screen. Only one of the infrared bands was used due to high absorption of energy in the water areas. Three brightness readings were made of the image at each sampling station using a Photo Science Spot Brightness Meter. The image brightness of MSS bands 4, 5, and 6 was thus obtained and a regression analysis performed with respect to: average extinction coefficient, total suspended particles, and chlorophyll a. Table 9 on the following page shows the image brightness at different sampling stations for the three MSS frames.

Extinction Coefficient

The relation of screen brightness in each band and extinction coefficients was plotted. These relationships are shown in Figures 30 and 31 for 24 April 1973 and 17 June 1973. These specific frames were selecte for linear regression due to the availability of more data points.

Station No.	North Latitude	West Longitude	8 October 1972 Image Brightness ft. Lamberts			24 April 1973 Image Brightness ft. Lamberts			17 June 1973 Image Brightness ft. Lamberts		
			4	5	6	4	5	6	4	5	6
H1	41°06.8'	71°51.5'	8.8	1.88	1.82	26.45	2.27	17.00			
H2	41°10.4'	71°51.5'	7.67	1.86	1.84	27.20	2.02	15.25			
H3	41°13.8'	71°51.5'	7.73	1.87	1.87	32.40	2.38	14.80			
H4	41°16.5'	71°51.5'	11.65	3.48	1.92	30.50	2.38	14.00			
HB1	41°04.8'	71°49.4'				27.40	2.61	13.80	10.30	47.4	56.0
HB2	41°05.8'	71°46.3'				26.40	2.57	13.00	10.17	46.5	52.0
HB3	41°06.7'	71°43.3'				26.00	2.37	12.35	9.69	42.0	55.5
HB4	41°07.5'	71°40.2'				28.30	2.25	12.54	9.47	42.0	63.0
HB5	41°08.4'	71°37.3'				31.00	3.40	20.90	9.15	40.7	55.0
BR1	41°15.7'	71°34.8'				25.40	2.45	14.00	10.04	46.2	52.0
BR2	41°18.0'	71°33.0'				27.00	2.60	14.50	11.64	58.0	70.0
BR3	41°20.8'	71°30.5'				30.00	2.60	15.00	13.40	61.0	110.0

Table 9

ERTS image brightness measurements for data acquired over Block Island Sound on 8 October 1972, 24 April 1973, and 17 June 1973.

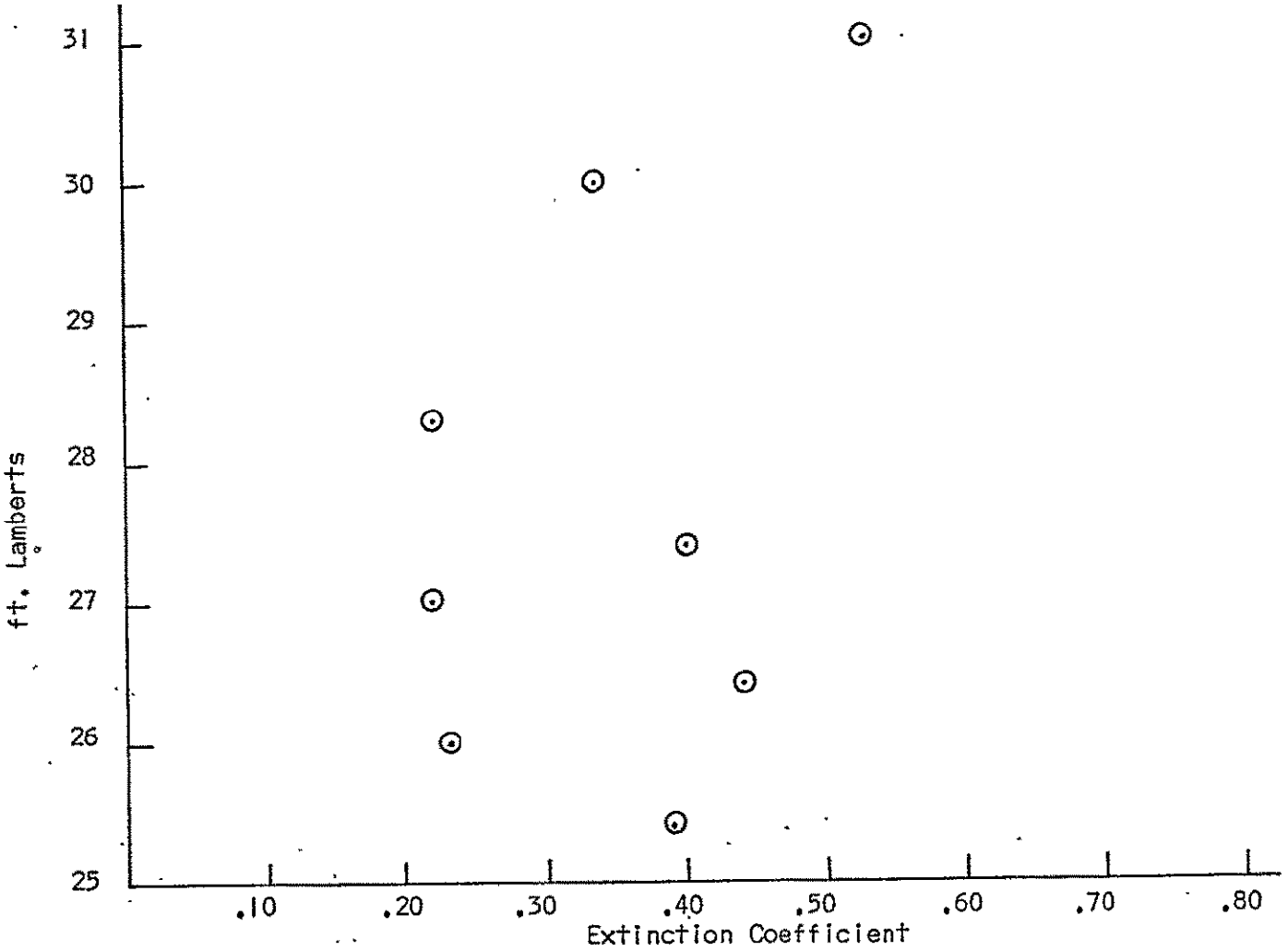

Figure 30. 24 April 1973 - Block Island Sound. ERTS MSS Band 4 image brightnes versus extinction coefficient.

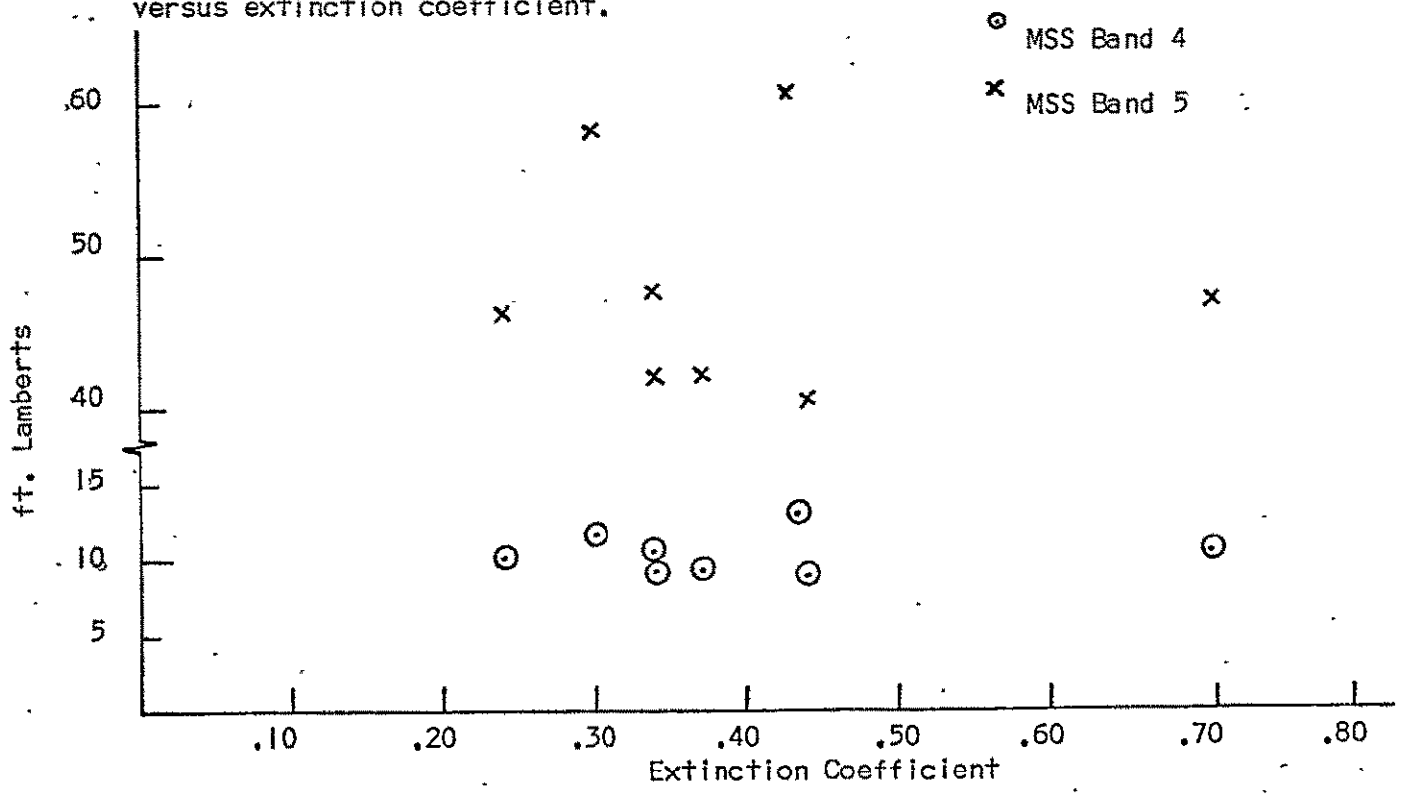

Figure 31. 17 June 1973 - Block Island Sound. Image brightness of bands 4 and 5 versus extinction coefficient measured by ship sampling.

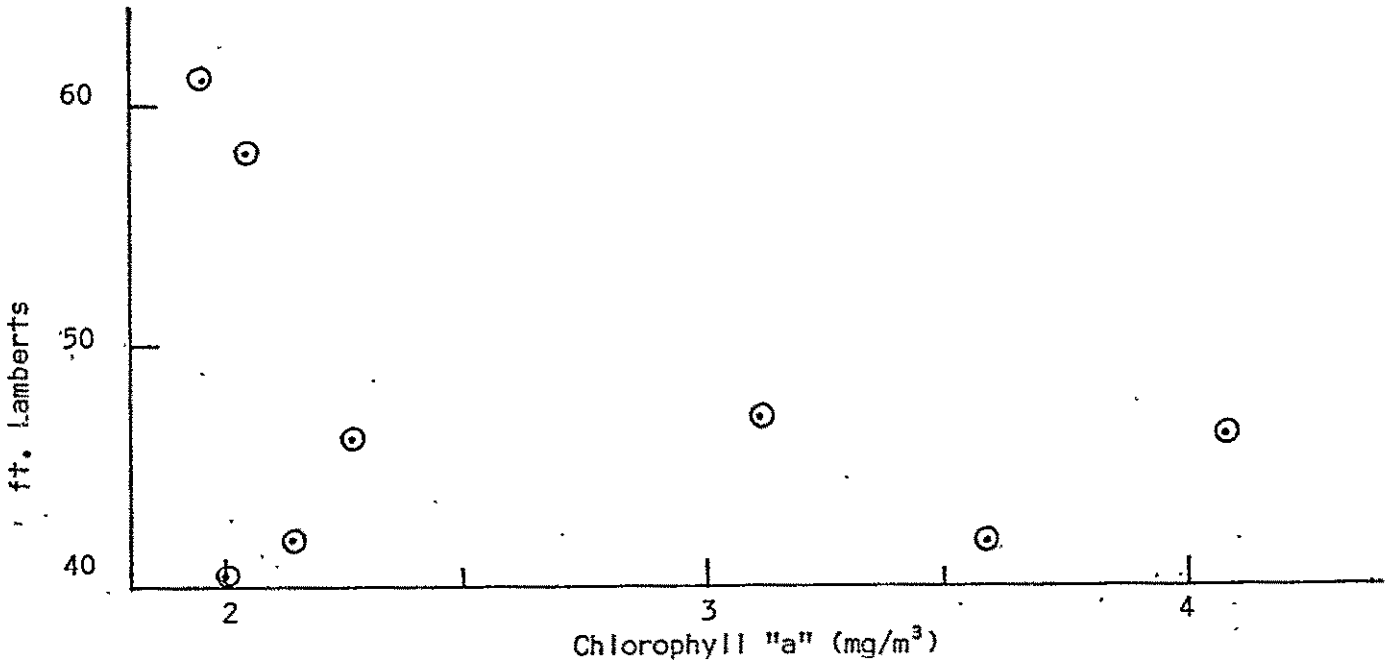

Figure 32. 17 June 1973 - Block Island Sound. ERTS MSS band 5 image brightness versus chlorophyll "a".

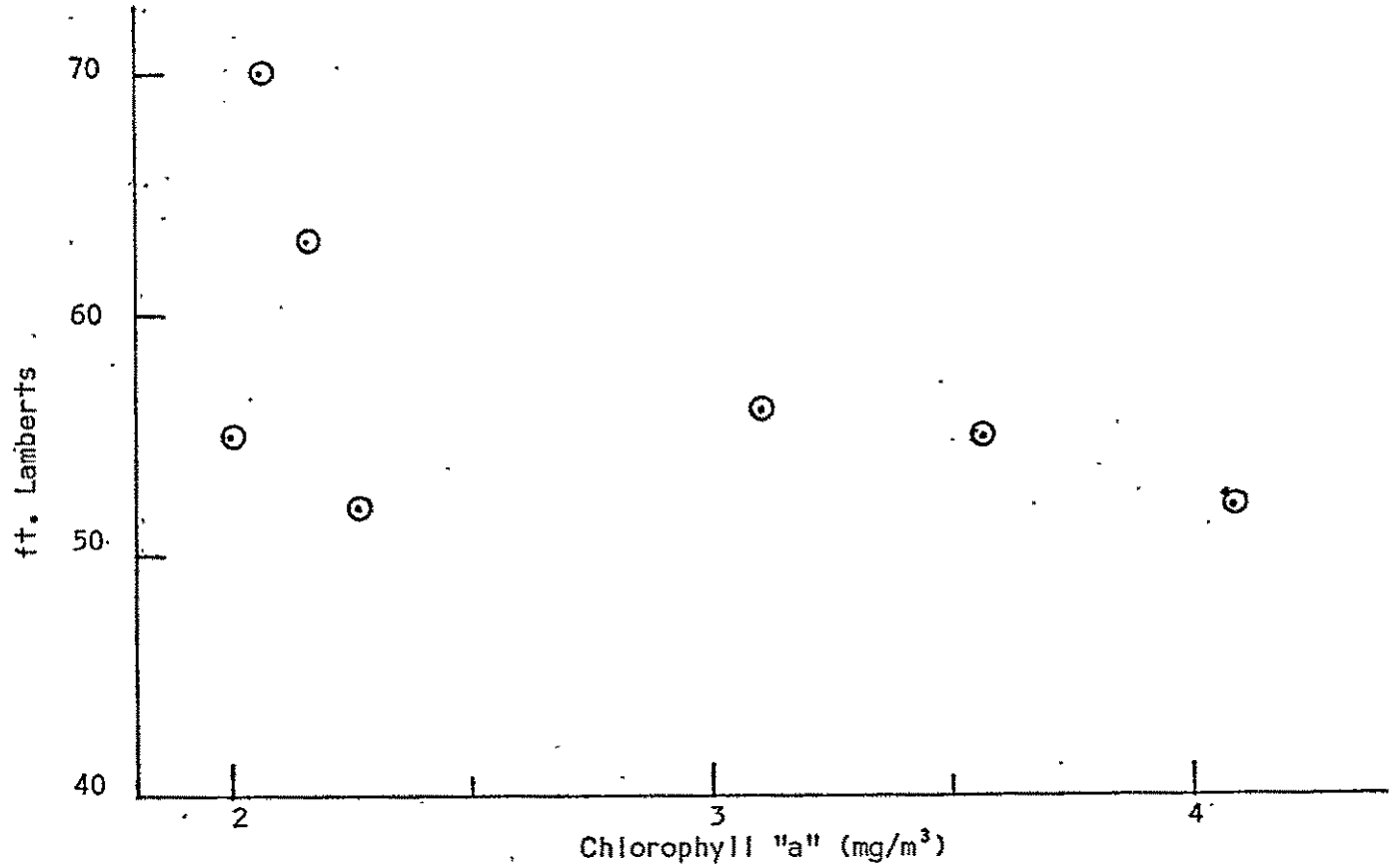

Figure 33. 17 June 1973 - Block Island Sound. Image brightness of band 6 versus chlorophyll "a".

Examination of the Figures 30 and 31 reveal little relationship between extinction coefficient and image brightness in contrast to the analysis discussed previously by using ERTS imagery over the New York Bight area where such a relationship exists. It is believed this is due to the fact that oceanographic data could not be acquired at the exact instance of ERTS overpass at a relatively large number of sampling stations. However, as shown in the preceding sub-sections, by using the density slicer attached to the additive color viewer, a visual display of the relative extinction coefficient in qualitative terms could be obtained.

Chlorophyll a

Analysis of ERTS imagery over the New York Bight area and ship sampling showed that only gross approximations of chlorophyll a are possible. For Block Island Sound, image brightness of ERTS data and chlorophyll a were plotted for linear relationship. Figures 32 and 33 reveal no relationship which could be measured in quantitative terms. Similar analysis was performed for total particle counts and total cell counts, but no correlation between these parameters and image brightness was found.

Section 5

Conclusions

As a result of this study, the following conclusions were made.

1. The fundamental problem in oceanography is sampling and, in particular, synoptic sampling analagous to the sampling programs in meteorology. It is, however, economically impossible to operate ships on an adequate scale to cover the needs of not only the oceans, but more importantly, the coastal zones and estuaries. Currently, the placing of buoys equipped with adequate transducers to provide the required information is also problematical from both an engineering and economic standpoint. ERTS MSS data, however, provides the synoptic over-view of an area that forms the basis for further monitoring.

2. In general, temperature and salinity are by themselves inadequate indicators of different water masses in combined coastal zones and estuaries. Other chemical and biological parameters are required to adequately delineate such water masses. Unfortunately, these analyses are costly. ERTS imagery has given the means to design such costly sampling programs - that is, from viewing such imagery as discussed before, it can be determined where to go, how to sample (with what frequency), and what to look for. In effect, the element of chance is removed from initial exploratory experiments.

3. The greatest value of the imagery has been in identifying and locating water masses in local waters from their color differences. Such identification would, in general, not be possible through conventional sampling techniques from aboard surface vessels.

4. ERTS multispectral scanner imagery of the New York coastal waters can be photographically reprocessed to show the presence of subtle spectral differences in the water when viewed using an additive color viewer. In Block Island Sound and Rhode Island Sound suspended materials, most probably organic in nature, were permanent in the 600-700 nm and 700-800 nm spectral bands.

5. Photographic reprocessing techniques have been developed which when applied to the ERTS multispectral imagery supplied to investigators yields greatly improved detectability of subtle water and land phenomena. These techniques have been related to the gray scale supplied with each of the four multispectral images in order to provide quantified data on the photographic transformations applied to the imagery.

6. In Block Island Sound, ERTS imagery has made it possible to delineate water masses from the Peconic Bay system, from Long Island Sound, and from Rhode Island Sound. The imagery has given visual proof of the existence of such phenomena that previously had only been suspected from water sample analysis. The degree, or intensity, of the color differences can also be shown to be of importance in detecting such occurrences as planktonic blooms, unusual run-off conditions from rivers and streams, and the indications of unusual beach erosion and sand transport processes. Some of the clouds of material noted in the imagery appear to be persistent; in particular, the cloud of material at Montauk Point, Long Island. It is suspected that this cloud may be associated with upwelling processes, i.e., the advection of bottom materials and organisms into the surface layer.

7. ERTS-1 photographic imagery can be photographically enhanced to give color signatures which correlate with water turbidity in sewage dump areas, such as the New York Bight. Bands 4, 5, and 6, when reprocessed and viewed in additive color, provide color signatures of water turbidity. By projecting band 4 as red, band 5 as green, and band 6 as blue, a distinct reddish-yellow color signature which correlates with suspended materials in coastal waters is observed.

8. Color signatures can be utilized to chart the position of sewage dump areas as a function of time using time-sequential multispectral analysis. Thus, the dissipation of such effluent can be charted and monitored in relation to tidal currents and the effects of weather.

9. Predictions of the absolute value of the number of total particles contained in New York Bight can be made using ERTS-1 bands 5 and 6 which have been carefully reprocessed to bring out maximum water detail. Predictions of the relative extinction coefficient of New York Bight waters can be made using ERTS-1 bands 4 and 5. Atmospheric effects in band 4 apparently cause variability in image characteristics which prevent absolute measurements from being attained. Display of these bands in an additive color viewer provides the scientist with a color composite in which variations in color are related to total particles or extinction coefficients. An electronic density slicer can be used with an additive color viewer to provide semi-automatic thematic charts of total particles or extinction coefficient. Charts of these basic water characteristics derived from ERTS-1 should be incorporated in any ship sampling program to establish ship sampling stations, periodicity of sampling, and extend ship sampling data on a continuous basis.

10. In New York Bight, two prominent features dominate the ERTS MSS data - the effluent from the Hudson River and the sludge dumping dispersion patterns. The discharge pattern of Hudson River water agrees with ground truth data shown on the maps. Here, too, the concepts of the flow and mixing patterns in the Bight are being revised in light of these ERTS images.

11. The dumping of treated sewage material in the New York Bight is a source of controversy as to the extent of its impact upon the biota. The discharge of this material is clearly outlined in the imagery, and since an urgent need exists to monitor total, as well as instantaneous dispersion of such material, the imagery affords a most convenient and unique method of monitoring such dispersion.

12. Conceptual models of Block Island Sound and Long Island Sound were simplified idealizations. Anomalous findings in physical and chemical parameters were generally classified as "noise". However, the ERTS imagery has shown that there are areas where color differences are persistent, in particular, off Montauk Point on Long Island and the shores of Rhode Island. These areas are where more concentrated investigations of physical, chemical, and biological processes should be conducted. Such studies will provide the needed input to environmental models both mathematical and hydraulic whose framework will now involve a more realistic, albeit more complex conceptual model.

13. The clouds of material seen in most of the ERTS imagery acquired over Block Island Sound can be attributed to: (a) plankton blooms (organics), (b) suspended particles, (c) nutrients that are related to plankton populations,

and (d) inorganic materials - erosion from stream beds transported to the sea by rivers and transported material in the form of dust that has settled out from the atmosphere, particularly prevalent around the south shore of Long Island. If it can be proven that the ERTS MSS imagery is "seeing" phytoplankton and if an adequate relationship between particulate phosphate and pigment can be determined, then the nutrient load in the water can be "estimated" and hence the potential for eutrophication from ERTS imagery.

Section 6
New Technology

The research reported herein involves the additive color analysis of ERTS multispectral scanner data and the collection of chemical, biological, and physical data in Block Island Sound and adjacent New York waters.

The significant theories and the description of the techniques used to create the additive color displays has been given in Sections 2 and 4 of this report.

REFERENCES

Williams, Robert (1967): "The Physical Oceanography of Block Island Sound", a review report. New London, Connecticut.

Yost, Edward and S. Wenderoth (1969): "Ecological Applications of Multispectral Color Aerial Photography", Remote Sensing in Ecology, University of Georgia Press.

Hollman, Rudolph (1970): "The Physical Oceanography of the New York Bight" Water Pollution, Gordon and Breach, New York, pp. 3-12.

Yost, Edward and S. Wenderoth (1970): "Multispectral Remote Sensing of Coastal Waters", SERG TR-10, Long Island University, New York.

Yost, Edward and R. Kalia et al. (1972): "The Estuarine and Coastal Oceanography of Block Island Sound and Adjacent New York Coastal Waters", ERTS-1 Symposium Proceedings, Goddard Space Flight Center, Greenbelt, Maryland.

APPENDIX A

II PHYSICAL OCEANOGRAPHY

by

Rudolph Hollman
Research Scientist in Physical Oceanography
New York Ocean Science Laboratory
Montauk, New York

Stephen K. Gill
Technician in Physical Oceanography
New York Ocean Science Laboratory
Montauk, New York

II PHYSICAL OCEANOGRAPHY

Contents

INTRODUCTION

This section concerns itself with the physical properties of the water, in particular, its temperature, salinity, density, optical characteristics, and tidal currents.

The distribution of the physical properties of the waters of Block Island Sound has been reviewed by Williams (1964) and is the most comprehensive to date.

In the New York Bight area, the physical properties of the waters and their seasonal and diurnal variations have been reviewed by Hollman (1971).

METHODS

Temperature, salinity, and calculated density values were obtained at multidepths for most stations sampled in Block Island Sound. Only surface salinity samples were taken on the New York Bight cruises.

When stations were sampled more than once per cruise, averages of temperature, salinity, and density (δ_t) were calculated at standard depths of 0, 10, 20, 30, 35, and 40 meters. Flood and ebb averages of these parameters were also calculated over each cruise. Horizontal profiles (contours of t° C, S‰, and δ_t in depth versus distance) were made for each crossing of a transect.

The downwelling irradiance of the visible spectrum was measured at each station in Block Island Sound using an upward-facing irradiance meter (submarine photometer), comprising a photocell and cosine collector equipped with glass filters.

The extinction coefficient, $\bar{k}$, for these light values is defined by the equation:

$$I(z) = I(z=0) \exp - \bar{k}z \qquad (1)$$

where I(z=0) is the total visible light energy in a particular wavelength band that is

incident upon the naviface, I(z) is the remaining light energy at the depth z(m), and $\bar{k}$ is the total "extinction" coefficient for the particular wavelength band in units of m^{-1}.

On most cruises, irradiance measurements were taken as near to noon as possible at each station. Linear regression analyses were performed and correlation coefficients calculated for data sets using total particle counts and average extinction coefficients for each of the Block Island Sound and New York Bight stations.

Regression analysis and correlations were also calculated between monthly freshwater discharge into Long Island Sound and the monthly surface and bottom salinity values at the Block Island Sound stations. Dilution factors, D, defined by:

$$D = (\Delta S/\bar{S}) \times 100\% \qquad (2)$$

where ΔS is the annual range and $\bar{S}$ the mean salinity at a station, were also calculated.

RESULTS

Block Island Sound: Distribution of Temperature, Salinity, and Density

Fundamental to an understanding of the temperature and salinity fields is a picture of their annual variations, both in space and time. In other words, an instantaneous picture of the temperature or salinity field can be placed in a better perspective with a foreknowledge of the annual variations that can be expected. Such annual variations of temperature and salinity for the 12 stations in Block Island Sound are tabulated in Table II-1 through II-3 in the appendix to this section.

As readily seen in the tables, the warmest month in all cases is August, with temperatures of approximately 19° C, and the coldest month is February, with temperatures of approximately 2° C. These results agree with previous results obtained in Block Island Sound. These data are graphically displayed as a function of time in Figure II-1 through II-3 in the

same transect order as found in the tables. The lower portion of each figure shows the variation of both surface and bottom (where applicable) temperatures in °C over the year. The upper portion shows the variation of both surface and bottom (where applicable) salinity in parts per thousand (‰) over the same time period, together with the mean monthly values for the Total Stream Discharge (SD) into Long Island Sound in cubic feet per second (cfs) as provided by the U.S. Department of the Interior, Geological Survey, Water Resources Division in Hartford, Connecticut.

The temperature profiles show that the average surface waters are warmer than the bottom waters during the warm months and cooler than the bottom waters (inversion) during the coldest months of January and February. This is again typical of the temperature regime in Block Island Sound.

An examination of the salinity profiles shows that the bottom waters are consistently more saline than the surface waters. This is typical of estuaries. The figures also show that a good inverse correlation exists between the surface salinity and the total stream discharge at approximately a 1-month lag. The stream discharge is an important factor in the annual distribution of salinity in Block Island Sound.

Monthly values of the averaged surface temperatures, salinities, and corresponding densities (σ_t) for each station in Block Island Sound are plotted as a function of distance (station location) and shown in Figure II-4. The solid curves are the average surface salinity distributions across the transects for the various dates; the dashed line is the accompanying surface temperatures, and the broken dashed line the corresponding densities.

In general, the lowest salinities are found at Station H1 of the H transect and HB1 of the HB transect, both by Montauk Point (Figure I-1). On the H transect, the most saline waters are found by the Rhode Island shore at Station H4. The highest salinities on the HB transect are located at Station H5 by Block Island. There is no apparent preference for either high or low saline waters on either end or the center of the BR transect. High-low salinity values appear to alternate between the southern end (BR1), the middle (BR2), and the northern end (BR3).

There does not appear to be any significant temperature difference across the transects.

That is to say that, on the average, over a tidal cycle, the surface waters are nearly isothermal on each transect with little difference from one station to another. The inference to be drawn is that the average surface temperatures over a tidal cycle are a relatively poor indicator of water masses, whereas the corresponding salinity averages do show the existence of different water types.

The average surface density distribution over a tidal cycle is largely governed by the salinity distribution, since the temperatures are, for practical intents, isothermal.

Three water masses can be inferred from these figures, particularly along the H and HB transects: significantly fresher and lighter (less dense) waters along the Long Island shore at Montauk that originates in the Peconic Bay System, a water mass in the middle of these two transects that is largely Long Island Sound water, and a water mass to the north offshore of Rhode Island that is significantly more saline and denser that has its origin in Rhode Island Sound to the east. This water mass also occupies most of the BR transect between Block Island and Point Judith, Rhode Island (Figure I-1).

The monthly variations in temperature and salinity from one figure to another are images of the distributions shown in Figure II-1 to II-3. As indicated above, the average surface density, as represented by σ_t, is dependent upon the salinity field. However, the annual variation in density is largely dependent upon the annual temperature variation. The vertical density structure is most stable in summer, with warmer and therefore lighter water overlying cooler and denser waters. In winter, however, the density structure is nearly uniform from surface to bottom, and in some brief instances cooler and denser water may be found to overlie warmer and slightly lighter waters. This is an unstable situation that generally leads to convective overturning, producing a well mixed and homogeneous water mass.

Horizontal isopleths of average values taken over half-tidal cycles (flood/ebb) for representative summer and winter cruises along each transect are shown in Figure II-5 through II-7 as a function of depth and distance (station position). The apparent absence of any significant difference in the distribution of temperature, salinity and particularly σ_t between flood and ebb conditions either in summer or winter, along the H transect (Figure II-5),

the HB transect (Figure II-6), or the BR transect (Figure II-7), is most surprising. A change of 180° in the flow of these waters between tidal currents was expected to produce at least a measurable change in the slopes of the 150 isopycnal surfaces, from an upward slope from north to south during a flood tidal cycle to a downward slope during an ebb cycle. The slope for all three variables is persistently downward when going from north to south (from right to left in each figure) regardless of the stage of the tidal cycle or the time of the year.

The most striking changes occur in the temperature distributions between the summer months and the winter months. Vertical gradients are approximately 5° C for the entire water column during the summer and less than 1° C during the winter months.

It is apparent from these figures that the tidal flow alters the values of the various variables such as temperature and salinity through advective processes, but does not appreciably alter the slopes of the isotherms or the isohalines. This implies that the horizontal gradients of temperature and salinity are virtually unaffected by changes in the direction of the tidal flow.

Optical Properties

Values for the extinction coefficients defined by Equation 1 over a wavelength band comprising the visible spectrum (white light) are tabulated in Table II-4 in the appendix to this section for each station in Block Island Sound. The magnitude of the coefficients is related to the amount of suspended particles and dissolved materials in the water column and is, in effect, a measure of the turbidity of the water. As can readily be seen in the table, particularly from the averages from each station, the highest extinction values, and consequently the waters with the greatest turbidity, are those stations by Montauk Point (H1 and HB1), by Block Island (HB5 and BR1), and by Rhode Island (H4 and BR3). These areas with high extinction coefficients coincide with areas of high turbidity, particularly around Montauk Point and Point Judith, Rhode Island, as determined from visual inspections of ERTS-1 imagery. The clearest waters are generally found near the center of each transect (Station H2, H3, HB3, HB4, and BR2).

The depth to which 1% of the visible radiation energy incident at the naviface penetrates can be determined from Equation 1, using the average station values for $\bar{k}$ from Table II-4. This depth represents the compensation depth below which energy produced by photosynthesis is counterbalanced by that energy that is used up by respiration. Major photosynthetic activity, therefore, takes place above this level. For the H transect, these levels occur at 12.1m, 15.4m, 18.4m, and 17.7m for Station H1 through H4 respectively; for the HB transect, the levels are 12.8m, 14.4m, 14.8m, 15.9m, and 12.4m for Station HB1 through HB5; for the BR transect, the depths for the compensation level are 12.4m, 13.2m, and 10.0m for Station BR1 through BR3 respectively. The shallowest depth (10.0m) occurs at Station BR3 at Point Judith, Rhode Island, generally also the most turbid area in the ERTS imagery for Block Island Sound

Extinction coefficients in the blue, green, and red spectral bands for the Block Island Sound stations are tabulated in Table II-5 of the appendix. The blue band has a maximum transmission of 87% between approximately 300 nm and 550 nm; the green band transmits a maximum of 65% between 460 nm and 660 nm, and the red band transmits a maximum of 85% between 500 nm and 720 nm. As the averages for each station show, the maximum extinction is found in the red band, as would be expected, the minimum in the green, and a secondary maximum in the blue. These conditions are typical for mean coastal waters (see for example, Sverdrup, Johnson and Fleming, 1942, Fig. 20, pg. 85). Here again, the higher extinction values in all wavelengths are found at the stations closest to land, as was the case for the extinction coefficients for the visible spectrum.

Compensation depths using average spectral extinction coefficients from Table II-5 were calculated and tabulated in Table II-6 (appendix). The shallowest depth (6.8m) is in the red band for Station HB1 off Montauk Point. The greatest depth of 18.4m in the green band occurs at Station H3 and BR1.

In general, the clearest waters are found along the H transect. The average transmittance per meter along this transect is 74.3%/m for the visible spectrum band, and 72.8%/m for the blue, 77.1%/m for the green, and 62.7%/m for the red band. The most turbid water over the visible spectrum band in along the BR transect, with an average transmittance of 67.5%/m. In comparison, the average transmittance for the HB transect in visible bands

was 71.9%/m. Over the blue and green spectral band, the most turbid waters were along the HB transect, where the average transmittance values were 63.8%/m and 72.2%/m respectively. The lowest transmittance values in the red band were from the BR transect, with an average value of 54.7%/m.

Interpolated Parameters

Surface values of temperature, salinity, chlorophyll *a*, total particle count, and extinction coefficients were interpolated to coincide with the time of the satellite overpasses on 8 October 1972 and on 19 March, 24 April, and 17 June, 1973. The phases of the tidal cycle at the time of the overpass were used to find the corresponding interpolated times from data obtained from cruises closest in time to the overpass. This is possible since the data acquired on each transect generally covers a tidal excursion during each season of the year. We have, therefore, the variation of any parameter in space and time over a tidal cycle for each period of the year.

The results of such interpolations, or estimations, are tabulated in Table II-7 of the appendix. In the case of the extinction coefficients, $\bar{k}$, the ratio of particle counts to extinction coefficients for the preceding cruises was employed to calculate the values found in the table.

New York Bight: Distribution of Temperature and Salinity

Surface values of temperatures and salinity for the nine stations within the apex of the New York Bight (Figure I-2) are tabulated in Table II-8 in the appendix. As can be seen in the table, the most saline waters are found at the easternmost stations, i.e., B1 and B9. In winter, these two stations are also the warmest, and in summer (May) the coolest. The least saline waters are found to the west (B3), representing the combined waters of the Hudson and Raritan rivers that have mixed with the harbor waters and are exiting along the Sandy Hook side of the harbor entrance.

Optical Properties

Extinction coefficients (Equation 1) for the stations in the New York Bight are tabulated in Table II-9 in the appendix together with the compensation depth calculated from the individual station averages. The clearest (least turbid) waters are found the furthest offshore at Station B6. The value at B6 (0.47) is still almost a factor of 2 greater than the corresponding values at Station H3 (0.25) in Block Island Sound and is, in fact, comparable to the most turbid station, BR3, that had an average value of 0.46 (Table II-4). The most turbid waters are those off of Sandy Hook (B3).

The compensation depths for the stations in the Bight range from approximately 4m to 9m as compared to an approximate range of from 10m to 18m in Block Island Sound, almost a factor of 2 less.

The average spectral extinction coefficients for the stations in the Bight are tabulated in Table II-10 (appendix), with station averages for each color band and associated compensation depths. The band of maximum extinction is now in the blue band and the secondary maximum in the red, indicating more turbid waters. The band of least extinction is still in the green. A shift in the wavelength of maximum penetration from the blue-green band to the orange-red band is expected with an increase in turbidity (see, for example, Sverdrup et al 1941, pg. 84). The compensation depths for these average spectral values are approximately half of the corresponding values from Block Island Sound.

Summary

These results are summarized in Figure II-8 through II-10. Each figure shows the isopleths for surface temperature, salinity, -kr and total particle counts for 20 December 1972 and 25 January and 31 May 1973 respectively.

DISCUSSION

The annual temperature regime within Block Island Sound and the New York Bight is largely governed by solar radiation and correlates with the mean month temperatures in the atmosphere, lagged 1 month. For example, maximum air temperatures occur in July, minimum temperatures in January. For these waters, the maximum temperatures occur in August, the minimum in February. Vertical temperature gradients are largely governed by vertical mixing and diffusion between a surface layer composed of largely Harbor and Sound water and a bottom layer of coastal water.

The annual salinity regime is mainly regulated by the stream discharge entering Long Island Sound and New York Harbor. The two major sources of this stream discharge are the Connecticut River for the Sound and the Hudson River for the Harbor. There is also approximately a 1-month lag between maximum stream discharge and the corresponding salinity minimums (Figure II-1 through II-3).

Linear correlations at a 1-month lag and dilution factors, D, as defined by Equation 2, were calculated for Block Island Sound and are tabulated in Table II-11 in the appendix. The highest correlations occur at the center stations of the H and HB transects and the weakest correlation occurs at Station BR3 (55%). Weak correlations at depth (30m) imply a two-layered system, with a surface layer that is composed of less saline Long Island Sound waters and a bottom layer of saline coastal waters. Vertical mixing and diffusion is relatively weak in Block Island Sound, as indicated by these high correlations and dilution factors.

Average tidal flood and ebb currents for Block Island Sound are shown in Figure II-11. With velocities of greater than 1 knot along most transects, one would expect a shift in the slopes of the isopycnals with a change in the direction of the tidal flow (Figure II-5 to II-7). The only exceptions are the uppermost isopycnals between Station HB2 and HB3 (Figure II-6), where a slight change in slope can be noticed between the flood and ebb cycles. In general, the fact that the isopycnals slope upward from left to right implies a net flow of water in the ebb direction.

The average extinction coefficient for Block Island Sound in the visible spectral band was 0.335, as compared to a mean value for the New York Bight of 0.663, almost a factor of 2 greater. The mean value for the blue band is 0.400 in Block Island Sound and 1.048 in the New York Bight; for the red band, the value is 0.554 and 0.876 in the Sound and the Bight respectively. The disparity in these two wavelength bands dramatizes the shift of the peak of maximum transmissivity from shorter to higher wavelengths with increasing turbidity.

The average extinction coefficients for each transect in Block Island Sound were correlated with total particle counts as determined with a Coulter Counter (to be discussed in Section IV) and for particle counts greater than 5μ in equivalent diameter. The results are tabulated in Table II-12 in the appendix. Highest correlations occur with particles greater than 5μ but less than 10μ in size. Similar results obtain for the Bight stations, as can be seen in Table II-13 (appendix). These results reflect nonselective attenuation, particularly absorption, since the lower limit of the total particle count is approximately 0.7μ in equivalent size (see Section IV), so that selective or Raleigh scattering is not included in these calculations. The correlations would be significantly improved if the resolving power of the Coulter Counter could be increased; however, this is an engineering design problem that hopefully will be resolved in the future.

REFERENCES

Hollman, Rudolph. 1970. The physical oceanography of the New York Bight. In *Water Pollution*, A.A. Johnson, ed. Gordon and Breach, New York. pp 3-12.

Sverdrup, H.U., M.W. Johnson, and R.H. Fleming. 1942. *The Oceans: Their Physics, Chemistry, and General Biology*. Prentice Hall, Englewood Cliffs, N.J. 1061 pp.

Williams, Robert G. 1967. The Physical Oceanography of Block Island Sound, a review report. New London, Conn., U.S. Navy Underwater Sound Laboratory. 15 pp. (USL Technical Memorandum No. 2212-33-67)

TABLE II-1

Average monthly values of temperature and salinity in the H transect of Block Island Sound (1972-1973)

Station	Variate	Depth	August	October	November	December	February	March	April	June
H1	$\bar{T}$°C	Z=0	19.3	17.3	11.8	8.4	1.9	3.9	6.6	14.5
		Z=30m	-	-	-	-	-	-	-	-
	$\bar{S}$‰	Z=0	30.27	30.85	31.05	30.27	29.65	31.29	29.00	28.96
		Z=30m	-	-	-	-	-	-	-	-
H2	$\bar{T}$°C	Z=0	18.8	17.7	11.9	8.7	2.4	3.8	6.9	13.9
		Z=30m	16.9	17.7	12.0	9.2	-	3.8	5.8	11.0
	$\bar{S}$‰	Z=0	30.24	31.10	31.20	30.17	29.67	29.43	28.67	28.69
		Z=30m	30.90	31.12	31.36	30.89	-	29.80	31.20	31.20
H3	$\bar{T}$°C	Z=0	20.1	17.5	12.2	8.7	2.8	3.5	7.0	14.2
		Z=30m	15.7	17.5	12.4	10.1	-	3.5	5.5	10.5
	$\bar{S}$‰	Z=0	30.67	31.39	31.21	30.80	30.25	30.88	29.59	29.94
		Z=30m	31.46	31.59	31.74	31.58	-	31.12	31.60	31.00
H4	$\bar{T}$°C	Z=0	19.7	17.4	11.4	8.8	2.8	3.7	7.3	13.7
		Z=30m	15.9	17.4	11.6	9.0	-	3.6	5.3	11.5
	$\bar{S}$‰	Z=0	30.52	31.71	31.39	31.01	30.98	31.09	29.42	29.92
		Z=30m	31.70	31.81	31.93	31.36	-	31.28	31.96	31.30

TABLE II-2

Average monthly values of temperature and salinity in the HB transect of Block Island Sound (1972-1973)

Station	Variate	Depth	August	November	December	February	March	April	June
HB1	$\bar{T}$°C	Z=0	18.0	12.3	8.5	2.8	3.7	7.8	14.7
		Z=30m	-	-	-	-	-	-	-
	$\bar{S}$‰	Z=0	30.65	31.49	30.18	30.15	29.41	29.52	29.31
		Z=0	-	-	-	-	-	-	-
HB2	$\bar{T}$°C	Z=0	17.7	12.4	8.8	3.2	3.9	7.7	14.3
		Z=30m	-	-	-	-	-	-	-
	$\bar{S}$‰	Z=0	30.80	31.65	30.32	30.49	29.71	29.68	29.74
		Z=30m	-	-	-	-	-	-	-
HB3	$\bar{T}$°C	Z=0	18.0	12.5	9.0	3.2	3.6	7.9	14.6
		Z=30m	13.1	12.4	9.5	4.6	-	5.7	11.2
	$\bar{S}$‰	Z=0	30.80	32.05	31.09	30.70	29.84	29.33	29.69
		Z=30m	32.27	32.12	32.11	32.11	-	32.23	31.46
HB4	$\bar{T}$°C	Z=0	18.4	12.5	9.1	3.5	3.8	8.1	14.5
		Z=30m	-	-	-	-	-	-	-
	$\bar{S}$‰	Z=0	31.14	32.11	31.56	31.20	30.25	29.78	30.42
		Z=30m	-	-	-	-	-	-	-
HB5	$\bar{T}$°C	Z=0	18.1	12.3	9.2	3.8	3.6	8.5	13.9
		Z=30m	-	-	-	-	-	-	-
	$\bar{S}$‰	Z=0	31.35	32.12	31.81	31.58	30.51	29.95	30.77
		Z=30m	-	-	-	-	-	-	-

TABLE II-3

Average monthly values of temperature and salinity in the BR transect of Block Island Sound (1972-1973)

Station	Variate	Depth	September	November	December	March	April	June
BR1	$\bar{T}$°C	Z=0	18.8	10.7	8.6	3.5	7.4	14.0
		Z=30m	18.5	10.8	8.6	3.6	5.1	10.5
	$\bar{S}$‰	Z=0	31.41	31.91	31.55	31.14	30.68	30.13
		Z=30m	31.62	31.93	31.65	31.46	31.48	31.50
BR2	$\bar{T}$°C	Z=0	19.1	10.6	8.2	3.5	7.9	14.0
		Z=30m	17.4	11.3	8.6	3.4	5.1	9.3
	$\bar{S}$‰	Z=0	31.58	31.50	31.38	31.34	31.12	30.58
		Z=30m	31.79	31.91	31.56	31.70	32.24	31.83
BR3	$\bar{T}$°C	Z=0	19.2	9.8	6.1	3.4	7.8	14.2
		Z=30m	-	-	-	-	-	-
	$\bar{S}$‰	Z=0	31.56	31.23	30.30	31.40	30.61	30.64
		Z=30m	-	-	-	-	-	-

TABLE II-4

Average extinction coefficients ($\bar{k}$) in Block Island Sound

a) H Transect

Date	Cruise	Station			
		H1	H2	H3	
20 Mar 1973	K7310	0.42*	0.35	0.29	(
24 Apr 1973	K7318	0.35*	0.25	0.21	(
Averages		0.38	0.30	0.25	(

*Extrapolated

b) HB Transect

Date	Cruise	Station				
		HB1	HB2	HB3	HB4	HB5
29 Aug 1972	K7218	0.39	0.29	0.31	0.29	0.34
24 Apr 1973	K7318	0.36	0.30	0.23	0.19	0.44
25 Apr 1973	K7319	0.35	0.31	0.37	0.36	0.27
19 Jun 1973	K7336	0.33	0.39	0.34	0.31	0.44
Averages		0.36	0.32	0.31	0.29	0.37

c) BR Transect

Date	Cruise	Station		
		BR1	BR2	BR3
5 Sep 1972	K7219	0.35	0.37	0.50
16 Nov 1972	K7232	0.40	0.42	0.52
19 Mar 1973	K7310	0.32	0.42	0.59
20 Mar 1973	K7311	0.54	0.38	0.46
24 Apr 1973	K7318	0.32	0.23	0.31
18 Jun 1973	K7335	0.31	0.28	0.37
Averages		0.37	0.35	0.46

TABLE II-5

Average spectral extinction coefficients (-k[λ]) in Block Island Sound

a) H Transect

Cruise & Date	Color Band	Station			
		H1	H2	H3	H4
K7318 24 Apr 1973	Blue	-	0.35	0.27	0.33
	Green	-	0.27	0.25	0.26
	Red	-	0.42	0.45	0.53

b) HB Transect

Cruise & Date	Color Band	Station				
		HB1	HB2	HB3	HB4	HB5
K7319 25 Apr 1973	Blue	0.56	0.42	0.38	0.46	0.39
	Green	0.41	0.33	0.31	0.34	0.28
	Red	0.73	0.58	0.63	0.60	0.52
K7336 19 Jun 1973	Blue	0.60	0.46	0.34	0.31	0.57
	Green	0.29	0.27	0.30	0.23	0.42
	Red	0.64	0.51	0.48	0.48	0.59
Averages	Blue	0.58	0.44	0.36	0.39	0.48
	Green	0.35	0.30	0.31	0.32	0.35
	Red	0.68	0.54	0.56	0.54	0.56

c) BR Transect

Cruise & Date	Color Band	Station		
		BR1	BR2	BR3
K7232 16 Nov 1972	Blue	0.48	0.49	0.47
	Green	0.36	0.38	0.38
	Red	0.68	0.61	0.80
K7318 24 Apr 1973	Blue	0.35	0.39	0.31
	Green	0.19	0.16	0.25
	Red	0.38	0.67	0.51
K7335 18 Jun 1973	Blue	0.39	0.38	0.33
	Green	0.19	0.25	0.26
	Red	0.55	0.60	0.62
Averages	Blue	0.41	0.42	0.37
	Green	0.25	0.26	0.30
	Red	0.54	0.63	0.64

TABLE II-6

Compensation depths (depths at which 1% of the incident energy is found) in meters

a) H Transect

Wavelength Band	Station			
	H1	H2	H3	H4
Blue	-	13.2	17.0	14.0
Green	-	17.0	18.4	17.7
Red	-	11.0	10.2	8.7

b) HB Transect

Wavelength Band	Station				
	HB1	HB2	HB3	HB4	HB5
Blue	7.9	10.5	12.8	11.8	9.6
Green	13.2	15.4	14.8	14.4	13.2
Red	6.8	8.5	8.2	8.5	8.2

c) BR Transect

Wavelength Band	Station		
	BR1	BR2	BR3
Blue	11.2	11.0	12.4
Green	18.4	17.7	15.4
Red	8.5	7.3	7.2

TABLE II-7

Interpolated values for temperature, salinity, density, chlorophyll *a*, particle count, and extinction coefficient to coincide with ERTS-I overflights

a) 8 October 1972 Overflight: 1101 EDST

Interpolated Variate	Station			
	H1	H2	H3	H4
Temperature (°C)	16.9	17.6	17.4	17.4
Salinity (‰)	31.60	31.18	31.20	31.65
Density (σ_t)	22.94	22.48	22.53	22.89
Chlorophyll *a* (mg/m^3)	2.85	1.46	2.28	3.00
Particle Count (1/L)	-	-	-	-
$-\bar{k}$ (1/m)	-	-	-	-

b) 19 March 1973 Overflight: 1002 EST

Interpolated Variate	Station		
	BR1	BR2	BR3
Temperature (°C)	3.5	3.6	3.3
Salinity (‰)	30.96	31.31	31.37
Density (σ_t)	24.65	24.92	24.99
Chlorophyll *a* (mg/m^3)	1.00	2.20	2.79
Particle Count (1/L)	140×10^6	155×10^6	270×10^6
$-\bar{k}$ (1/m)	0.22	0.38	0.49

c) 24 April 1973 Overflight: 1002 EST

Interpolated Variate	Station				
	HB1	HB2	HB3	HB4	HB5
Temperature (°C)	7.8	7.8	8.2	8.2	8.2
Salinity (‰)	28.90	29.95	29.42	29.36	30.05
Density (σ_t)	22.55	22.82	22.90	22.85	23.40
Chlorophyll *a* (mg/m^3)	0.75	1.14	0.75	0.51	1.10
Particle Count (1/L)	177×10^6	219×10^6	164×10^6	163×10^6	163×10^6
$-\bar{k}$ (1/m)	0.40	0.44	0.23	0.22	0.53

TABLE II-7 (Continued)

c) continued

Interpolated Variate	Station		
	BR1	BR2	BR3
Temperature (°C)	7.4	7.9	7.7
Salinity (‰)	30.55	31.15	30.75
Density (σ_t)	23.90	24.29	24.01
Chlorophyll *a* (mg/m^3)	2.30	0.80	0.84
Particle Count (1/L)	175x10^6	111x10^6	240x10^6
$-\bar{k}$ (1/m)	0.39	0.22	0.34

d) 17 June 1973 Overflight: 1102 EST

Interpolated Variate	Station				
	HB1	HB2	HB3	HB4	HB5
Temperature (°C)	14.4	14.2	15.0	14.4	13.6
Salinity (‰)	28.92	29.71	29.95	30.82	31.00
Density (σ_t)	21.46	22.09	22.11	22.90	23.20
Chlorophyll *a* (mg/m^3)	3.11	4.08	3.58	2.15	2.00
Particle Count (1/L)	175x10^6	240x10^6	285x10^6	200x10^6	175x10^6
$-\bar{k}$ (1/m)	0.34	0.71	0.34	0.37	0.44

Interpolated Variate	Stati	
	BR1	BR
Temperature (°C)	14.0	13.
Salinity (‰)	30.32	30.
Density (σ_t)	22.60	22.
Chlorophyll *a* (mg/m^3)	2.26	2.
Particle Count (1/L)	197x10^6	238x
$-\bar{k}$ (1/m)	0.24	0.

(1/L = per liter)

TABLE II-8

Surface temperatures (°C) and salinities (‰) for Station 1 through 9 in the New York Bight

		Station								
Date & Cruise	Variate	B1	B2	B3	B4	B5	B6	B7	B8	B9
20 Dec 1972	Temperature	8.0	5.1	3.6	5.0	5.9	5.6	5.5	6.1	6.8
K7239	Salinity	31.74	23.41	18.11	23.75	27.50	26.84	27.32	29.18	31.25
25 Jan 1973	Temperature	7.0	5.3	4.3	4.9	5.4	5.8	5.6	6.3	7.0
K7302	Salinity	32.62	27.59	23.58	27.01	30.10	31.67	30.90	32.28	32.92
31 May 1973	Temperature	13.7	15.8	15.9	15.8	16.2	15.5	16.5	16.0	16.0
K7327	Salinity	29.23	23.05	19.64	23.43	24.10	23.44	23.91	26.58	29.08

TABLE II-9

Average extinction coefficients (-k) in the New York Bight

Date & Cruise	Station								
	B1	B2	B3	B4	B5	B6	B7	B8	B9
20 Dec 1972 K7239	1.30	0.96	1.20	0.63	0.53	0.51	0.43	0.51	0.77
25 Jan 1973 K7302	0.92	0.71	0.98	0.85	0.69	0.48	0.63	0.59	0.75
31 May 1973 K7327	0.14	0.67	0.93	0.44	0.30	0.43	0.50	0.54	0.52
Average	0.787	0.780	1.037	0.640	0.506	0.473	0.520	0.547	0.680
Compensation Depth (m)	5.85	5.90	4.44	7.200	9.101	9.74	8.86	8.42	6.77

TABLE II-10

Average spectral extinction coefficients ($-\bar{k}[\lambda]$) in the New York Bight

Date & Cruise	Color Band	Station								
		B1	B2	B3	B4	B5	B6	B7	B8	B9
25 Jan 1973 K7302	Blue	1.33	0.98	1.41	1.10	0.96	0.82	0.76	0.79	0.85
	Green	0.79	0.62	1.04	0.70	0.65	0.56	0.55	0.51	0.64
	Red	1.35	1.00	1.17	1.10	0.99	0.86	0.88	1.01	1.18
31 May 1973 K7327	Blue	0.38	1.20	1.78	1.21	0.77	1.17	1.29	1.21	0.86
	Green	0.17	0.78	1.33	0.36	0.28	0.72	0.66	0.60	0.54
	Red	0.34	0.91	0.57	0.74	0.46	0.92	0.66	0.88	0.75
Average	Blue	0.855	1.090	1.595	1.155	0.865	0.995	1.025	1.000	0.855
	Green	0.480	0.700	1.185	0.530	0.465	0.640	0.605	0.555	0.590
	Red	0.845	0.955	0.870	0.920	0.725	0.890	0.770	0.945	0.965
Compensation Depth (m)	Blue	5.4	4.2	2.9	4.0	5.3	4.6	4.5	4.6	5.4
	Green	9.6	6.6	3.9	8.7	9.9	7.2	7.6	8.3	7.8
	Red	5.4	4.8	5.3	5.0	6.4	5.2	6.0	4.9	4.8

TABLE II-11

Correlations between salinity and stream discharge into Long Island Sound between August 1972 and July 1973 at a 1-month lag, together with dilution factors, D(%)

Station	Depth	Correlation Coefficient	Dilution Factor D(%)
H1	Z=0m	-0.94	7.7
H2	Z=0m	-0.95	8.5
	Z=30m	-0.29	5.1
H3	Z=0m	-0.84	5.9
	Z=30m	-0.44	3.0
H4	Z=0m	-0.79	7.5
	Z=30m	-0.38	2.1
HB1	Z=0	-0.94	7.2
HB2	Z=0	-0.96	6.5
HB3	Z=0	-0.95	8.9
	Z=30m	-0.22	2.5
HB4	Z=0m	-0.91	7.5
HB5	Z=0m	-0.85	6.9
BR1	Z=0m	-0.73	5.7
	Z=30m	-0.80	1.4
BR2	Z=0m	-0.64	3.2
	Z=30m	-0.26	2.1
BR3	Z=0m	-0.55	4.1

TABLE II-12

Linear correlation coefficients between average extinction coefficients (visible band) and suspended particles in Block Island Sound

Transect	$-\bar{k}$ vs Total Particles	$-\bar{k}$ vs Particles >5μ
H	0.73	0.73
HB	0.58	0.79
BR	0.71	0.67

TABLE II-13

Linear correlation coefficients between average extinction coefficients (visible band) and suspended particles in the New York Bight

Cruise	Correlation	
	$-\bar{k}$ vs Total Particles	$-\bar{k}$ vs Particles >5μ
K7329	0.63	0.92
K7302	0.61	0.72
K7327	0.88	0.90

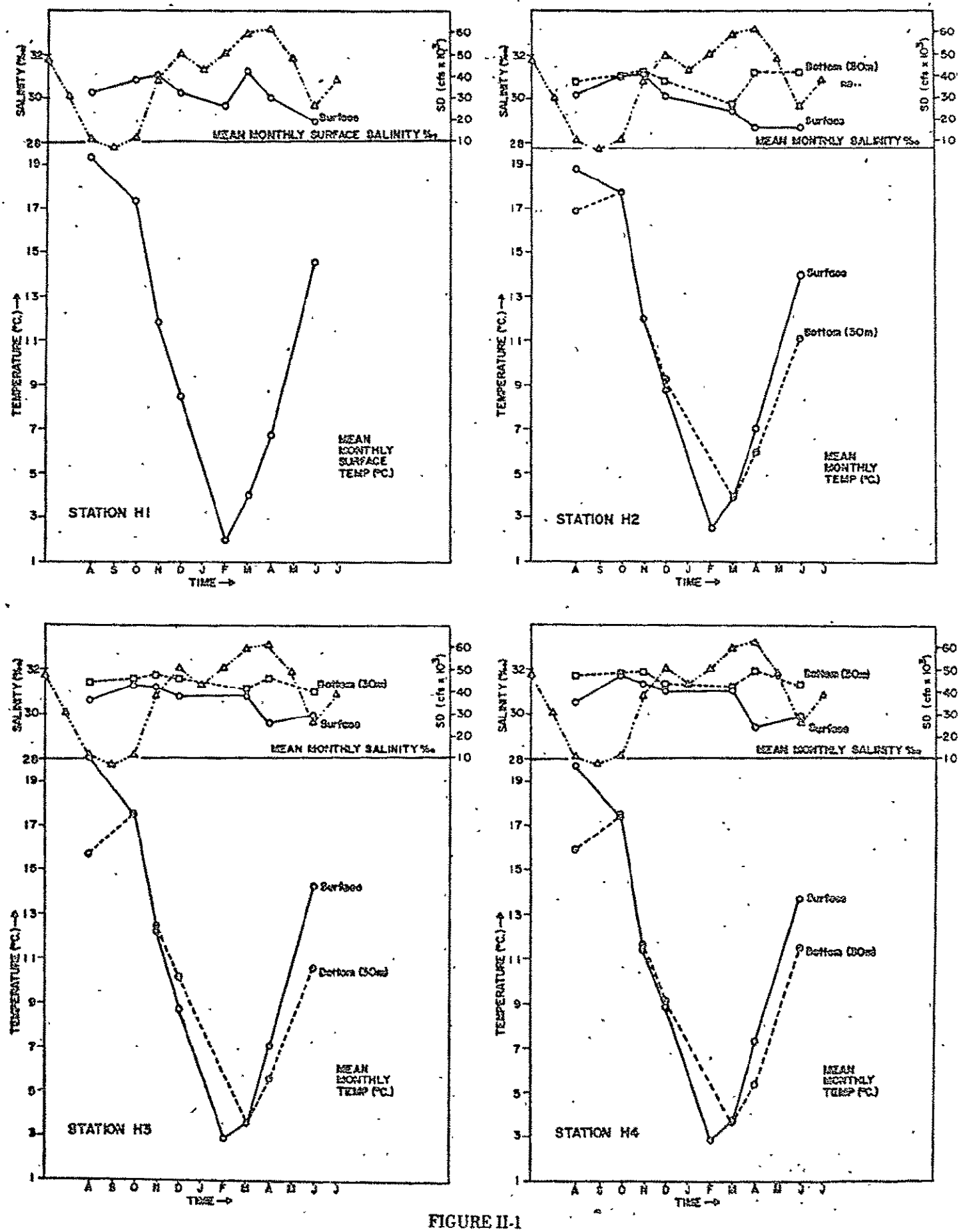

FIGURE II-1

Annual variation of mean monthly temperature, salinity, and stream discharge (SD) into Long Island Sound for the 4 stations in the H transect

ORIGINAL PAGE IS
OF POOR QUALITY

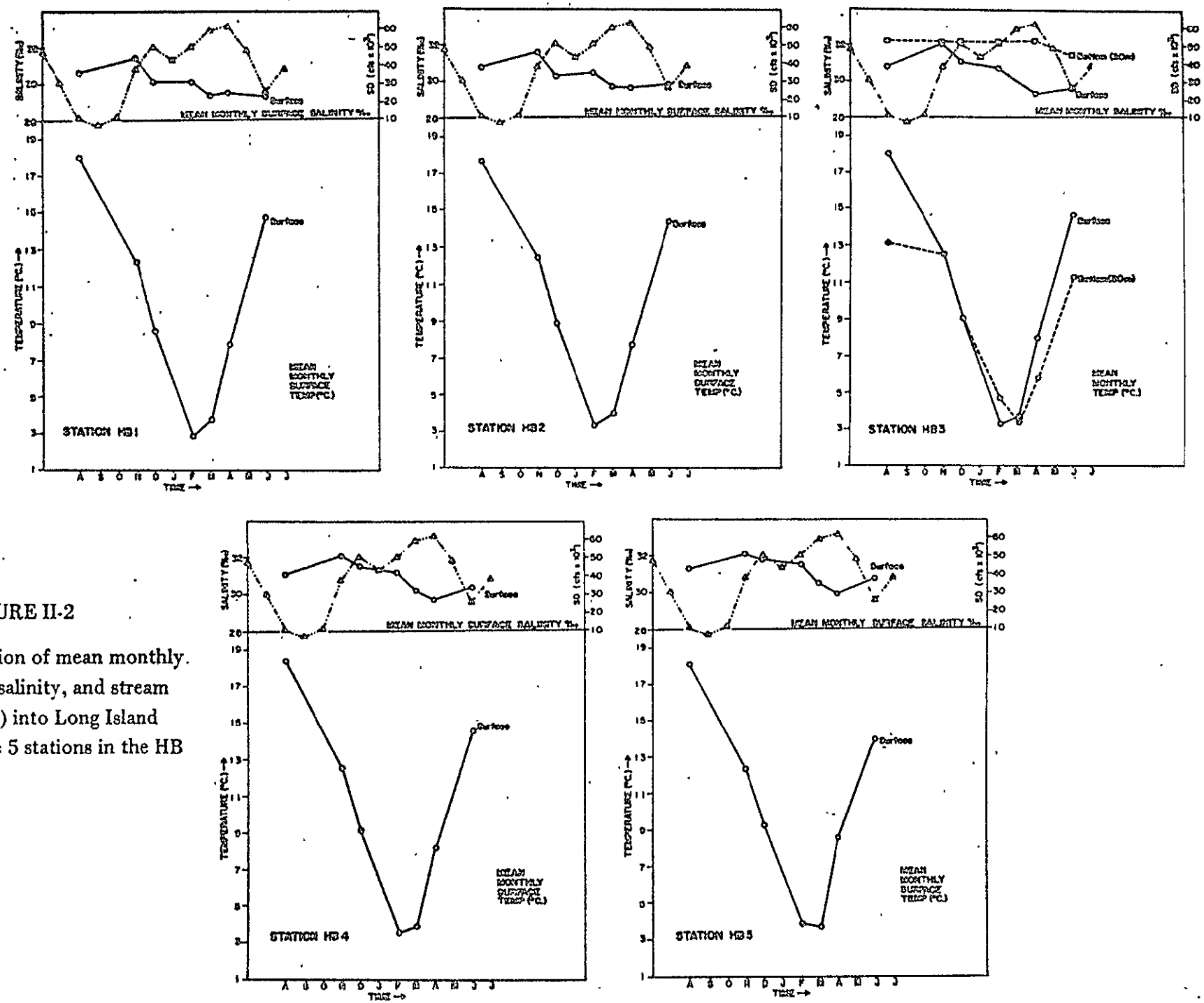

FIGURE II-2

Annual variation of mean monthly. temperature, salinity, and stream discharge (SD) into Long Island Sound for the 5 stations in the HB transect

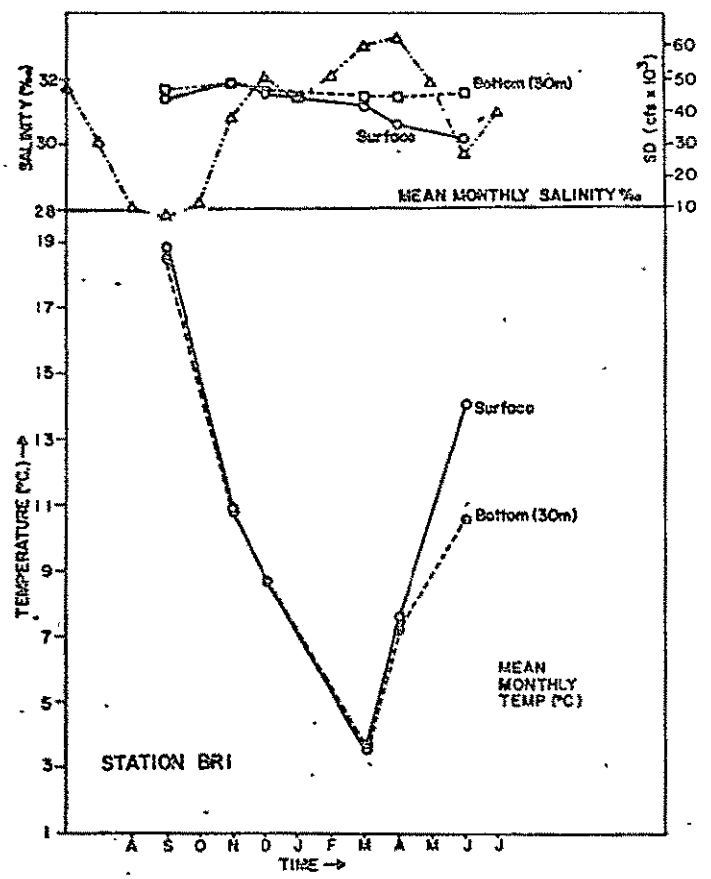

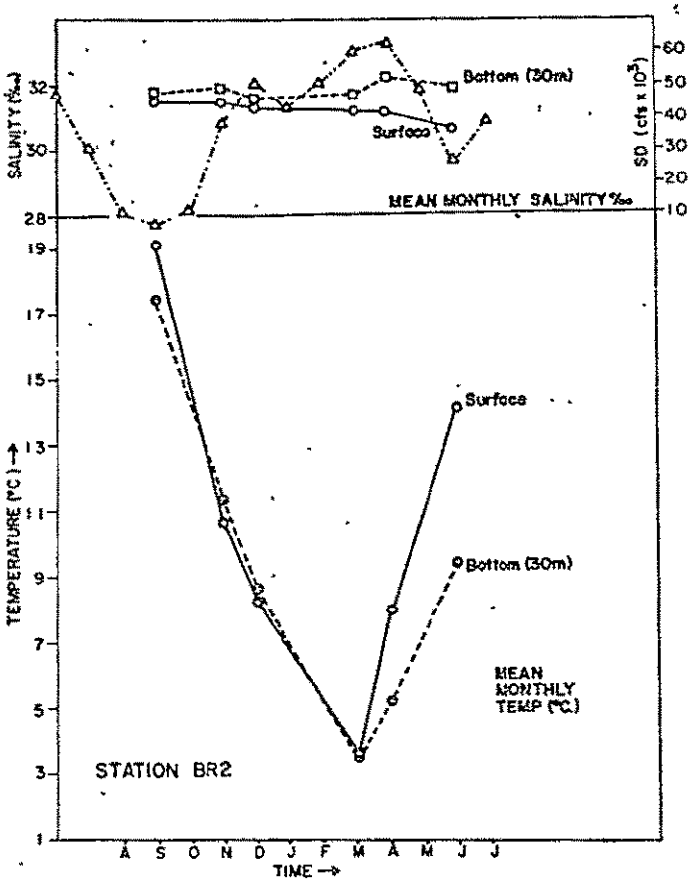

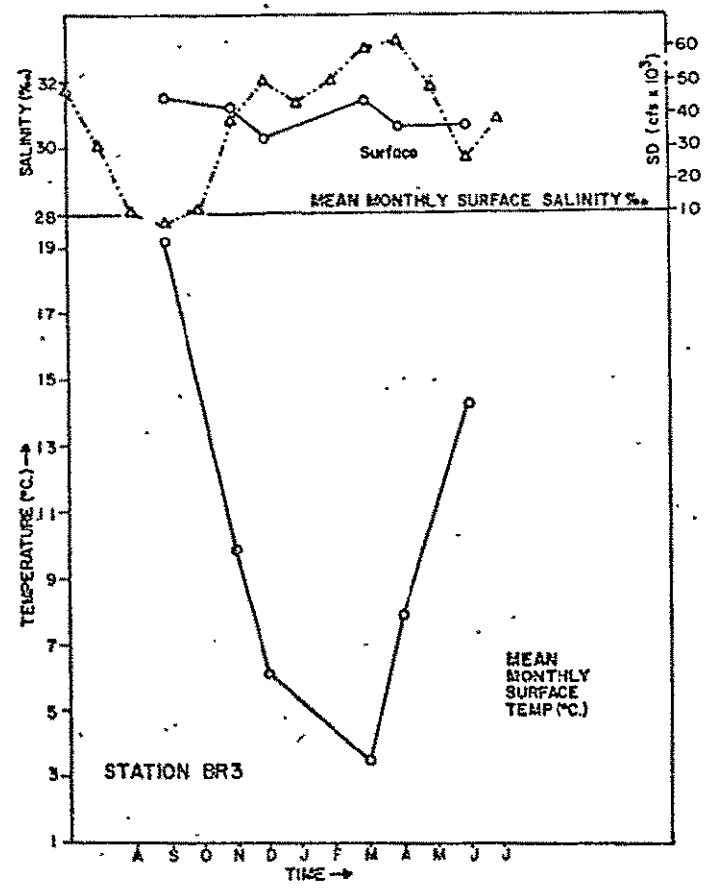

FIGURE II-3

Annual variation of mean monthly temperatur salinity, and stream discharge (SD) into Long Island Sound for the 3 stations on the BR transect

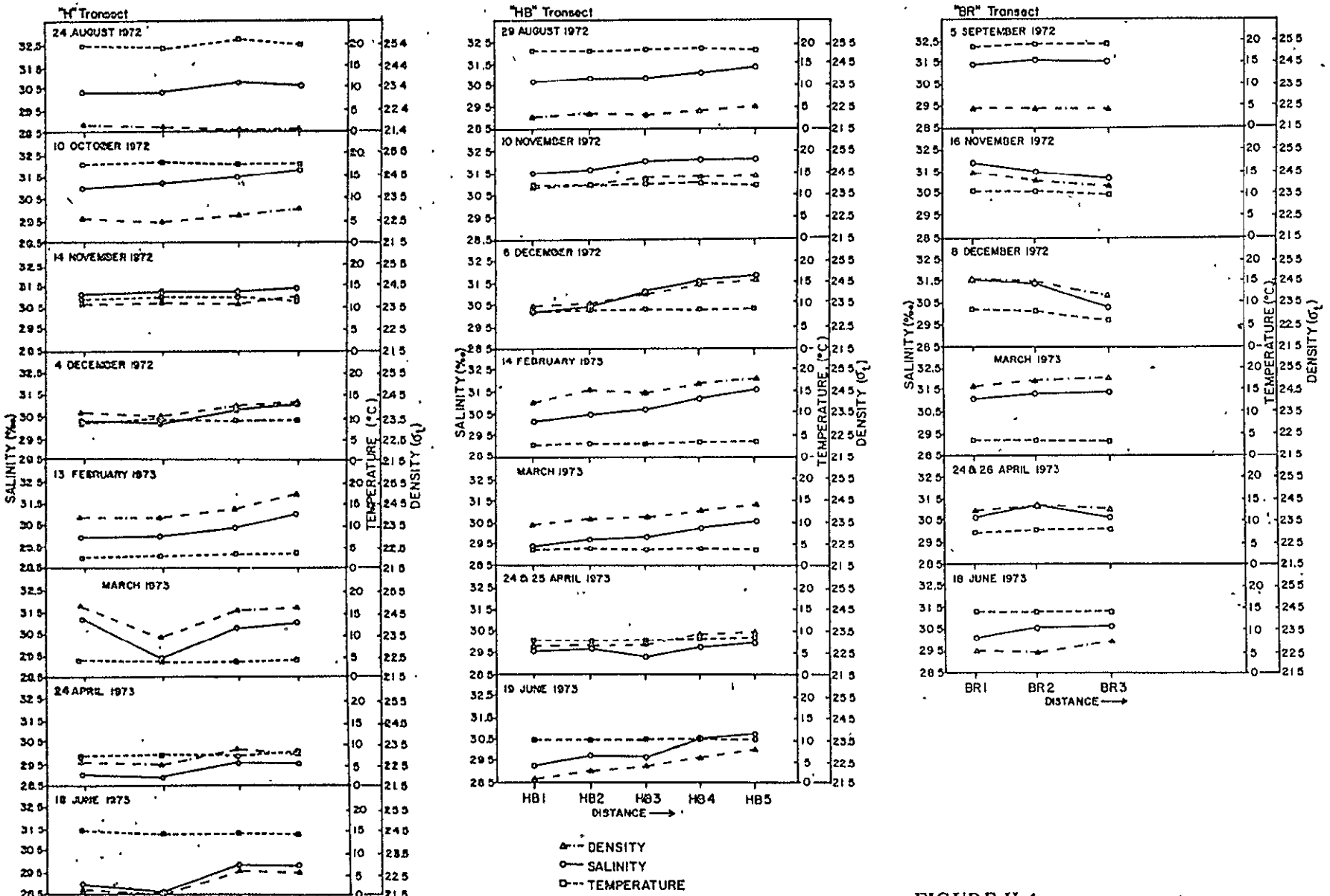

FIGURE II-4

Monthly values of the average surface temperatures, salinities, and σ_t across each transect in Block Island Sound

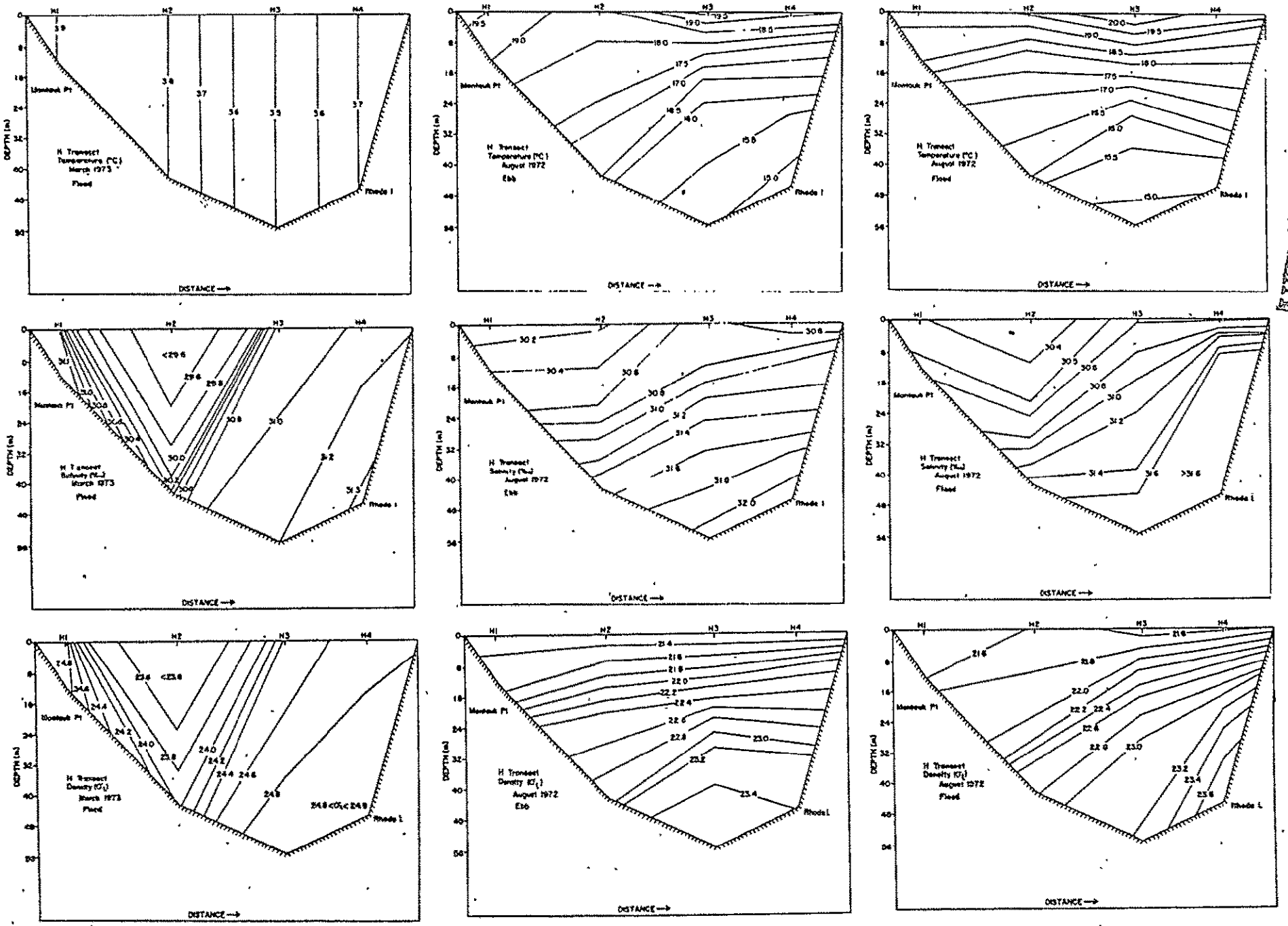

FIGURE II-5

Lateral isopleths of temperature, salinity, and σ_t during the flood tidal flow on 20 March 1973 (winter conditions) and average values for ebb and flood tidal flow on 24 August 1973 (summer conditions)

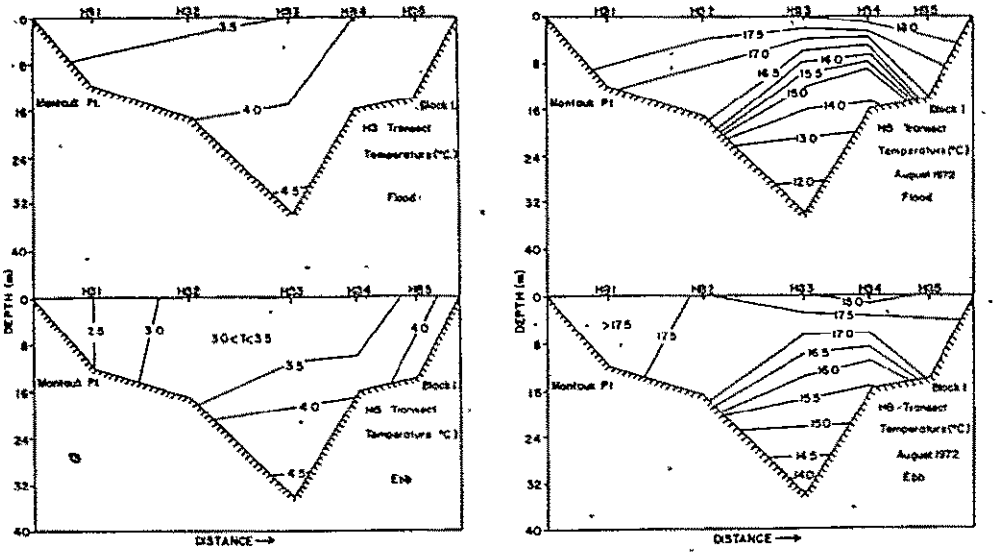

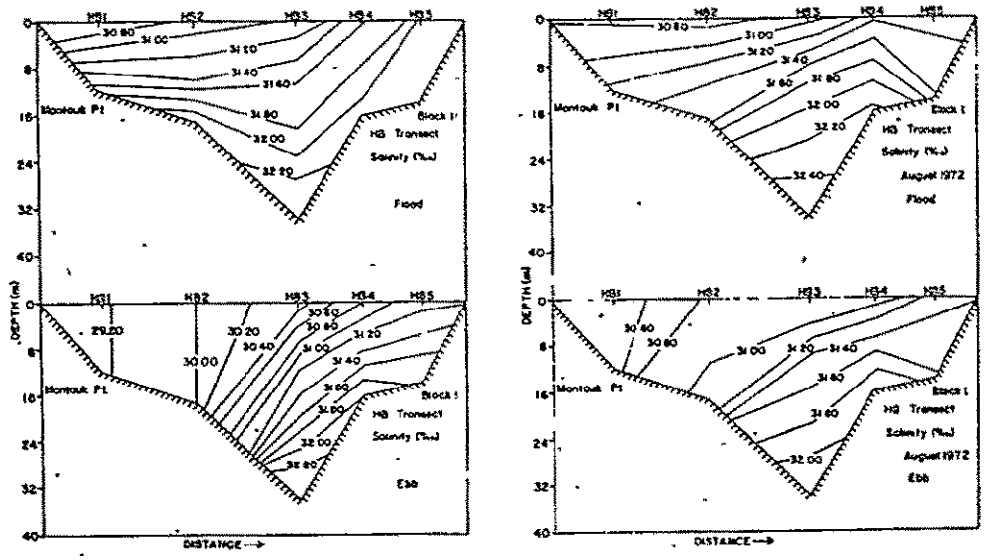

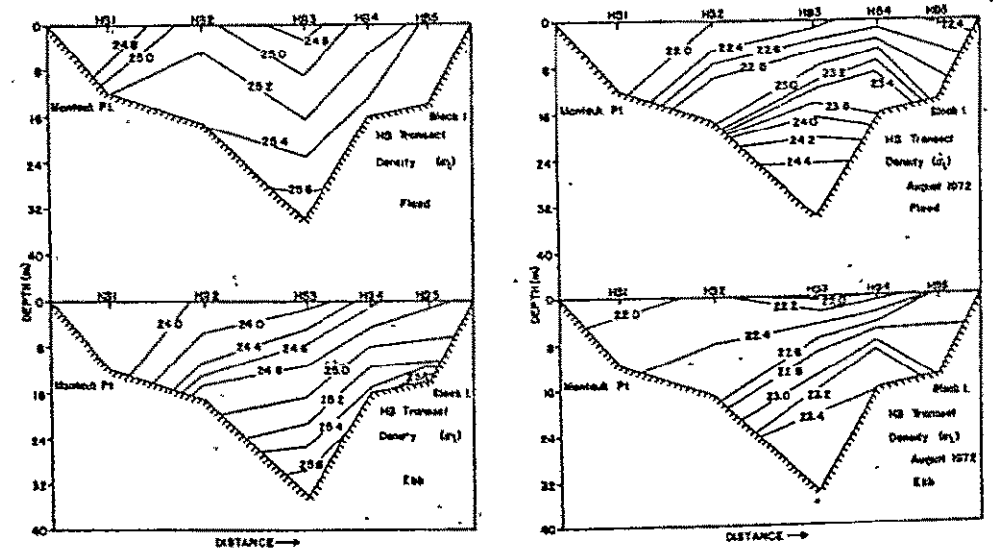

FIGURE II-6

Lateral isopleths of average temperature, salinity, and σ_t for ebb and flood tidal flows on 14 February 1973 (winter conditions) and 29 August 1972 (summer conditions)

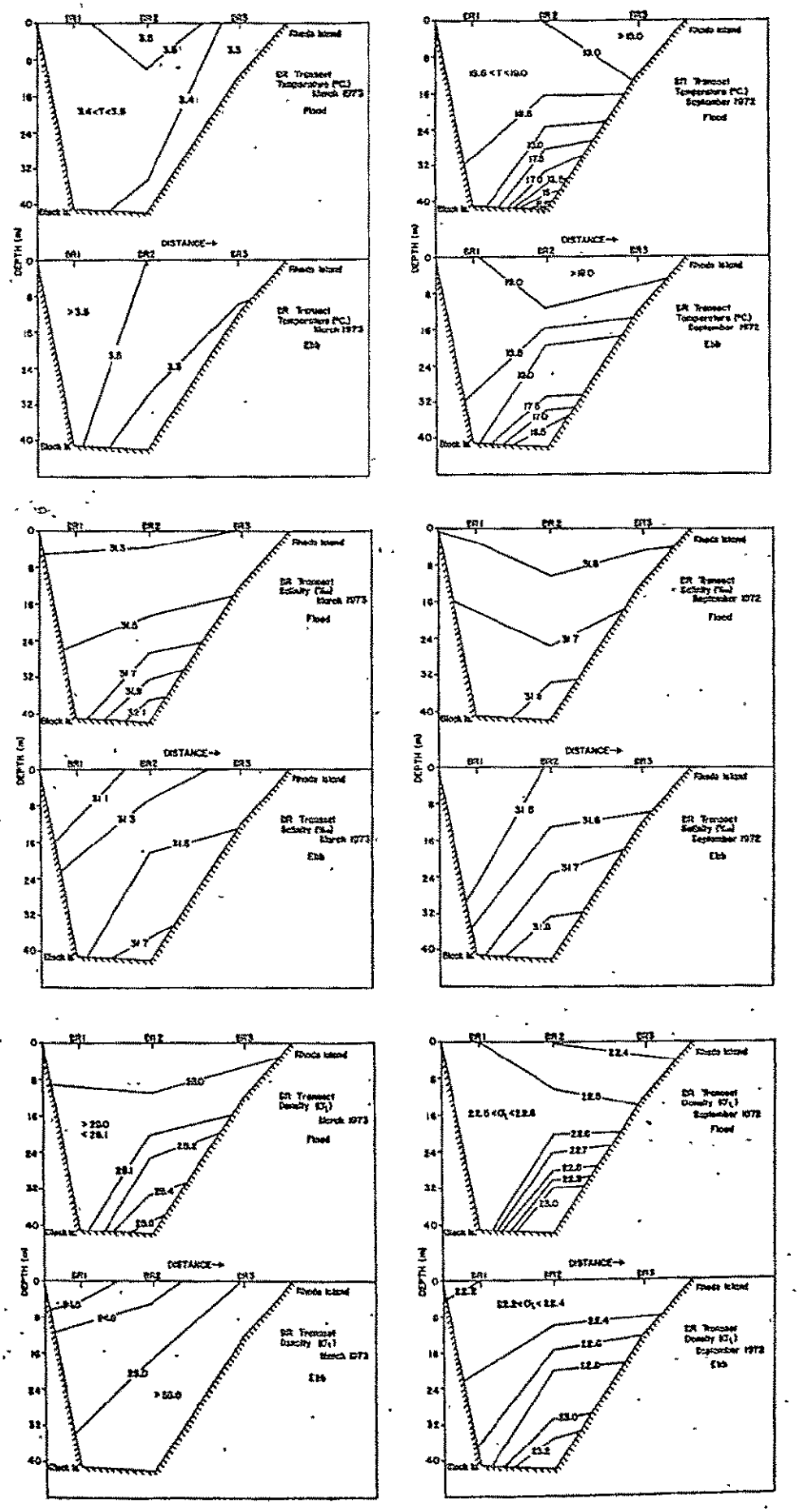

FIGURE II-7

Lateral isopleths of average temperature, salinity, and σ_t for ebb and flood tidal flows on 21 March 1973 (winter conditions) and 5 September 1972 (summer conditions)

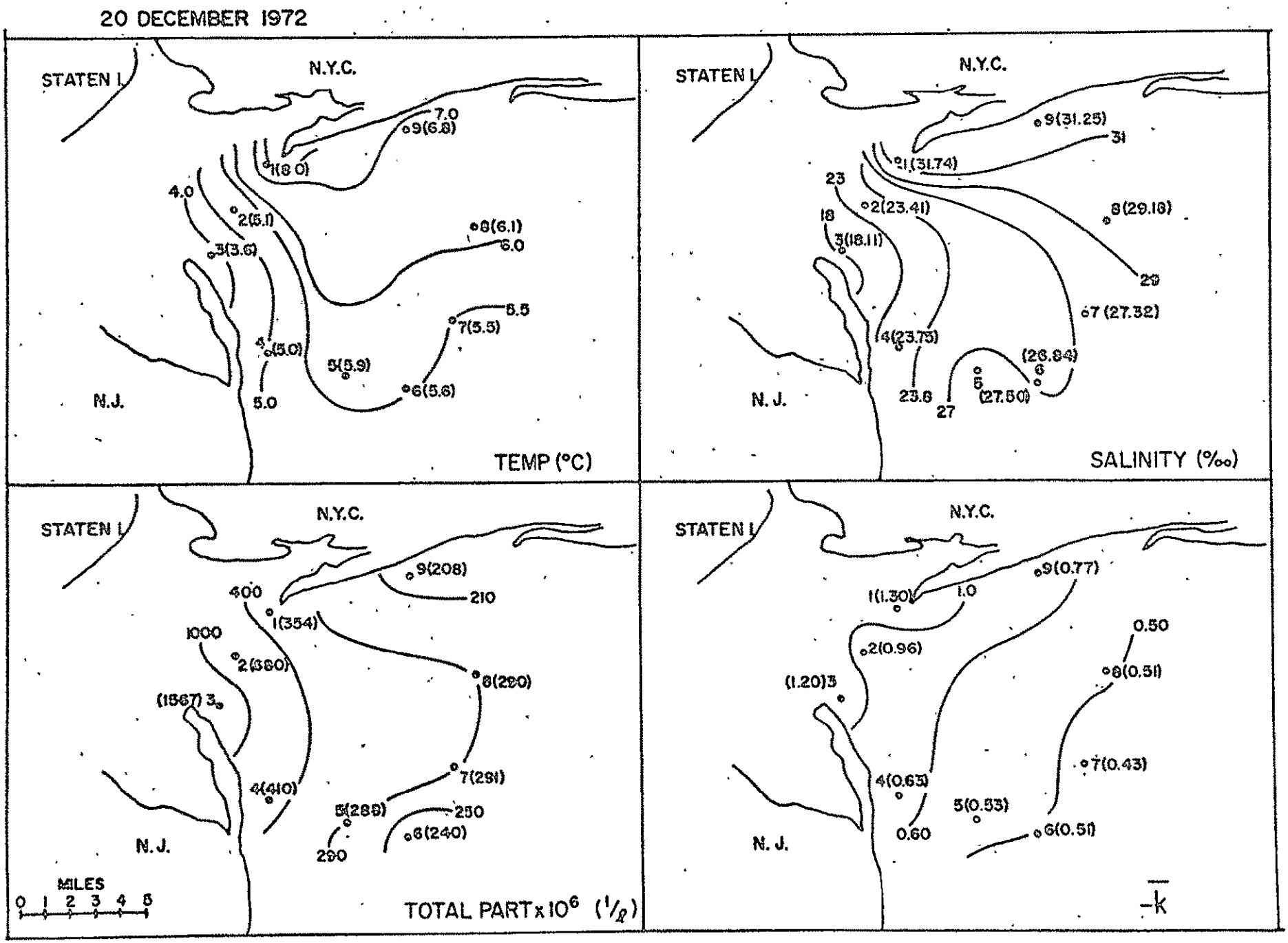

FIGURE II-8

The spatial distribution of surface temperatures, salinities, and total particulate matter and mean "extinction coefficients" for the 9 stations in the apex of the New York Bight on 20 December 1972

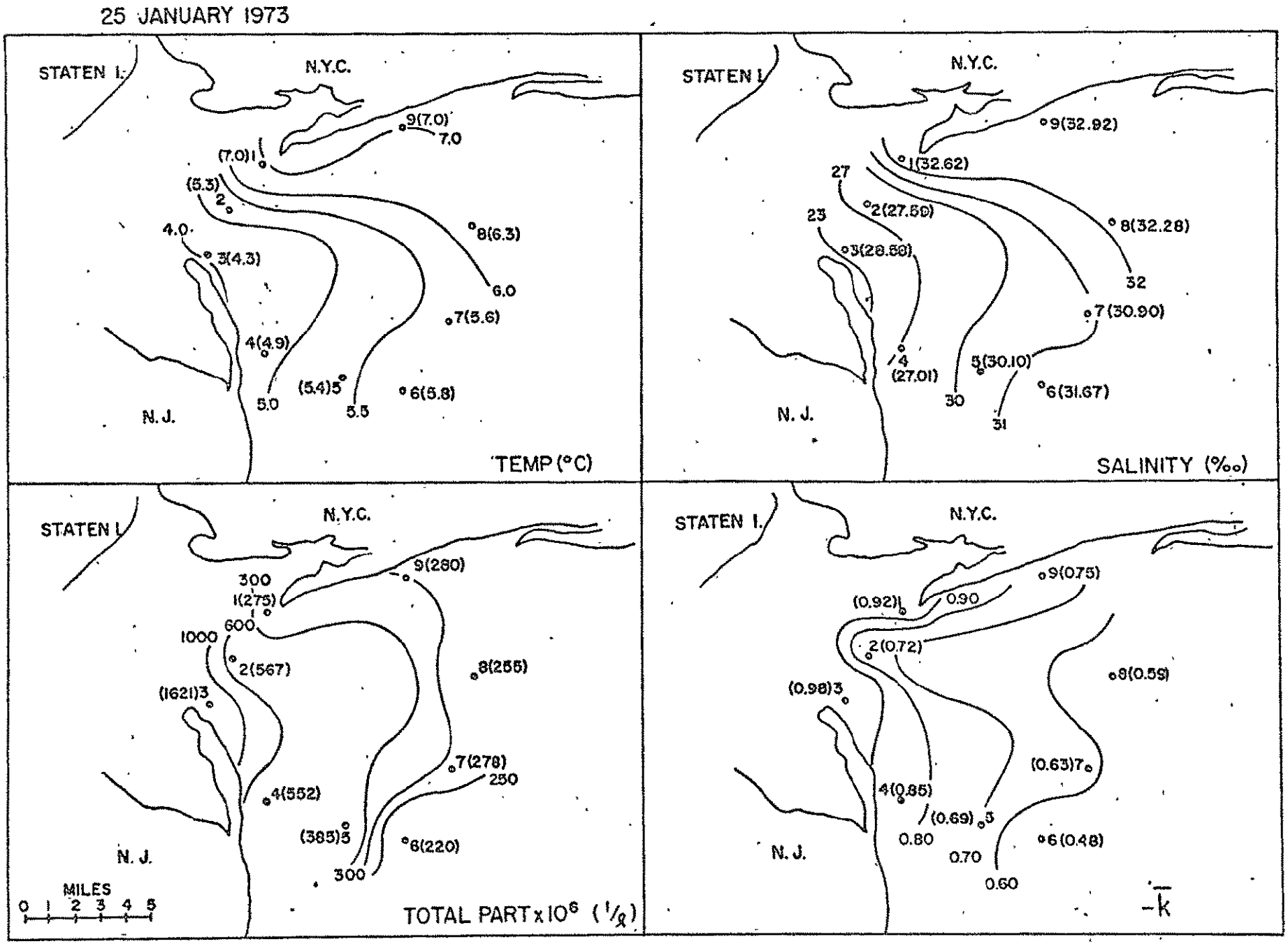

FIGURE II-9

The spatial distribution of surface temperatures, salinities, and total particulate matter and mean "extinction coefficients" for the 9 stations in the apex of the New York Bight on 25 January 1973

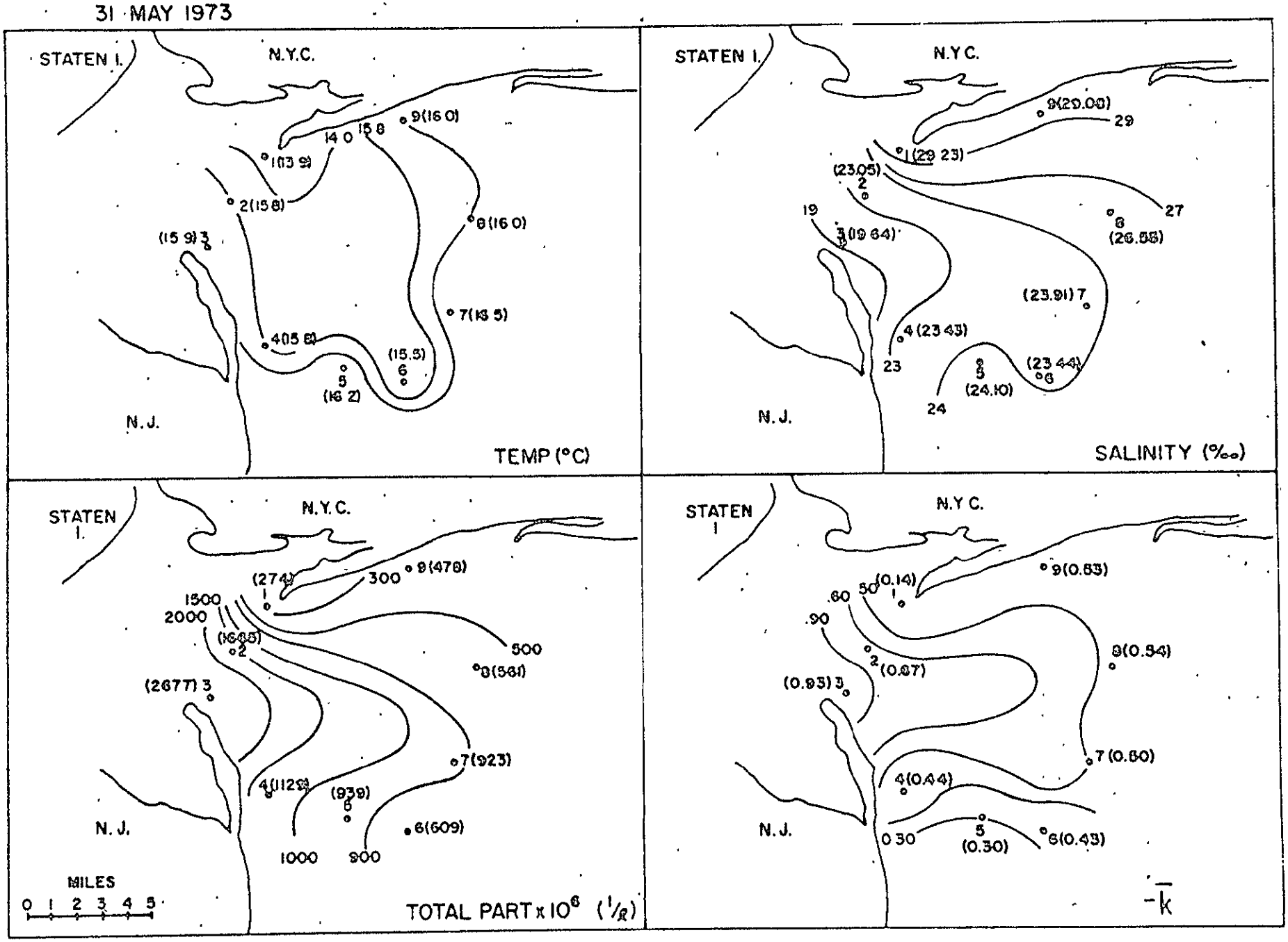

FIGURE II-10

The spatial distribution of surface temperatures, salinities, and total particulate matter and mean "extinction coefficients" for the 9 stations in the apex of the New York Bight on 31 May 1973

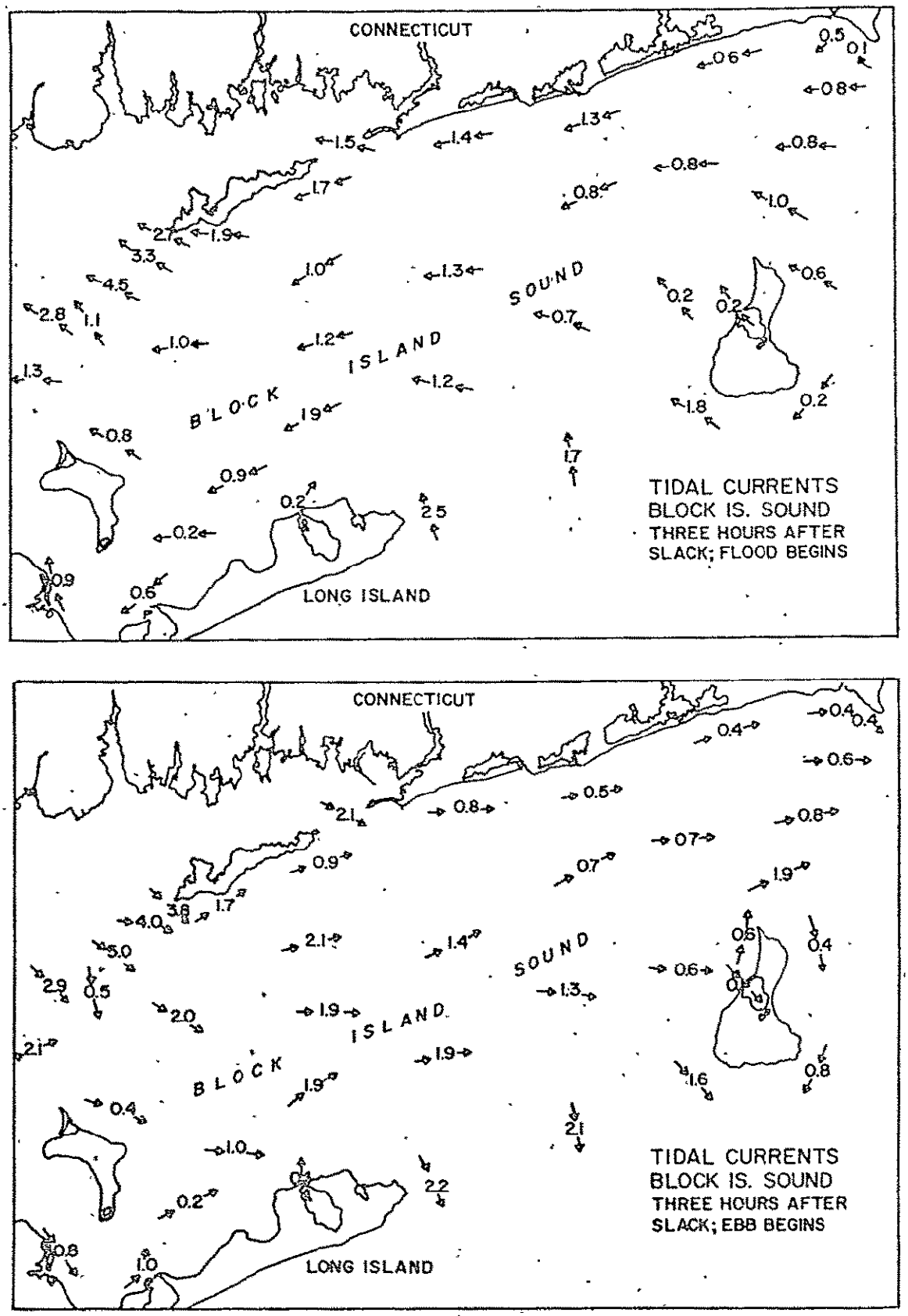

FIGURE II-11

The average flood and ebb tidal currents for Block Island Sound (taken from Tidal Current Charts, Block Island Sound and Eastern Long Island Sound, National Ocean Survey, NOAA, U.S. Dept. of Commerce, 1971)

APPENDIX B

III CHEMICAL OCEANOGRAPHY

by

James E. Alexander
Senior Research Scientist in Chemical Oceanography
New York Ocean Science Laboratory
Montauk, New York

Theodore T. White
Research Assistant in Chemical Oceanography
New York Ocean Science Laboratory
Montauk, New York

III CHEMICAL OCEANOGRAPHY

Contents

INTRODUCTION

In the fall of 1972, a study of the biological, chemical, and physical oceanography of Block Island Sound as a whole was initiated. Prior to this time, observations of these same features in the waters entering the Sound from the west had been made. Particular emphasis had been placed on four stations lying on a transect established between Montauk Point, Long Island, New York, and Watch Hill, Rhode Island.

The aim of this present investigation was to determine the relationship between ERTS-1 imagery and the characteristics of the surface waters in this area. In a previous study (Alexander et al 1973), it was noted that in coastal oceanography the sampling program should be designed around the fact that this zone is highly dynamic, and particular attention must be paid to both tidal and nontidal forces in program design.

METHODS

At each station, the locations of which have been previously described, samples were collected from selected depths with 5-ℓ Niskin bottles. Once on board, samples for the measurement of salinity, oxygen, and phytoplankton analyses were removed. The remainder of the sample was then filtered through Whatman GF/C filters in an all glass filtrations system. The filter pads were then placed in individual vials and frozen for later analysis of chlorophyll and particulate phosphorus. Samples of the filtrate were removed for the measurement of reactive and total soluble phosphorus, nitrite and nitrate nitrogen, and silica.

Salinity was determined with a conductivity system (Beckman RS7-B) and oxygen was determined by the method described by Carpenter (1966). Reactive, total soluble and particulate phosphorus, silica, and chlorophyll were determined according to the methods described by Strickland and Parsons (1968). Nitrite and nitrate nitrogen were determined by the method described by Wood et al (1967).

On 12 May 1973, through the cooperation of the local power squadrons and other private

yachts, a synoptic sampling of the surface waters was conducted. Salinity and suspended solids samples were collected at 0900, 1200, and 1500 hours. The method described by Strickland and Parsons (1968) was used for these analyses.

RESULTS AND DISCUSSION

A. Block Island Sound

The seasonal distribution of oxygen along the H transect is depicted in Figure III-1a-c. No significant differences were apparent between the four stations at the surface. Similar concentrations were found along the HB and BR transect. As anticipated, the observed surface oxygen concentrations, which ranged from approximately 4.5 ml/ℓ in September to 8.5 ml/ℓ in March, were inversely correlated with surface temperatures ($r = -0.863$). On an annual basis, the surface waters of Block Island Sound had a predicted oxygen concentration of $O_2 = -0.18\ (t^\circ C) + 8.15$. The overall correlation of oxygen with chlorophyll *a* in these surface waters was not significant ($r = -0.167$).

The observed changes in reactive and soluble organic (total soluble-reactive) phosphorus, nitrite, nitrate, and silicate for the various transects are tabulated in Table III-1, III-2, and III-3.

The nutrients (phosphates, nitrates, and silicates) showed the seasonal variations typical of temperate waters. Indications are that the supply of nitrogen to these waters is limited and that, under the appropriate conditions, the nutrients are utilized by the phytoplankton rather quickly. Although relatively large seasonal changes in concentration were noted, the correlations between these parameters and chlorophyll *a* were not considered significant.

Particulate phosphorus and chlorophyll *a* (Figure III-1a, b, c and III-2a, b, c) showed a strong correlation ($r = 0.815$). The equation of the line depicting the relationship was $P\text{-}PO_4 = 0.58$ chl. $a + 0.85$. Particulate phosphorus generally ranged between 0.5 and 3.5 μg-at/ℓ. The maximum concentration (6.36 μg/ℓ) was noted at Station H1 in March. Subsurface concentrations (30 m depth) generally paralleled those found at the surface.

In early October, what appeared to be the remnants of an autumn bloom were found at those stations occupied along the H transect. Little evidence of such conditions was found for the other transects. Chlorophyll *a* concentrations generally remained low (0.5-1.0 mg/m^3) through the remainder of the fall and winter. A spring flowering of relatively short duration was present in March. Peak chlorophyll *a* concentrations of 9.4 mg/m^3 were present at Station H1. The amount of chlorophyll *a* present in the surface waters of this transect gradually decreased from the high value noted at Station 7 to 2.1 mg/m^3 at Station 4. No evidence of a spring outburst of similar magnitude was found in the waters of the other transects. The reasons for this may be that the frequency of sampling was such that the bloom was missed along the other transects, or the data reduction techniques affected the graphical presentation. In respect to the latter, the range of chlorophyll *a* at BR1 was 1.69-3.39; at BR2 a range of 2.01-2.60 mg/m^3, and at BR3 a range of 0.85-3.04 mg/m^3. Along the HB transect, inclement weather prevented our sampling from 14 February until 25 April, and undoubtedly the spring bloom was missed.

This study was designed to determine the relationship between ERTS-1 imagery and the characteristics of surface waters in this area. It was also necessary to determine how representative any of these data were for that day, since in the present ERTS-1 program an image of an area represents the conditions for that moment in time only. Our sampling program was designed to collect data on the effect of both tidal and nontidal forces upon a given parameter and consequently to yield information pertinent to the above. The effect of these upon the distribution of particulate phosphorus and chlorophyll *a* on 10 October 1972 is shown in Figure III-3. Satellite time was at approximately 1100 hours, and at that time higher concentrations of both particulate phosphorus and the pigmented population were present at Station H1 than at the remaining stations. This station also showed the greatest range of concentration for both of these parameters. Since this range of variation is typical of the variability to be expected for most parameters, it is particularly important that additional information be gathered relevant to the variability of all parameters in both short- and long-term space and time.

With respect to the former, we conducted an experiment on 12 May 1973, with the help of the local power squadrons and private yachts, to collect synoptic samples for the

measurement of suspended material, salinity, and temperature in the surface waters of Block Island Sound and adjacent waters. In this preliminary experiment, logistics prevented the collection of samples for chlorophyll. The location of each of the sampling vessels is shown in Figure III-4. The sampling times were 0900, 1200, and 1500 hours. It should also be noted that, although care was exercised in the storage of the samples, certain of those collected early in the day remained in the plastic containers for more than 10 hours prior to filtration.

The synoptic distribution of temperature, salinity, and suspended solvents is shown in Figure III-6a, b, c, III-7a, b, c, and III-8a, b, c. For each of the three parameters observed, large ranges in values and concentrations were noted. The effect of the tidal forces upon the distribution of these parameters was apparent.

B. New York Bight

Only three cruises in the New York Bight were completed (December, January, and May), and during each of these any particular site was sampled only once. This places strong limits on the interpretation of the data. The observed data for the TR and NYB transects are shown in Table III-4 and III-5 respectively.

The concentration of nutrients and chlorophyll was generally higher along the New York Harbor transect than along the TR transect. This was especially apparent in the nitrate concentrations. Evidences for seasonal trends were particularly evident in the nitrate and silicate data. Table III-6 lists the average data for all of the parameters for both the TR and NYB transects in December, January, and May.

No significant correlation between the nutrients, particulate phosphate, and chlorophyll *a* was found for the TR transect at any time. Along the NYB transect, however, strong correlations were found between the concentration of chlorophyll *a* and soluble organic phosphorus. It was also noted that the correlation was strongest in May. For example, the overall correlation of soluble organic phosphorus with chlorophyll *a* for the NYB transect was 0.88. In December and January, the correlations were not significant ($r = 0.01$ and 0.12 respectively), while in May the correlation was 0.95.

SUMMARY

Observations on the spatial and temporal distribution of particulate phosphate, reactive phosphate, and soluble organic phosphate, nitrate nitrogen, silica, and chlorophyll *a* were conducted in both Block Island Sound and the New York Bight from August 1972 to June 1973. The frequency of sampling was greatest in the former area.

Evidence of the presence of the seasonal cycles expected for these temperate waters was present. The waters of Block Island Sound and those along the southern shore of Long Island were deficient in nitrogen. With the exception of particulate and soluble organic phosphorus, no significant correlations were found between any of the measured parameters and chlorophyll *a*. In Block Island Sound, correlations of 0.815 were found between particulate phosphorus and chlorophyll *a*. No correlation was found for these parameters in the New York Bight. In the latter area, a strong correlation (0.88) existed between soluble organic phosphorus and chlorophyll *a* at the entrance to New York Harbor. Evidence was also presented indicating that the strength of this correlation fluctuates seasonally.

TABLE III-1

Seasonal variations in reactive and soluble organic phosphorus, nitrite and nitrate nitrogen, and silicate along the "H" transect

Date		10 Oct 1972				14 Nov 1972				4 Dec 1972				13 Feb 1973			
Station / Parameter		H1	H2	H3	H4	H1	H2	H3	H4	H1	H2	H3	H4	H1	H2	H3	H4
$R\text{-}PO_4$	0m	0.97	1.16	1.14	0.84	1.13	1.06	0.89	0.96	1.28	1.25	1.14	1.17	0.91	N.A.	1.00	0.90
µg-at/ℓ	30m	1.21	-	0.91	0.82	-	N.A.	N.A.	-	-	1.15	0.95	1.03	-	N.A.	N.A.	N.A.
$O\text{-}PO_4$	0m	0.38	0.42	0.33	0.49	1.71	0.37	1.34	0.51	0.29	0.23	0.21	0.16	0.75	N.A.	0.21	0.15
µg-at/ℓ	30m	-	0.26	0.60	0.50	-	N.A.	N.A.	N.A.	-	0.20	0.38	0.16	-	N.A.	N.A.	N.A.
NO_2	0m	0.48	0.81	0.53	0.13	0.19	0.24	0.11	0.30	0.19	0.33	0.25	0.16	-	N.A.	N.A.	N.A.
µg-at/ℓ	30m	-	0.84	0.42	0.12	-	1.01	0.11	0.11	-	0.21	0.21	0.16	-	N.A.	N.A.	N.A.
NO_3	0m	0.88	1.99	1.11	1.44	2.06	7.38	1.29	2.01	1.79	2.88	2.22	2.56	-	N.A.	N.A.	N.A.
µg-at/ℓ	30m	-	1.62	0.91	0.38	-	1.77	0.98	1.15	-	2.39	2.02	3.69	-	N.A.	N.A.	N.A.
Si	0m	4.73	5.46	4.26	1.82	1.61	2.07	3.58	2.73	3.39	5.44	3.45	3.18	10.5	N.A.	11.6	7.3
µg-at/ℓ	30m	-	5.89	4.50	1.66	-	3.20	2.40	3.93	-	3.84	5.28	2.50	-	N.A.	N.A.	N.A.

N.D. = Not Detectable
N.A. = No Data Available
- = Insufficient Depth

TABLE III-1 (cont'd.)

Date		20 Mar 1973				24 Apr 1973				18 Jun 1973			
Station / Parameter		H1	H2	H3	H4	H1	H2	H3	H4	H1	H2	H3	H4
$R\text{-}PO_4$	0m	0.68	0.77	0.65	0.62	0.66	1.13	0.76	0.63	0.43	0.60	0.27	0.32
µg-at/ℓ	30m	-	0.77	0.65	0.61	-	0.54	0.47	0.50	-	0.55	0.51	0.55
$O\text{-}PO_4$	0m	0.35	0.26	0.33	0.16	0.81	1.09	0.98	N.D.	0.76	0.59	0.71	0.51
µg-at/ℓ	30m	-	0.22	0.28	0.68	-	1.91	7.21	4.19	-	0.28	0.63	0.75
NO_2	0m	0.07	0.10	0.11	0.05	0.06	0.04	0.03	0.03	0.02	0.02	0.02	N.A.
µg-at/ℓ	30m	-	0.10	0.07	0.05	-	0.05	0.02	0.01	-	0.06	0.03	N.A.
NO_3	0m	1.69	5.05	2.35	2.05	1.47	1.39	1.15	0.90	0.28	0.09	-	0.01
µg-at/ℓ	30m	-	4.75	2.82	1.75	-	1.09	0.70	0.41	-	0.57	0.35	0.40
Si	0m	3.34	7.07	5.58	5.17	7.03	6.86	6.53	5.51	5.6	5.4	3.4	4.0
µg-at/ℓ	30m	-	8.04	7.24	4.67	-	7.91	6.39	5.77	-	7.70	6.55	7.23

TABLE III-2

Seasonal variations in reactive and soluble organic phosphorus, nitrite and nitrate nitrogen, and silica along the "BR" transect

Date		5 Sep 1972			16 Nov 1972			8 Dec 1972			21 Mar 1973			26 Apr 1973			18 Jun 1973		
Station / Parameter		BR1	BR2	BR3	BR1	BR2	BR3	BR1	BR2	BR3	BR1	BR2	BR3	BR1	BR2	BR3	BR1	BR2	BR3
$R\text{-}PO_4$	0m	0.40	0.46	0.70	0.92	1.16	1.43	0.90	0.92	1.03	0.53	0.50	0.37	0.25	0.29	0.30	0.31	0.32	0.47
µg-at/ℓ	30m	0.55	0.62	-	1.04	1.09	-	0.98	0.93	-	0.42	0.50	-	-	0.33	-	0.51	0.52	-
$O\text{-}PO_4$	0m	0.33	0.37	0.15	1.13	0.77	0.62	0.38	0.17	0.11	0.72	0.69	0.39	1.16	1.18	2.07	0.59	0.44	0.66
µg-at/ℓ	30m	0.21	0.31	-	0.54	0.45	-	0.11	0.09	-	0.93	0.60	-	-	1.12	-	0.37	0.93	-
NO_2	0m	0.02	0.02	0.06	0.21	0.30	0.35	0.28	0.24	0.40	0.06	0.04	N.A.	N.A.	0.03	0.01	0.01	0.02	0.01
µg-at/ℓ	30m	0.04	0.22	-	0.19	0.24	-	0.32	0.23	-	0.03	0.01	-	-	0.01	-	0.02	0.03	-
NO_3	0m	0.73	0.10	0.31	0.87	1.82	1.97	3.02	2.46	3.57	2.26	1.00	0.10	0.20	N.D.	0.01	0.01	0.02	0.07
µg-at/ℓ	30m	0.25	0.62	-	0.54	0.65	-	0.71	2.61	-	0.98	0.35	-	-	0.12	-	0.39	0.41	-
Si	0m	2.11	0.94	3.17	1.35	2.79	4.83	1.80	2.23	4.89	4.98	3.62	2.20	2.80	0.20	0.30	5.47	3.30	5.34
µg-at/ℓ	30m	2.00	3.42	-	1.35	2.02	-	2.12	2.42	-	3.39	3.23	-	-	3.41	-	5.96	7.40	-

N.D. = Not Detectable
N.A. = No Data Available
\- = Insufficient Depth

TABLE III-3

Seasonal variations in reactive and soluble organic phosphorus, nitrite and nitrate nitrogen, and silica along the "HB" transect

Date	29 Aug 1972					10 Nov 1972					6 Dec 1972				
Station / Parameter	HB1	HB2	HB3	HB4	HB5	HB1	HB2	HB3	HB4	HB5	HB1	HB2	HB3	HB4	HB5
$R\text{-}PO_4$ 0m	0.90	0.85	0.66	0.46	0.37	1.07	1.10	0.85	0.81	0.79	1.59	1.41	1.11	1.05	1.00
μg-at/ℓ 30m	-	-	0.67	-	-	-	-	0.67	-	-	-	-	0.80	-	-
$O\text{-}PO_4$ 0m	1.00	0.87	0.75	1.40	0.26	0.12	0.27	0.13	0.04	0.15	0.27	0.17	0.05	0.20	0.13
μg-at/ℓ 30m	-	-	0.99	-	-	-	-	0.10	-	-	-	-	0.08	-	-
NO_2 0m	0.07	0.06	0.03	0.02	0.03	0.22	0.21	0.12	0.20	0.33	0.31	0.39	0.29	0.30	0.44
μg-at/ℓ 30m	-	-	0.14	-	-	-	-	0.22	-	-	-	-	0.37	-	-
NO_3 0m	0.47	0.57	0.35	0.03	0.38	1.88	1.41	0.77	0.71	0.65	2.39	3.00	2.42	1.79	1.83
μg-at/ℓ 30m	-	-	1.53	-	-	-	-	0.52	-	-	-	-	1.44	-	-
Si 0m	3.50	3.86	2.60	1.75	1.33	2.98	2.18	1.72	2.03	1.50	4.45	5.70	2.38	1.85	1.70
μg-at/ℓ 30m	-	-	4.53	-	-	-	-	1.21	-	-	-	-	0.95	-	-

N.D. = Not Detectable
N.A. = No Data Available
- = Insufficient Depth

TABLE III-3 (cont'd.)

Date		14 Feb 1973					25 Apr 1973					19 Jun 1973				
Station / Parameter		HB1	HB2	HB3	HB4	HB5	HB1	HB2	HB3	HB4	HB5	HB1	HB2	HB3	HB4	HB5
$R\text{-}PO_4$	0m	0.99	1.07	1.03	0.91	0.84	0.60	0.49	0.44	0.41	0.35	0.41	0.47	0.32	0.32	0.42
μg-at/ℓ	30m	-	-	0.77	-	-	-	-	0.50	-	-	-	-	-	-	-
$O\text{-}PO_4$	0m	0.40	0.23	0.43	0.38	0.47	1.37	3.04	0.62	1.38	0.69	0.67	1.72	0.53	0.57	1.02
μg-at/ℓ	30m	-	-	0.17	-	-	-	-	2.02	-	-	-	-	-	-	-
NO_2	0m	0.09	0.12	0.12	0.15	0.14	0.08	0.05	0.06	0.05	0.05	0.02	0.02	N.A.	0.03	N.D.
μg-at/ℓ	30m	-	-	0.09	-	-	-	-	0.04	-	-	-	-	-	-	-
NO_3	0m	4.90	5.48	4.86	6.16	6.86	1.24	1.14	1.22	0.97	0.57	0.09	0.12	1.06	-	0.03
μg-at/ℓ	30m	-	-	0.02	-	-	-	-	0.88	-	-	-	-	-	-	-
Si	0m	8.77	9.78	10.10	8.14	7.56	7.72	6.74	7.85	7.14	5.16	4.54	5.08	4.36	3.97	3.82
μg-at/ℓ	30m	-	-	6.92	-	-	-	-	6.83	-	-	-	-	-	-	-

TABLE III-4

Observations on the variation of particulate, reactive and soluble organic phosphorus, nitrate nitrogen, silica and chlorophyll *a* along the TR transect in the New York Bight

Date	20 Dec 1972								24 Jan 1973							
Station / Parameter	1	2	3	4	5	6	7	8	1	2	3	4	5	6	7	8
$P\text{-}PO_4$ µg-at/ℓ	1.29	0.86	0.93	0.86	0.85	1.39	1.23	1.33	0.73	1.57	1.44	1.62	1.75	1.59	2.41	2.74
$R\text{-}PO_4$ µg-at/ℓ	1.87	1.39	1.19	1.12	1.02	1.95	1.53	1.60	1.16	0.76	0.77	0.76	0.81	0.71	0.80	0.90
$O\text{-}PO_4$ µg-at/ℓ	1.85	0.14	1.52	0.24	0.62	1.12	1.07	1.33	0.22	0.29	<0.01	0.13	0.14	0.08	0.15	0.05
NO_3 µg-at/ℓ	5.67	2.65	3.44	5.36	2.58	5.02	4.88	4.64	9.49	5.32	4.82	5.07	5.31	5.87	5.95	7.44
Si µg-at/ℓ	-	16.59	22.43	16.78	10.75	6.58	15.02	6.95	12.52	4.37	2.75	3.13	3.90	3.61	3.61	3.42
Chl *a* mg/m^3	2.32	5.46	1.43	0.78	1.04	1.23	0.98	0.99	0.91	5.32	1.91	1.95	1.30	1.91	2.69	3.07

TABLE III-4 (cont'd.)

Date	30 May 1973							
Station / Parameter	1	2	3	4	5	6	7	8
$P\text{-}PO_4$ µg-at/ℓ	1.01	0.28	0.17	0.20	0.49	0.29	0.11	0.08
$R\text{-}PO_4$ µg-at/ℓ	1.12	0.92	0.72	0.87	0.87	1.37	0.47	0.42
$O\text{-}PO_4$ µg-at/ℓ	0.44	0.99	1.58	3.33	1.31	0.41	1.87	3.09
NO_3 µg-at/ℓ	1.35	0.02		0.17	0.07	0.04	0.05	0.03
Si µg-at/ℓ	1.51	0.51	<0.10	<0.10	<0.10	<0.10	<0.10	<0.10
Chl *a* mg/m^3	1.63	3.01	1.62	2.10	1.30	0.78	1.26	2.72

TABLE III-5

Observations on the variation of particulate, reactive and soluble organic phosphorus, nitrate nitrogen, silica, and chlorophyll *a* along the NYB transect

Date	20 Dec 1972									24 Jan 1973								
Station / Parameter	1	2	3	4	5	6	7	8	9	1	2	3	4	5	6	7	8	9
$P\text{-}PO_4$ µg-at/ℓ	0.96	1.85	2.60	1.94	1.50	1.56	1.55	1.24	0.92	3.23	3.55	4.87	3.95	3.83	3.40	3.50	2.63	2.58
$R\text{-}PO_4$ µg-at/ℓ	1.22	2.54	3.16	2.60	1.87	1.77	2.17	2.06	1.29	1.00	1.90	2.48	1.84	1.24	0.71	0.96	0.82	0.90
$O\text{-}PO_4$ µg-at/ℓ	4.24	2.95	3.20	0.30	0.07	N.D.	N.D.	0.10	0.24	0.05	0.39	0.50	0.77	0.30	0.24	0.25	0.23	0.10
NO_3 µg-at/ℓ	4.01	13.24	19.31	14.46	8.98	7.34	11.36	6.10	2.79	6.67	13.36	17.04	10.55	12.76	6.99	9.54	6.38	5.73
Si µg-at/ℓ	2.95	12.04	2.08	2.17	1.69	0.92	5.71	5.91	5.91	5.28	16.50	22.25	12.52	5.93	3.39	6.21	3.80	3.71
Chl *a* mg/m^3	1.63	1.28	1.45	1.96	0.78	0.49	1.40	1.54	0.73	2.26	2.08	2.27	2.97	5.92	7.50	6.71	4.12	1.87

N.D. = Not Detectable

TABLE III-5 (cont'd.)

Date	30 May 1973								
Station / Parameter	1	2	3	4	5	6	7	8	9
$P\text{-}PO_4$ μg-at/ℓ	0.53	1.00	1.60	0.46	0.98	0.38	0.57	0.29	0.47
$R\text{-}PO_4$ μg-at/ℓ	1.42	1.88	2.64	1.12	2.63	1.12	1.62	1.17	1.22
$O\text{-}PO_4$ μg-at/ℓ	2.87	7.94	9.44	10.42	5.14	10.88	2.74	10.31	5.22
NO_3 μg-at/ℓ	1.03	12.10	19.14	8.75	10.42	5.57	10.27	1.68	1.25
Si μg-at/ℓ	0.06	1.05	2.95	1.24	0.15	0.51	0.51	0.15	0.60
Chl *a* mg/m^3	4.13	14.80	17.15	19.72	8.89	20.07	6.45	14.94	6.51

TABLE III-6

The average concentration of particulate, reactive and soluble organic phosphate, nitrate nitrogen, silica, and chlorophyll *a* along the TR and NYB transects for the months of December, January, and May

Date	Dec 1972		Jan 1973		May 1973	
Transect / Parameter	TR	NYB	TR	NYB	TR	NYB
$P\text{-}PO_4$ μg-at/ℓ	1.09	1.56	1.73	3.50	0.32	1.24
$R\text{-}PO_4$ μg-at/ℓ	1.45	2.06	0.83	1.31	0.84	1.64
$O\text{-}PO_4$ μg-at/ℓ	0.98	1.25	0.13	0.31	1.62	7.21
NO_3 μg-at/ℓ	4.28	9.73	6.15	9.89	0.24	7.80
Si μg-at/ℓ	13.58	4.37	4.66	8.84	0.32	0.80
Chl *a* mg/m^3	3.15	1.21	2.38	3.96	1.80	12.51

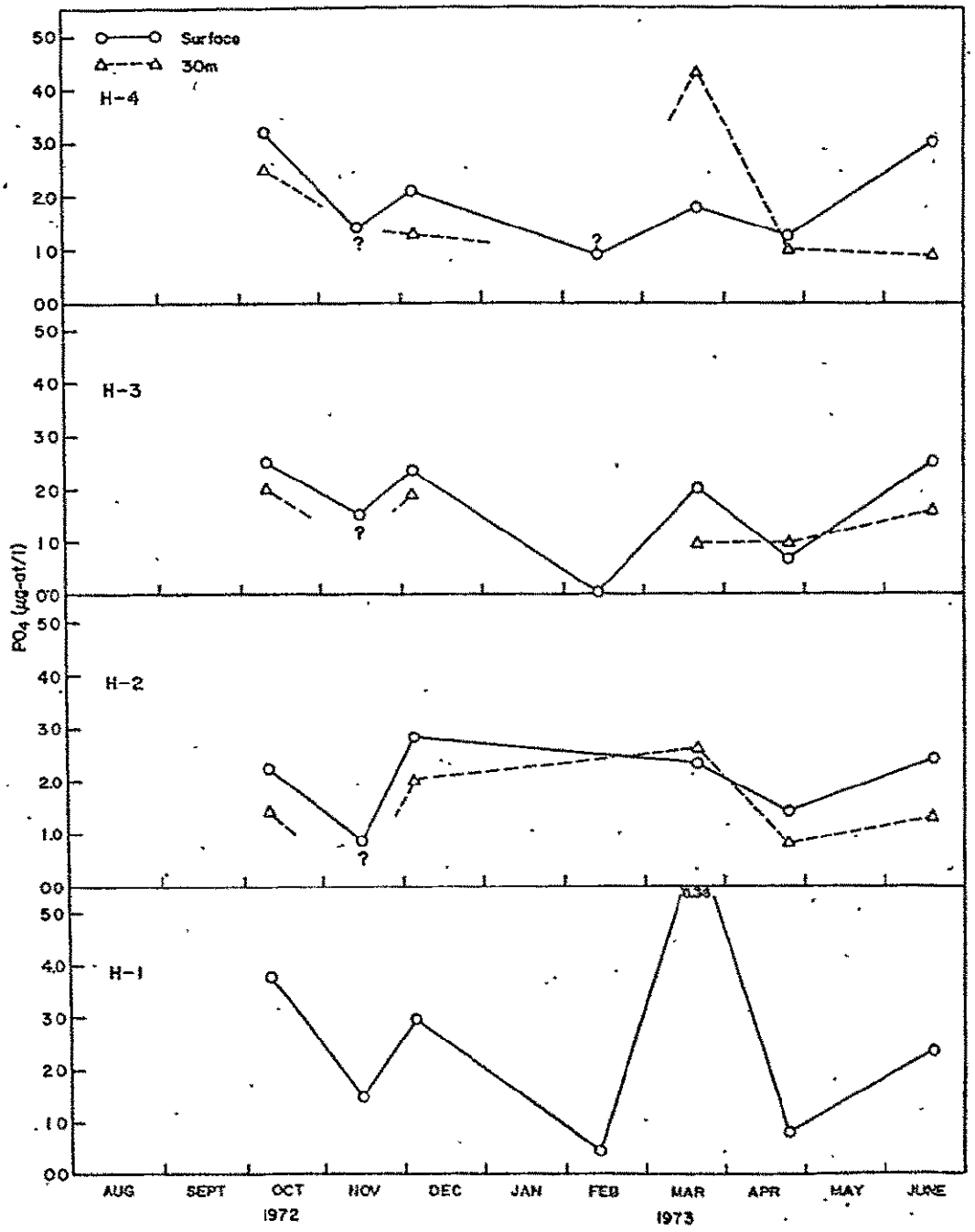

FIGURE III-1a

The seasonal distribution of particulate phosphorus along the H transect

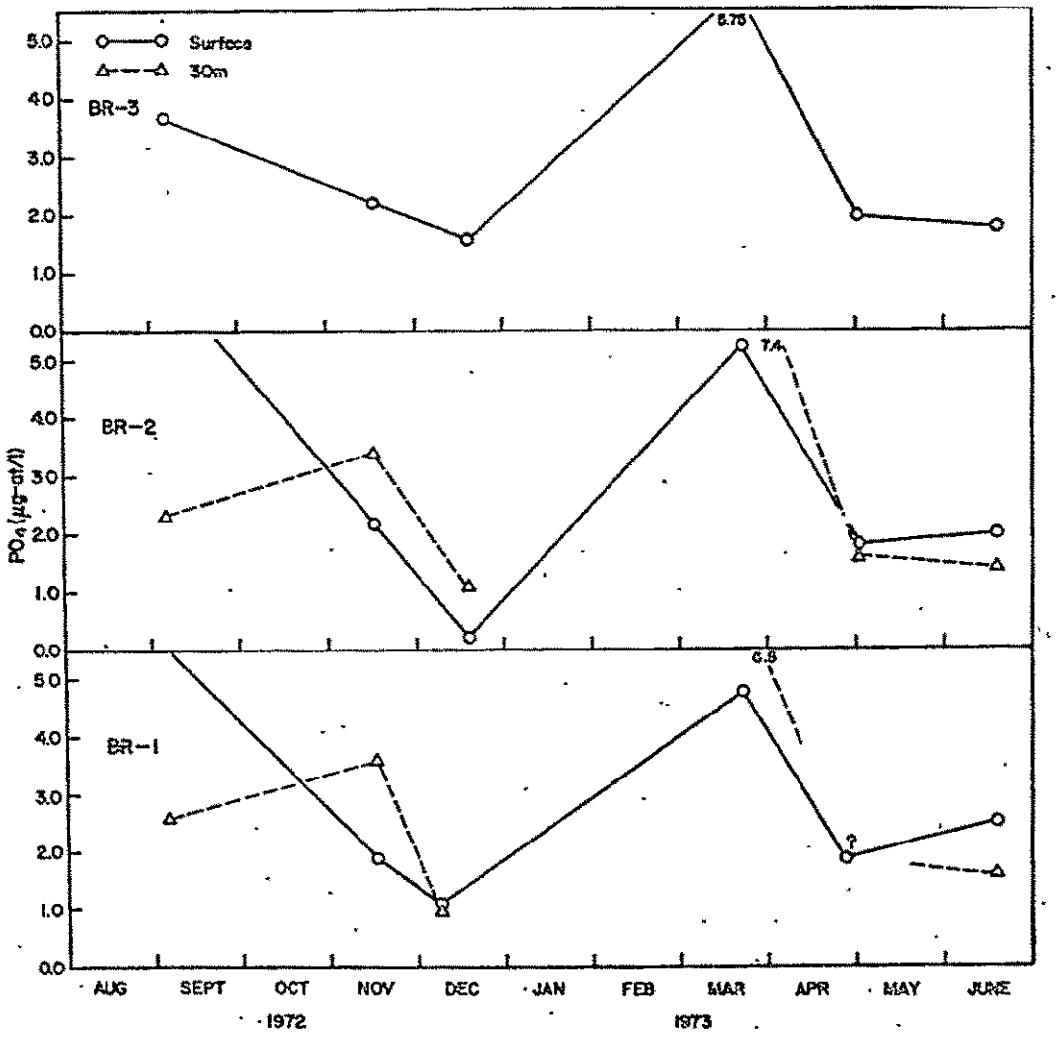

FIGURE III-1b

The seasonal distribution of particulate phosphorus along the BR transect

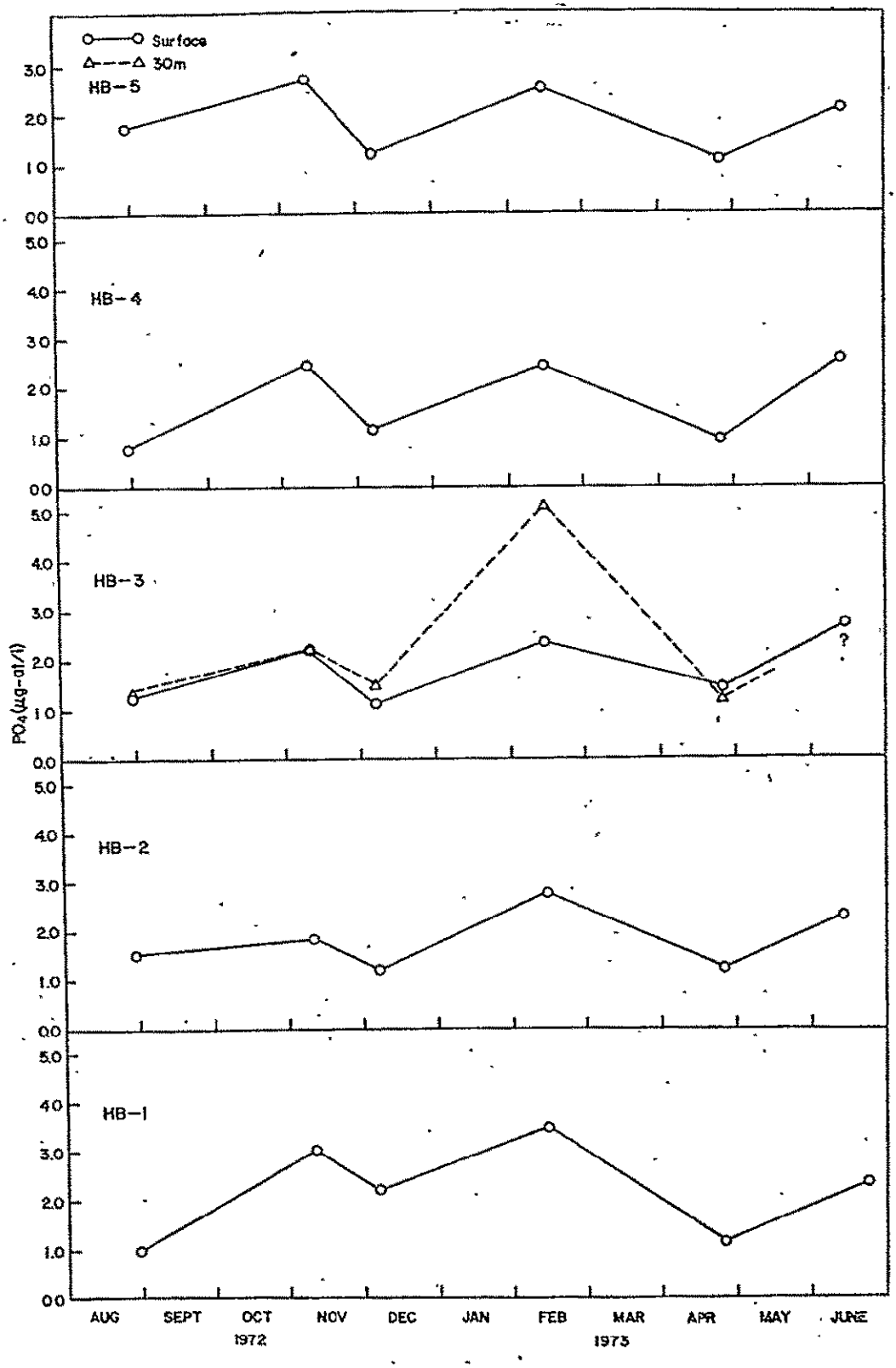

FIGURE III-1c

The seasonal distribution of particulate phosphorus along the HB transect

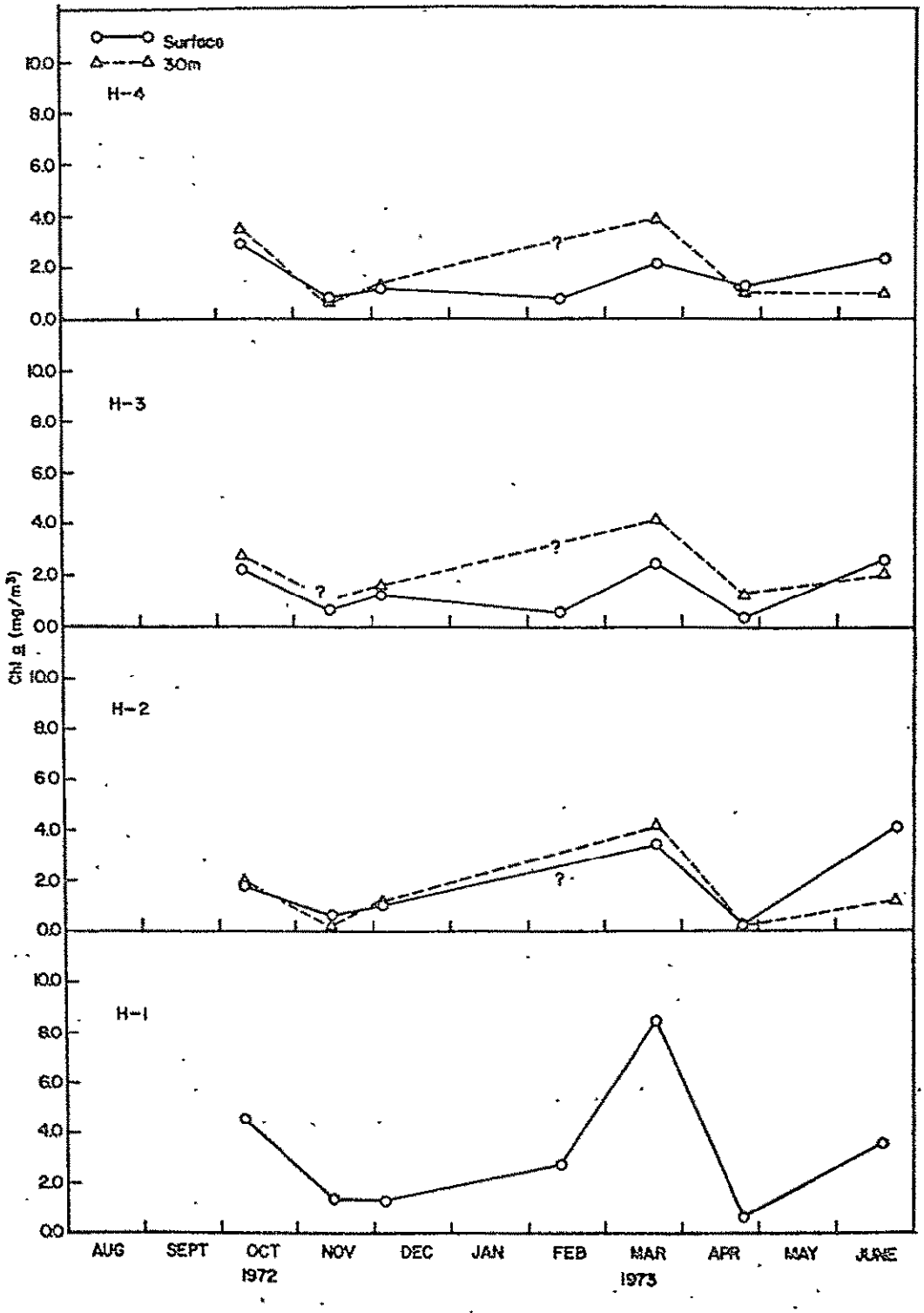

FIGURE III-2a

The seasonal distribution of chlorophyll *a* along the H transect

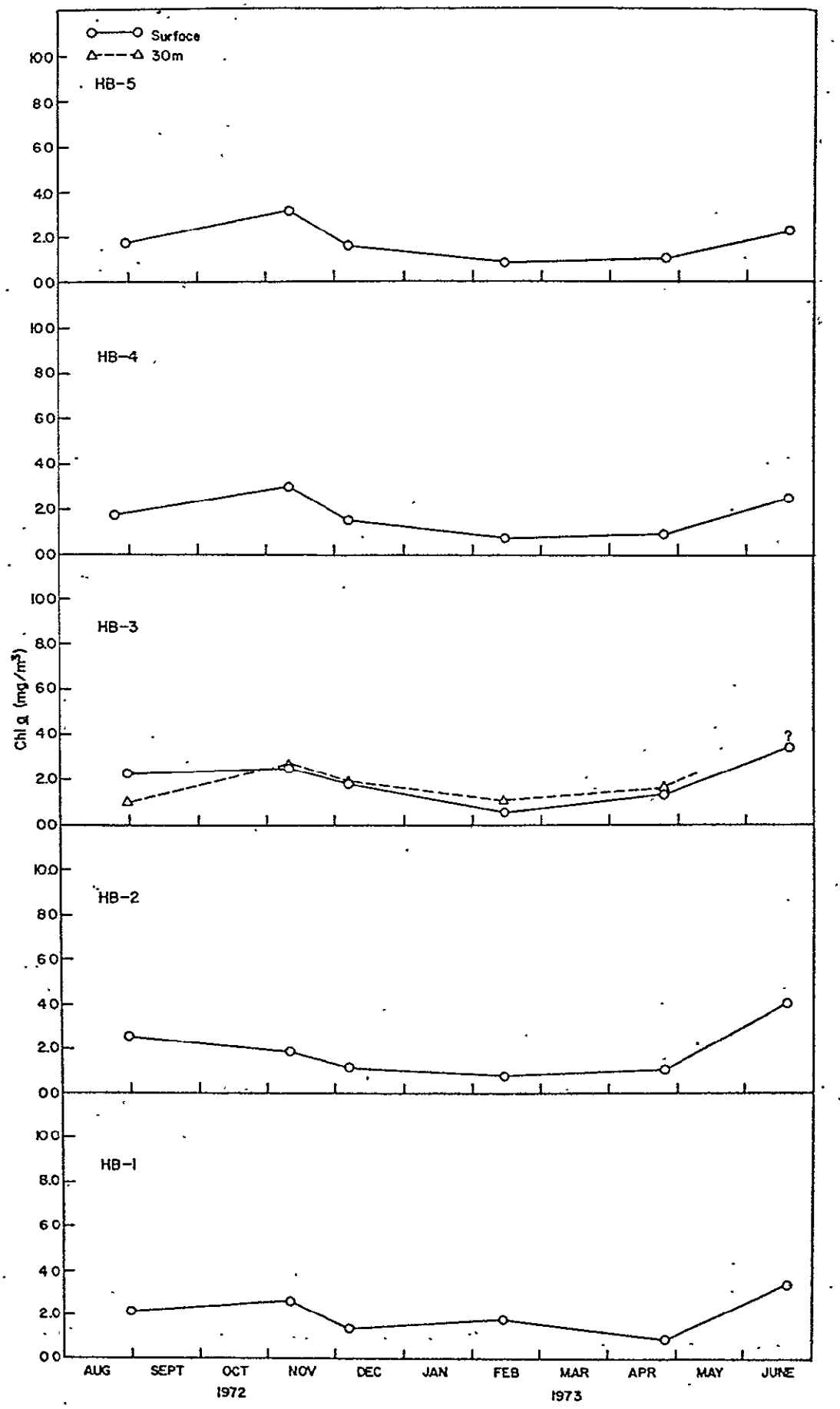

FIGURE III-2b

The seasonal distribution of chlorophyll *a* along the HB transect

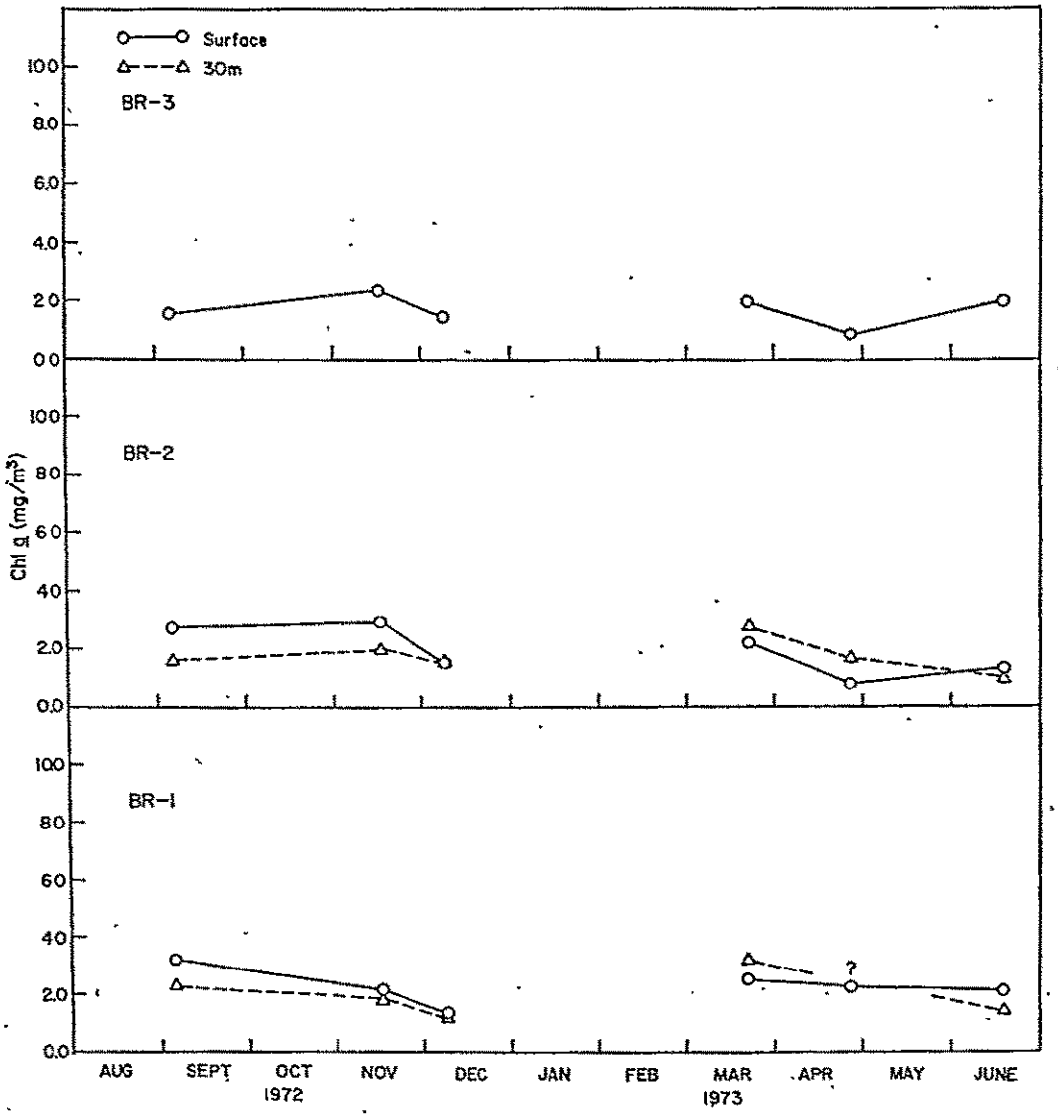

FIGURE III-2c

The seasonal distribution of chlorophyll *a* along the BR transect

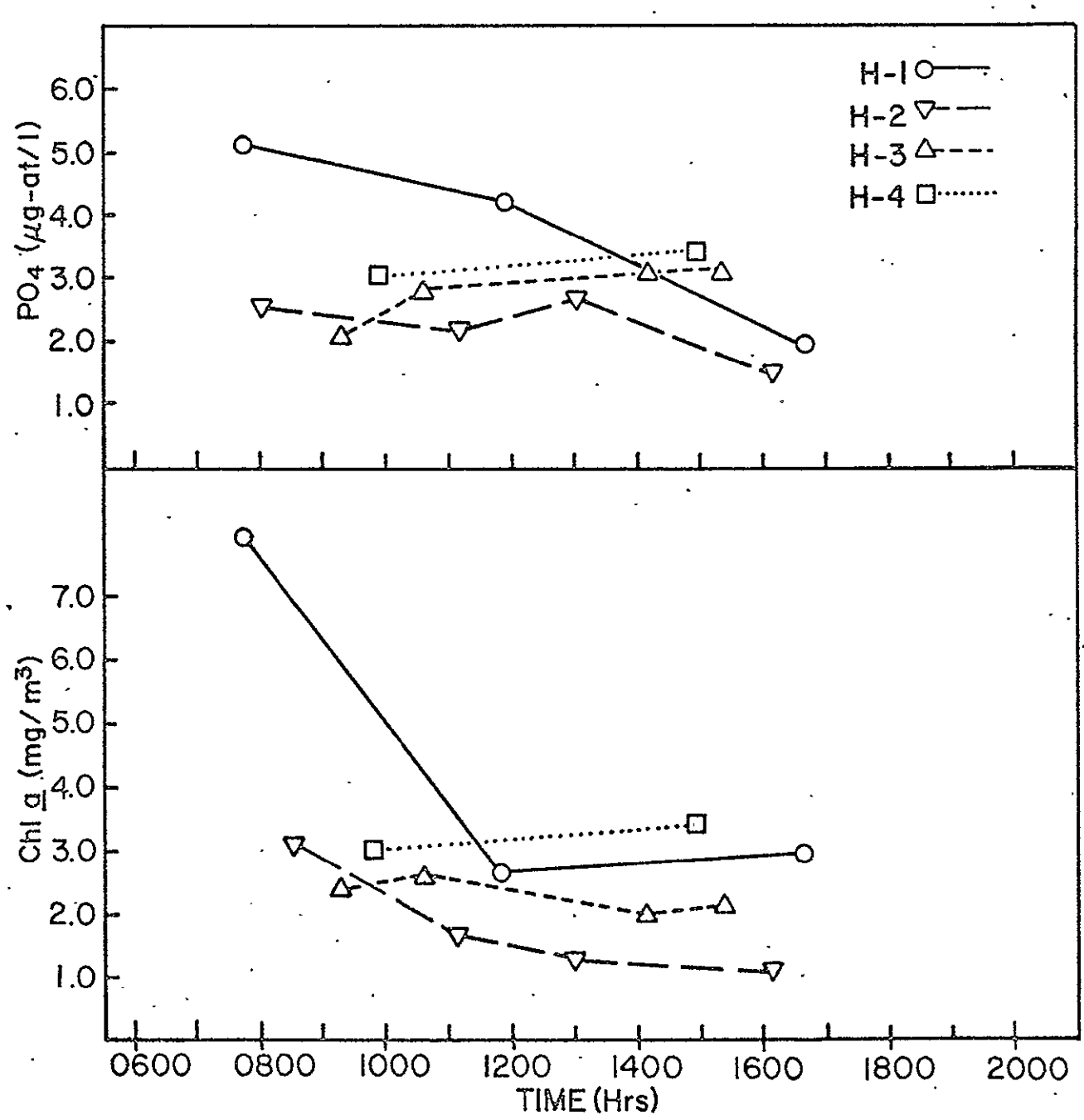

FIGURE III-3

Surface variations in particulate phosphorus and chlorophyll *a* along the H transect, 10 October 1972

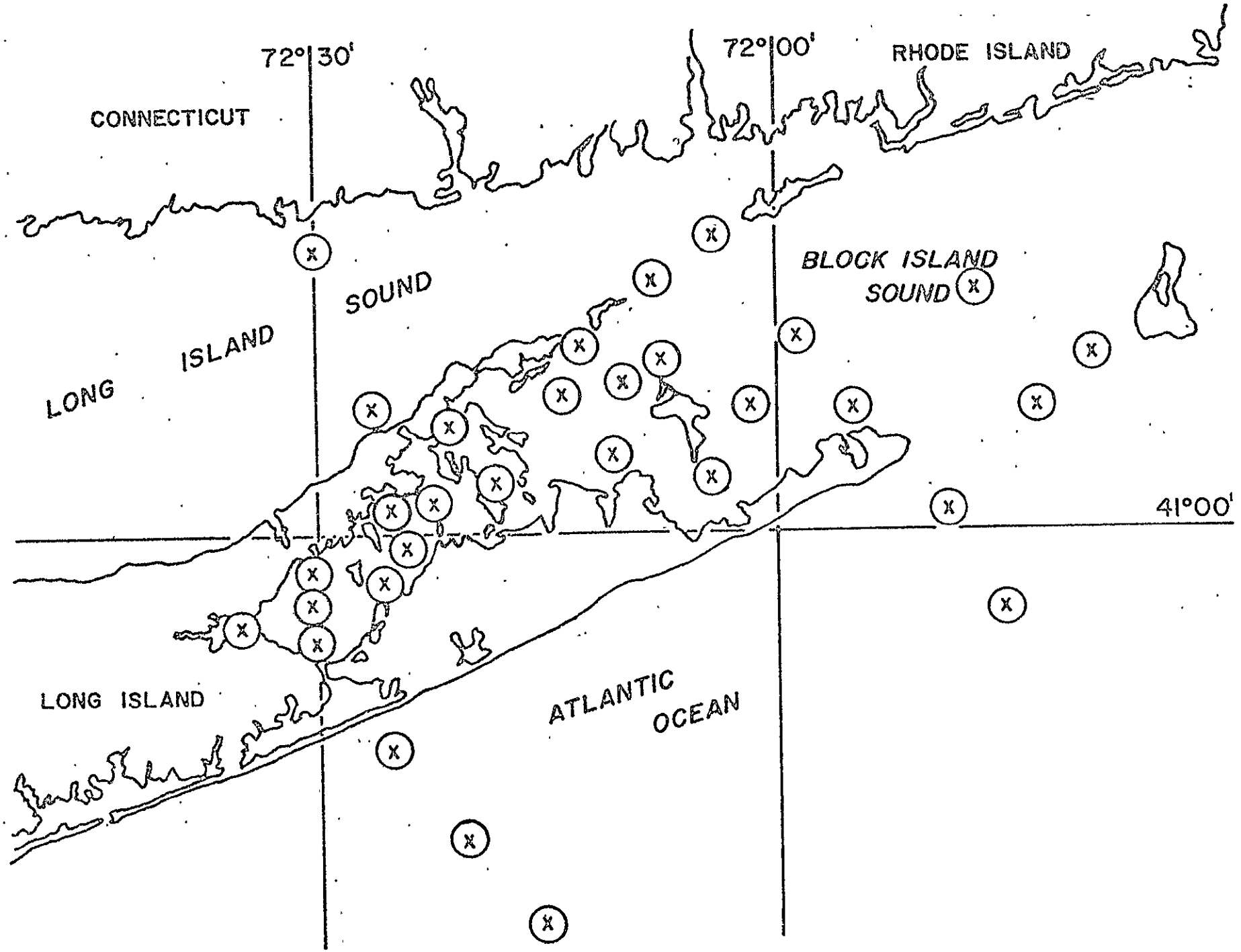

FIGURE III-4

The location of the sampling vessels for the synoptic study, conducted on 12 May 1973

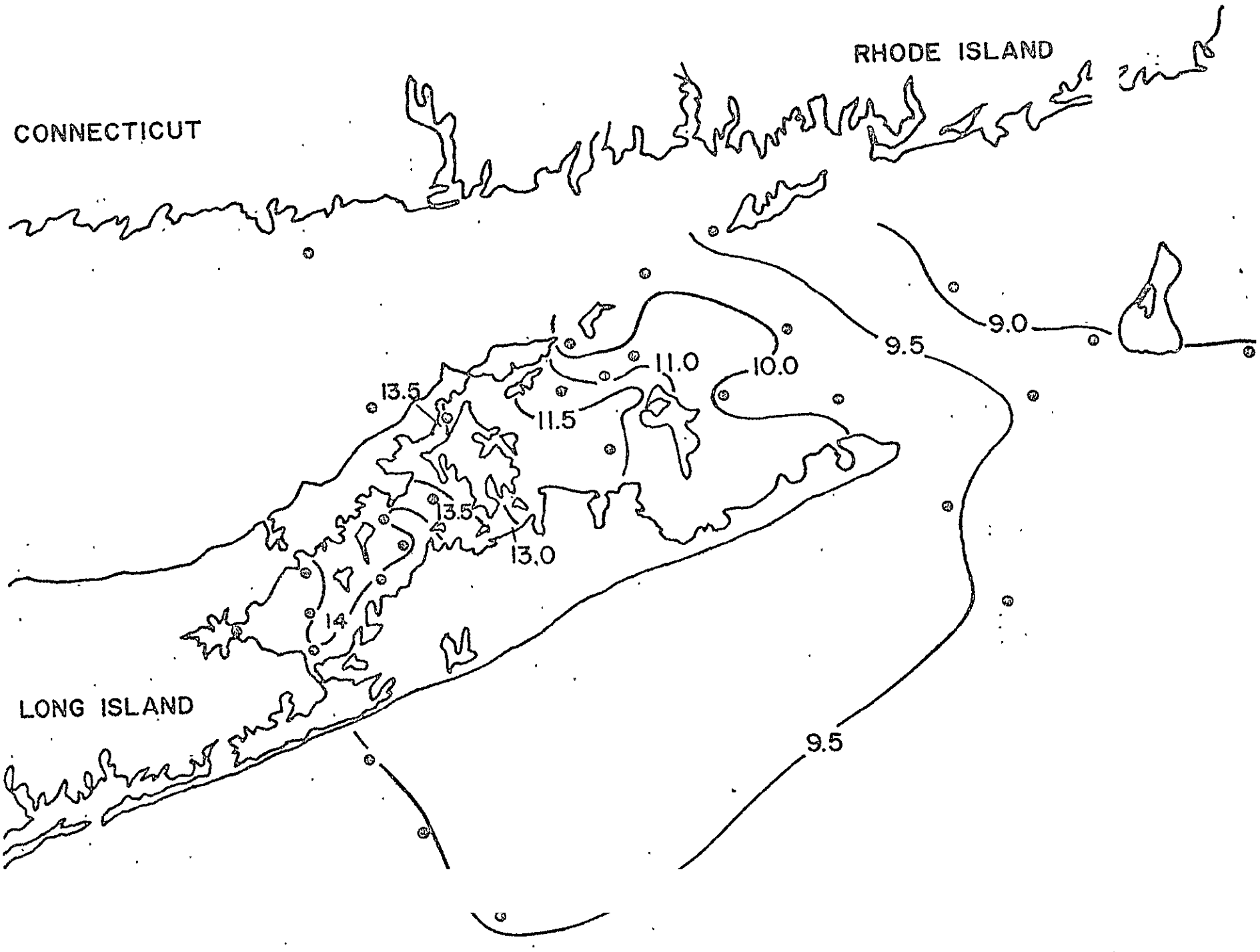

FIGURE III-5a

The distribution of temperature in the surface waters of Block Island Sound and adjacent waters (12 May 1973-0900)

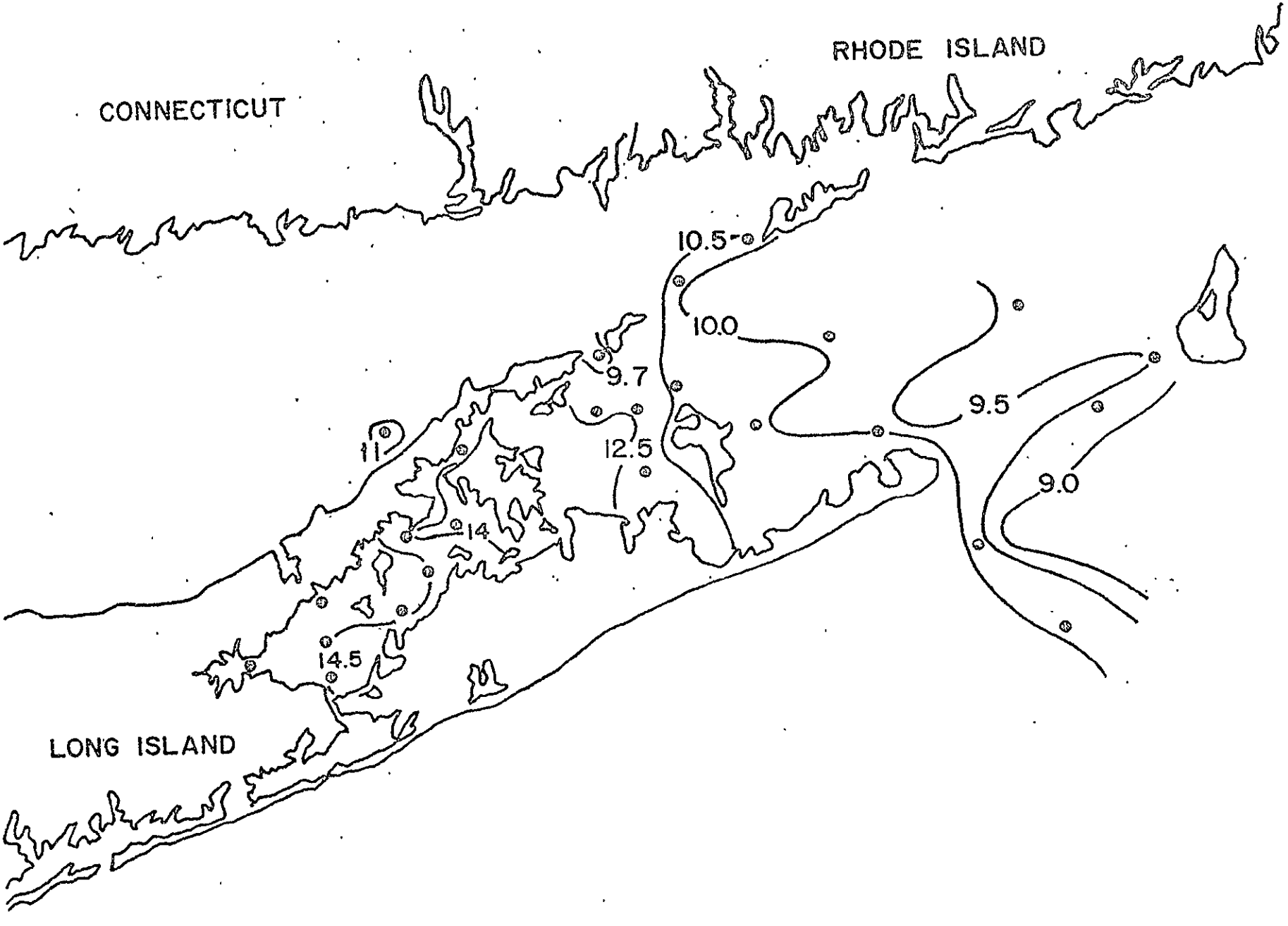

FIGURE III-5b

The distribution of temperature in the surface waters of Block Island Sound and adjacent waters (12 May 1973-1200)

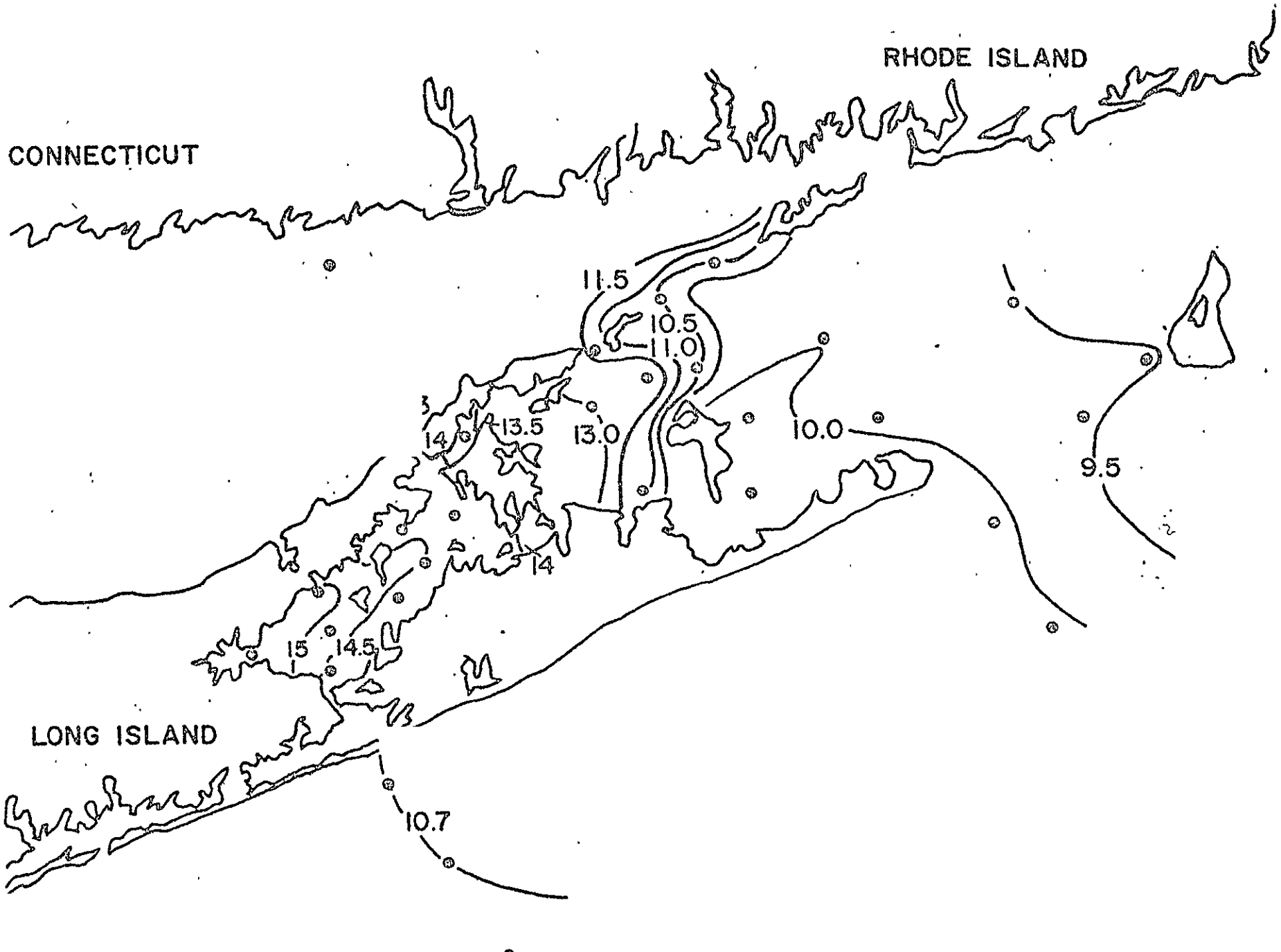

FIGURE III-5c

The distribution of temperature in the surface waters of Block Island Sound and adjacent waters (12 May 1973-1500)

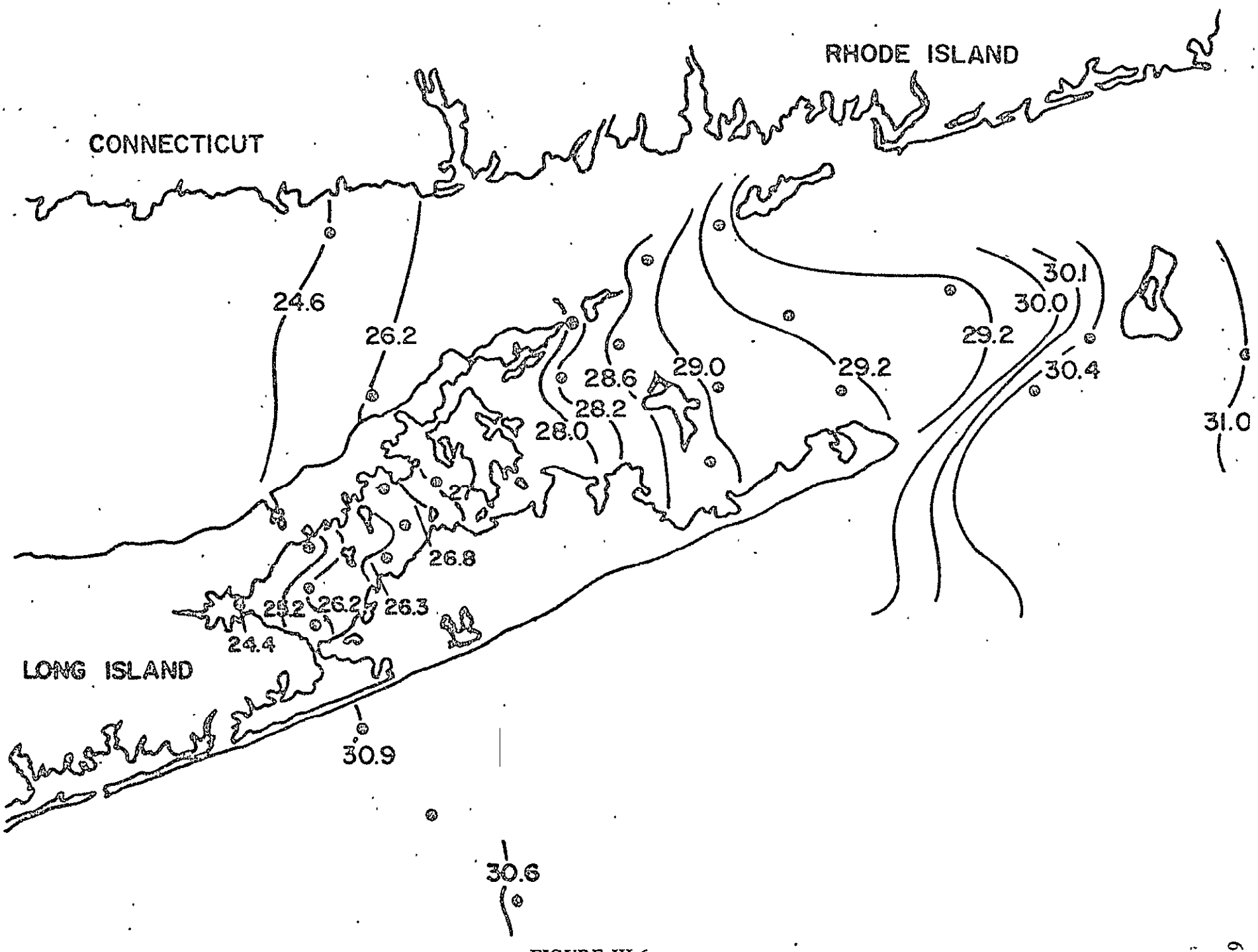

FIGURE III-6a

The distribution of salinity in the surface waters of Block Island Sound and adjacent waters (12 May 1973-0900).

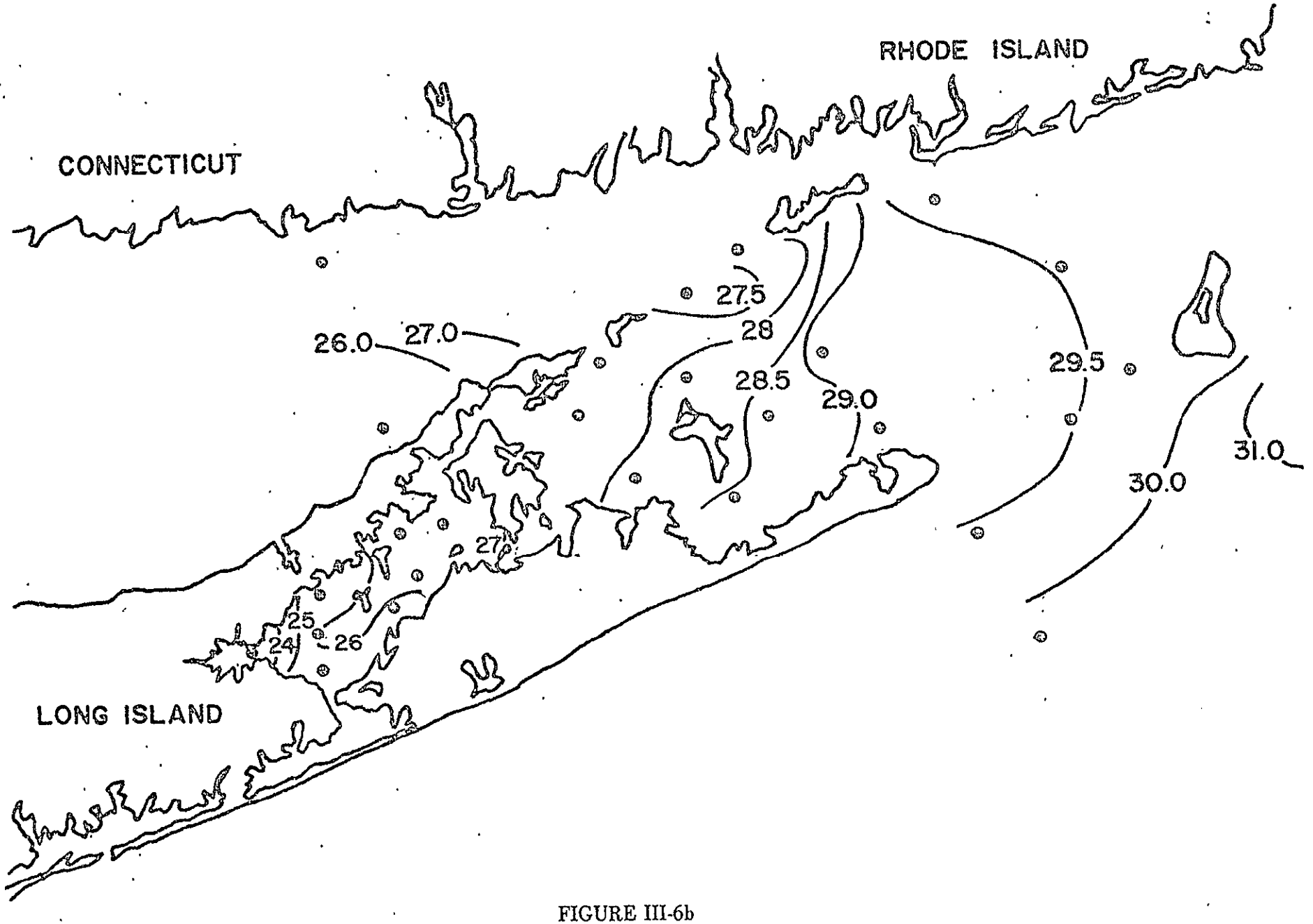

FIGURE III-6b

The distribution of salinity in the surface waters of Block Island Sound and adjacent waters (12 May 1973-1200)

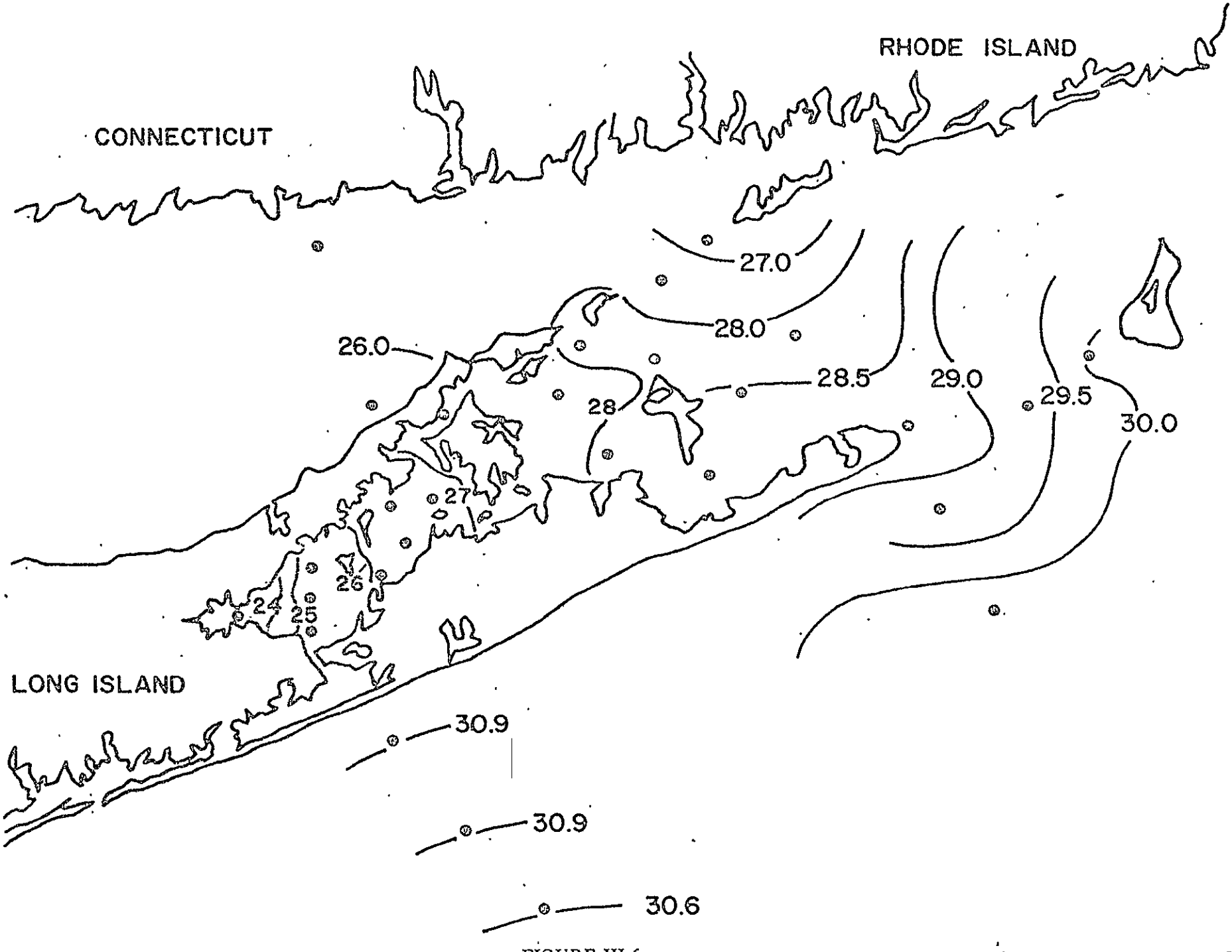

FIGURE III-6c

The distribution of salinity in the surface waters of Block Island Sound and adjacent waters (12 May 1973–1500)

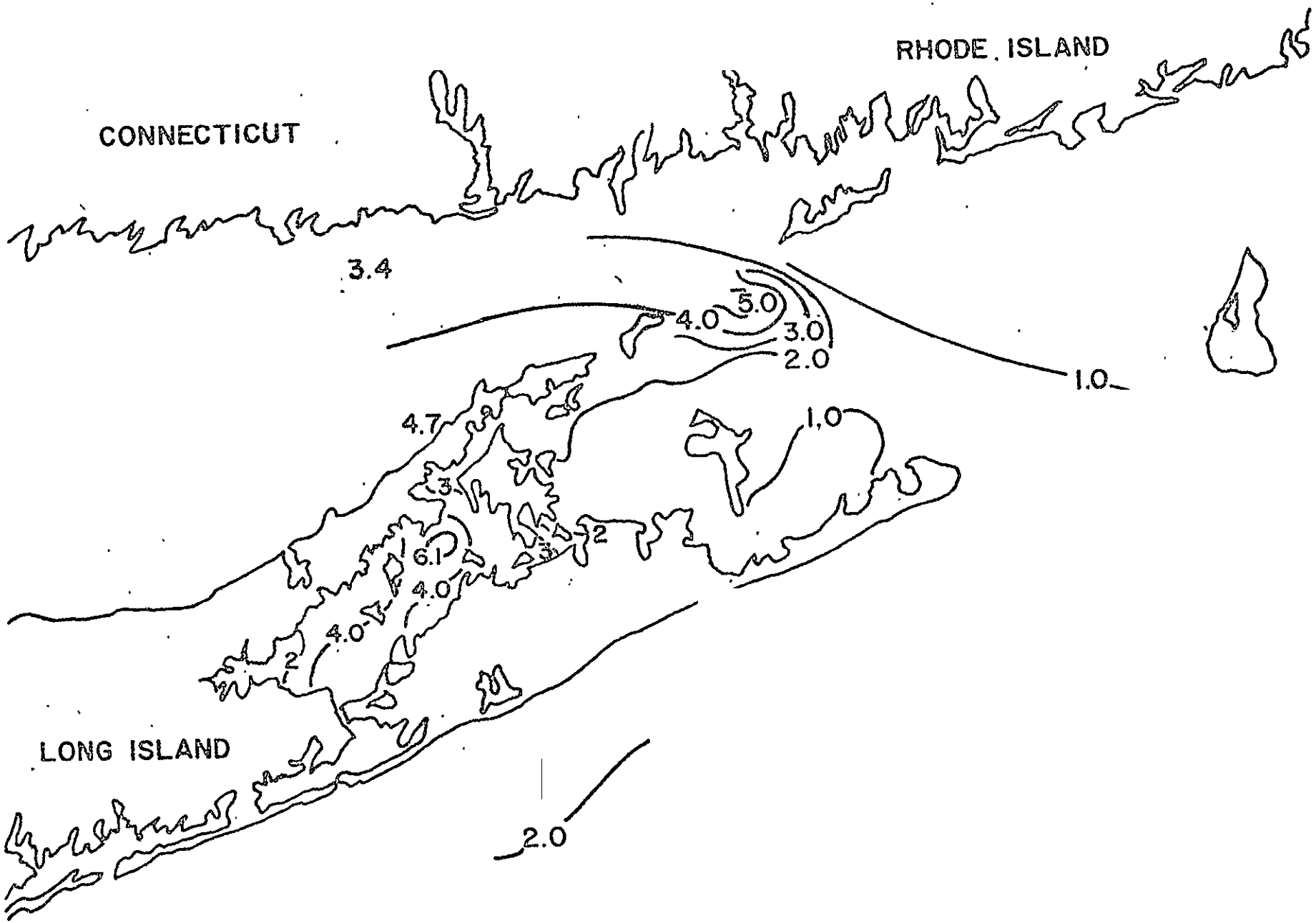

The distribution of suspended solids (mg/ℓ) in the surface waters of Block Island Sound and adjacent waters (12 May 1973-0900)

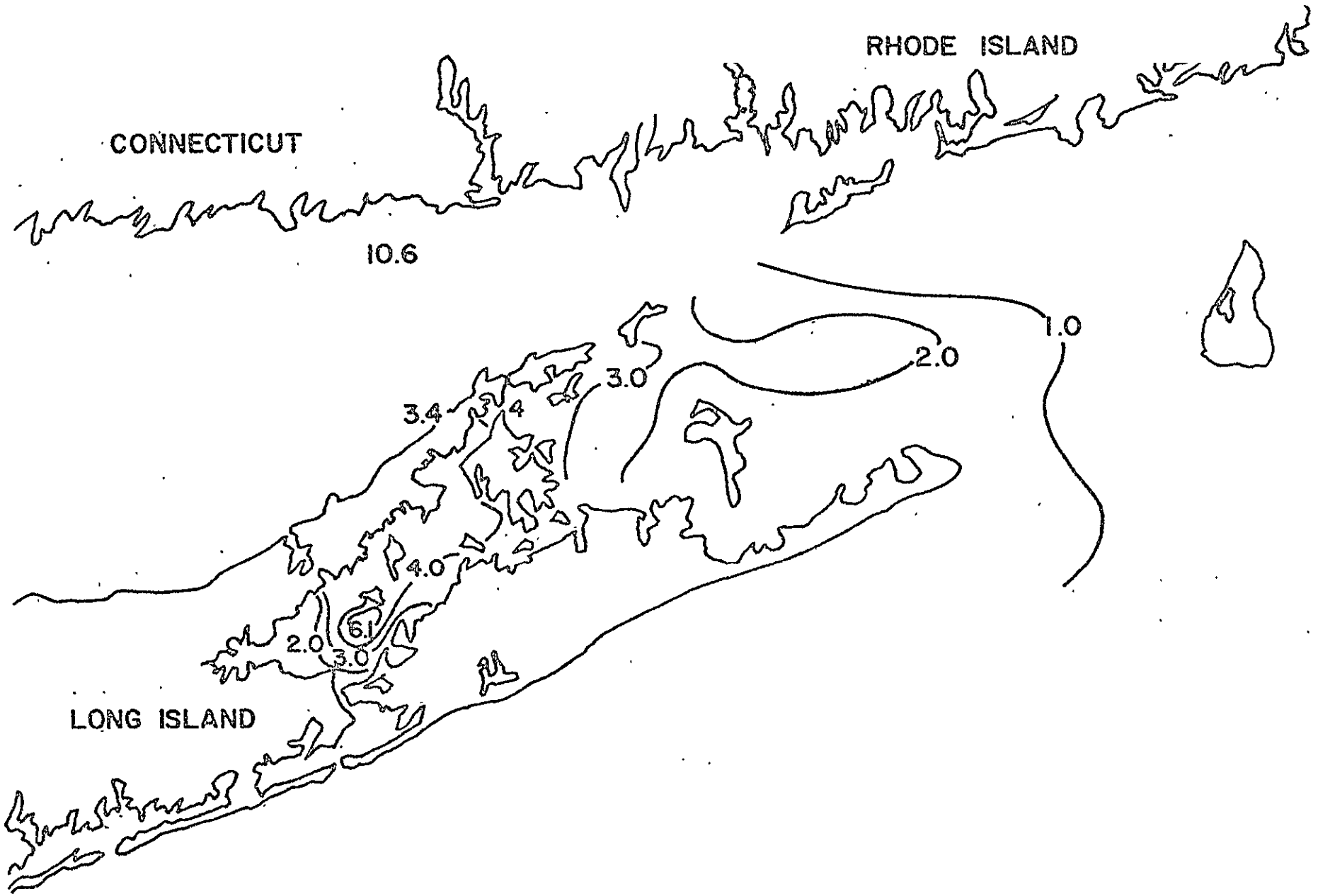

FIGURE III-7b

The distribution of suspended solids (mg/ℓ) in the surface waters of Block Island Sound and adjacent waters (12 May 1973-1200)

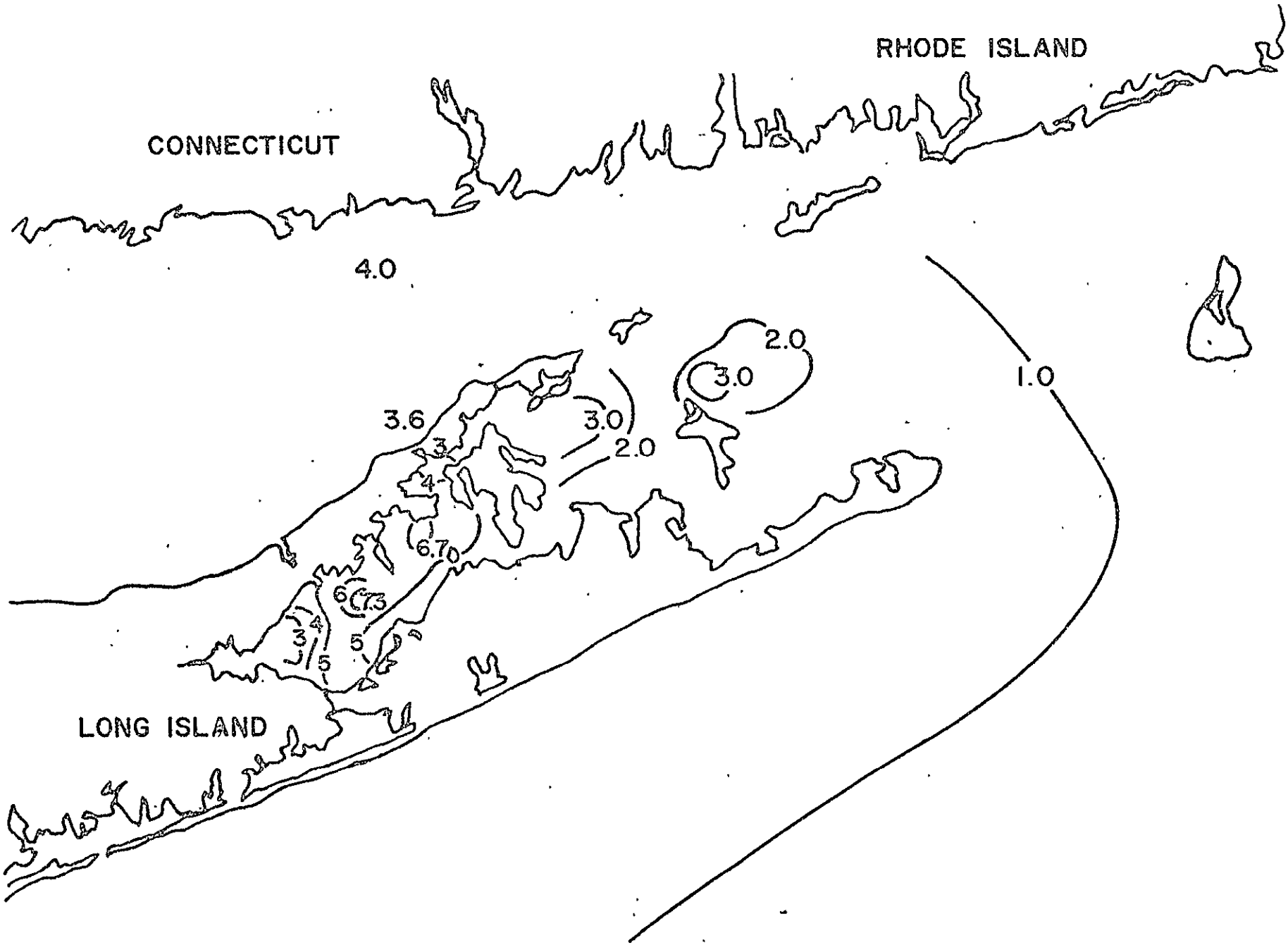

FIGURE III-7c

The distribution of suspended solids (mg/ℓ) in the surface waters of Block Island Sound and adjacent waters (12 May 1973-1500)

APPENDIX C

IV PHYTOPLANKTON AND SUSPENDED PARTICLES

by

Robert Nuzzi
Associate Research Scientist in Microbiology (Phytoplankton)
New York Ocean Science Laboratory
Montauk, New York

Ugo P. Perzan
Technician in Microbiology (Phytoplankton)
New York Ocean Science Laboratory
Montauk, New York

IV PHYTOPLANKTON AND SUSPENDED PARTICLES

Contents

METHODS

Sample Collection and Treatment

Samples for the analysis of phytoplankton and suspended particles were collected from the surface at each station in 5-ℓ Niskin bottles, concurrently with the chemical samples. One liter of water was removed from the bottle, immediately concentrated in a continuous plankton centrifuge to less than 10 mℓ, and brought to a final volume of 10 mℓ with filtered (0.45μ) seawater and neutral buffered formalin (a final concentration of 3%). This concentrated sample was returned to the laboratory for microscopic analysis of the phytoplankton population.

An additional 50-mℓ aliquot was withdrawn from the Niskin bottle and placed in a 50-mℓ glass vial. This sample was refrigerated until return to the laboratory, when it was immediately analyzed for suspended particles with a Coulter Counter, Model B (Coulter Electronics).

Phytoplankton Analysis

Aliquots of the concentrated sample were placed in a nannoplankton-counting chamber (Palmer and Maloney 1954) and various types of microscopic counts, depending on cell size and number, were performed under 100X and 400X magnification. At least 10 field counts (a wide field being delineated by the microscopic field and a narrow field by a whipple disc placed in one eyepiece) were performed under each magnification, and three survey counts (a scan of the entire counting chamber) were performed under 100X magnification. The average counts were multiplied by the appropriate factors to yield results as cells per liter.

Suspended Particle Analysis

Immediately upon return to the laboratory, the refrigerated 50-mℓ sample was analyzed for suspended particles with a Coulter Counter Model B. Two aperture tubes (30μ and 100μ) were employed so that particles between $0.16\mu^3$ and $635\mu^3$ (equivalent diameter of

0.68μ to 10.67μ) could be counted. Particles between 1 and 10μ equivalent diameter were counted at 1-micron intervals. Particles above 10.67μ equivalent diameter were also counted for most of the samples (Table IV-1).

Calibration of Coulter Counter

The calibration procedure followed was that of Sheldon and Parsons (1967). The 30μ aperture was calibrated with latex particles (1.947μ) and the 100μ aperture with paper mulberry pollen (12-13μ). The matching switch was set at 32-H, which ensured linearity between electrical pulses and particle volume at the aperture current switch setting of 1/2 that was used throughout the study. An amplification setting of 2 was routinely used for sample analysis. The number of particles counted in each sample was always low enough so that coincident passages could be ignored.

Since the samples could not be analyzed immediately after collection, the need for a method of holding the samples without changing the number of particles (or the particle sizes) within it had to be developed. Most chemical fixatives, while insuring the absence of biological replication, pose the problems of precipitation and flocculation. Therefore, refrigeration (4° C) was used to hold the samples until they could be returned to the laboratory for analysis. The percent of variation in counts after 24 hours (Table IV-2) was low enough that this method proved feasible. All samples were analyzed within 24 hours of collection, and generally within 12 hours.

Twenty mℓ disposable sample containers (Accuvettes, Coulter Electronics) were rinsed three times with freshly filtered (0.22μ) distilled water, followed by a triple rinse with freshly filtered (0.22μ) seawater. The same procedure was used to rinse a 24-mm membrane filter holder and 500-mℓ filter flask (Millipore) with a 25μ-mesh screen (Nitex HC nylon monofilament) used as a filter. The final seawater rinse was added to the sample container and background counts for the 30μ-aperture were performed for the various threshold settings listed in Table IV-1. Background counts for the 30μ-aperture were always less than 10% of the sample count. These counts were subtracted from the sample counts to yield results in particles per 0.05mℓ.

A second disposable sample container was rinsed as above, with the final rinse being used for a background count for the 100μ-aperture. These background counts were low enough (< 1% of the sample count) to be considered negligible. The volume of sample counted with the 100μ-aperture at each threshold setting was 0.5mℓ.

RESULTS AND DISCUSSION

Phytoplankton - New York Bight (NYB) and TR Stations

The surface populations resident at the NYB stations varied only slightly in quality in December and January, with *Skeletonema costatum* being dominant in all cases but one (Table IV-3). This was not the case during the May-June sampling, when *S. costatum* was dominant at only five stations.

Although the populations at the NYB stations generally resembled each other qualitatively, there were large quantitative differences. The mean phytoplankton standing crop for the entire period at Station 5, 6, and 7 was 1,059, 1,328, and 1,225 x 10^3 cells per liter respectively, five to six times that at Station 1 and 9, where means of 197. x 10^3 cells per liter were recorded. Station 2, 3, 4, and 8 had intermediate values (Table IV-4).

These differences may be due to the fact that Station 5, 6, and 7 are situated around the sewage-disposal site, an organically rich area. Similar results were found by Nuzzi in 1973.

The most singular feature of the phytoplankton population of the NYB area is its high numbers compared to the TR stations. For the same three sampling periods, the phytoplankton found off the southern shore of Long Island (TR transect) had a mean standing crop of 130 x 10^3 cells per liter, as compared to an overall mean of 799 x 10^3 cells per liter for the NYB stations (Table IV-4).

Quantitatively, the stations of the TR transect show moderate differences, with Station TR7 and TR8 yielding the highest mean counts. These stations are close to the NYB area and may be representative of the abundant growth that was observed there.

Qualitatively, the TR transect demonstrated a diversified phytoplankton composition (Table IV-3). *S. costatum,* the dominant species in the NYB area, showed moderate growth during December and January, but was never observed as the dominant species during the May-June sampling.

The composition of the phytoplankton in the NYB area and the TR transect demonstrates small variation in the number of taxa identified. A total of 85 taxa were identified in December, 66 in January, and 65 in the May-June period, the overwhelming majority being diatoms. Most species encountered, however, were subordinate to 9 diatoms and 4 flagellates, which accounted for 90% of the total phytoplankton. These 13 species were: *S. costatum, Thalassionema nitzschioides, Paralia sulcata, Thalassiosira subtilis, Chaetocerus* sp., *Leptocylindrus danicus, Navicula* sp., *Asterionella japonica, Thalassiosiria nordenskioldii, Gymnodinium* sp., *Ceratium tripos, Ceratium lineatum,* and *Ankistrodesmus falcatus* (a freshwater chlorophyte found only at Station NYB 2, 3, 5, and 7, and apparently originating in the Hudson River).

The pulses of *S. costatum, A. japonica, Gymnodinium* sp., and *C. lineatum* coincided to produce the May-June maxima in the NYB area. Despite this succession, it was almost entirely the variation in numbers of the overall most dominant species, *S. costatum,* that determined the pattern of abundance of the total population. *S. costatum* was present during all sampling periods—December, January, and May-June—and comprised 52%, 82%, and 44% of the total population respectively. The species composition for the waters off the southern shore of Long Island (TR transect) is somewhat different; here an active successional pattern can be seen (Table IV-3 and Figure IV-1).

Phytoplankton - Block Island Sound Stations

A total of 16 cruises were conducted during the period of October 1972 to June 1973. Although the transects were sometimes sampled on different days, they were all sampled during the months of November, December, February, March, April, and June, with the following exceptions: (1) the BR transect was not sampled in February; (2) the H-transect was additionally sampled in October; (3) a special synoptic sampling program, which will be discussed separately, took place in May.

Mean monthly phytoplankton counts for the three transects, HB, H, and BR (Table IV-5) show maxima occurring during the following months: March for the HB transect (645 x 10^3 cells per liter); October, March, and June for the H transect (1,230, 865, 645 x 10^3 cells per liter respectively), and June for the BR transect (497 x 10^3 cells per liter).

The mean phytoplankton standing crop for the entire period in Block Island Sound totaled 451 x 10^3 cells per liter for the H transect, over twice that recorded for the HB and BR transects, where means of 169 and 123 x 10^3 cells per liter respectively were recorded. The stations closest to Montauk Point generally exhibited the largest phytoplankton standing crop. Station HB1 and HB2 constituted 80% to 50% of the mean monthly count for the HB transect except for April and June, when they made up only 24% and 7% of the count respectively. Similarly, Station H1 composed 90% to 46% of the mean monthly count for the H transect except for April and June, when it constituted 18% and 15% respectively.

As in the New York Bight, *S. costatum* is quite abundant in Block Island Sound, where it comprised 60% of the H and HB transect population, excluding the months of April and June.

A total of 85 taxa were recorded during this investigation, the majority being diatoms. Transect H and HB were most similar in species composition, with 85 and 70 taxa identified respectively. A total of 20% of the taxa attained a frequency of >50% in the H transect and 23% of the taxa attained a frequency of >50% in the HB transect. A total of 59 taxa were identified in the BR transect, with 37% of these attaining a frequency of >50%. If only the dominant species (those accounting for 10% or more of any sample) are considered, the significant regional contrasts are: *T. decipiens*, occurring more frequently as a dominant in the BR transect, and *S. costatum* and *T. nitzschioides* in the H and HB transects. One exception was noticeable in the June sampling, when *Cerataulina bergonii* became the dominant species at all three transects.

Particle Counts - New York Bight (NYB) and TR Stations

The particle counts at the NYB and TR stations are given in Table IV-6. As with the

phytoplankton counts, the particle counts were higher in the NYB area. The average for the NYB stations was 667 x 10^6 particles per liter (total count) and 837 x 10^3 particles per liter (particles >10.7μ equivalent diameter), as opposed to 242 x 10^6 and 422 x 10^3 particles per liter for the TR stations.

Station NYB3 showed the highest total particle counts (1,567; 1,621, and 2,677 x 10^6 particles per liter for December, January, and May respectively) probably due to material being carried into the area by the Hudson River.

The increase in particles at all NYB stations, from December to May, might be due at least in part to increased biotic populations. A comparison of Table IV-5 and IV-6 indicates only a slight increase in both phytoplankton population and particle count during this time period at the TR stations as compared to the NYB stations. The correlation of coefficient (r) for phytoplankton cell counts vs particles >10.7μ equivalent diameter for 49 paired sets of values for the NYB and TR stations was 0.586, indicating that other factors besides phytoplankton are contributing to the particle counts.

Figure IV-2 compares phytoplankton cell counts with counts of particles >10.7μ diameter for the TR and NYB stations for all sampling periods.

Particle Counts - Block Island Sound Stations

Table IV-7 gives the results of the particle counts of the Block Island Sound stations. While there is only a slight variation in the total particle counts, the number of particles greater than 10.7μ equivalent diameter varied significantly from station to station. The highest counts of particles >10.7μ were found at Station H1 and HB1 (stations closest to Montauk Point), these counts corresponding to an increased phytoplankton population (Table IV-4). The counts at the BR stations varied only slightly.

The coefficient of correlation for phytoplankton cell counts and particles >10.7μ equivalent diameter for 101 sets of paired data in Block Island Sound was 0.858, with the correlation being highest during periods of high phytoplankton populations and lowest during periods when few cells were present. Table IV-8 contrasts the phytoplankton counts

and the counts of particles >10.7μ diameter for each transect in the Block Island Sound area for each sampling date.

Synoptic Sampling Program

On 12 May 1973, the surface waters of 29 stations were sampled synoptically by the New York Ocean Science Laboratory with the aid of the East Hampton and Peconic Bay power squadrons. Each station was sampled at 0900, 1200, and 1500 EDST (the times corresponding to maximum ebb current, slack, and approximately one hour before maximum flood current relative to the Race). Figure IV-3 presents the surface contours of *Thalassionema nitzschioides,* the dominant phytoplankter present during this sampling period.

The largest population occurred in the Peconic Bay-Gardiners Bay region, with a smaller population found in northern Long Island and Block Island Sound waters. These populations were separated by the sparsely populated waters apparently originating in central and southern Long Island Sound, passing through central Block Island Sound, and meeting the waters of the Atlantic Ocean between Montauk Point and Block Island. This type of circulation of the surface waters was shown previously by Nuzzi (1973) and Austin (1973).

SUMMARY

The high correlation between phytoplankton and suspended particles >10.7μ equivalent diameter in Block Island Sound (0.858) indicates that the phytoplankton may contribute largely to the suspended material in this region. In contrast, the lower correlation between these parameters in the New York Bight (0.586) indicates that other factors are adding to the suspended load in this area. Suspended materials are being brought into the area by the Hudson River outflow, as evidenced by the high total particle counts and lowered salinity values (see Section II) at Station NYB3.

The phytoplankton population was highest at the NYB and Block Island Sound stations,

with the TR stations having the lowest number of cells. There are indications that the organic enrichment caused by the disposal of sewage sludge in the New York Bight may play a role in maintaining the relatively high phytoplankton population in this region.

In Block Island Sound, the stations around Montauk Point generally exhibited the largest phytoplankton populations, these populations probably originating in the waters of the Peconic Bay-Gardiners Bay system.

Block Island Sound can be divided into three regions: (1) Northern Block Island Sound, influenced by the coastal waters of Connecticut, Rhode Island, and the Cape Cod region; (2) Southern Block Island Sound, influenced by the waters of the Peconic Bay-Gardiners Bay system; and (3) Central Block Island Sound, influenced by the waters of Long Island to the west and the Atlantic Ocean to the east.

REFERENCE

Austin, H.M. and P.M. Stoops. 1973. A synoptic study of the surface waters of Block Island Sound and surrounding waters, Part II. New York Ocean Science Laboratory Technical Report No. 0024.

Nuzzi, R. 1973. The distribution of phytoplankton in the New York Bight, September and November, 1971. In *The Oceanography of the New York Bight: Physical, Chemical, Biological* Vol. I (ed. R. Nuzzi). New York Ocean Science Laboratory Technical Report No. 0017.

_____. 1973. A synoptic study of the surface waters of Block Island Sound and surrounding waters, Part I. New York Ocean Science Laboratory Technical Report No. 0019.

Palmer, C.M. and T.E. Maloney. 1954. A new counting slide for nannoplankton. American Society of Limnology and Oceanography. Spec. Publ. No. 21.

Sheldon, R.W. and T.R. Parsons. 1967. A Practical Manual on the Use of the Coulter Counter in Marine Science. Coulter Electronics Sales Co., Toronto, Canada.

E75-10290
thru
E75-10299

EARTH RESOURCES SURVEY PROGRAM REPORT

TABLE IV-1

Aperture tubes and threshold settings used for suspended particle analysis by Coulter Counter Model B

Aperture	Threshold Settings		Volume (μ^3)	Equivalent Diameter (μ)
	Lower	Upper		
30μ	1	3.3	0.16 - 0.52	0.68 -1
	3.25	26	0.52 - 4.18	1 - 2
	26	88.4	4.18 - 14.14	2 - 3
100μ	2.3	5.3	14.25 - 33.51	3 - 4
	5.3	10.3	33.51 - 65.45	4 - 5
	10.3	17.8	65.45 - 113.03	5 - 6
	17.8	28.3	113.03 - 179.58	6 - 7
	28.3	42.3	179.58 - 267.97	7 - 8
	42.3	60	267.97 - 381.70	8 - 9
	60	82.5	381.70 - 523.63	9 - 10
	82.5	100	523.63 - 635	10 - 10.67
	100	out	>635	>10.67

TABLE IV-2

Variation in counts (Coulter Counter) after refrigeration for various periods of time. Numbers indicate the percentage difference from the sample analyzed immediately after collection.

Particle Diameter (μ)	Refrigerated for	
	1 day	3 days
0.68 - 1	+5.4%	+8.5%
1 - 2	-5.9	+20.7
2 - 3	-4.0	+15.9
3 - 4	-3.6	+31.0
4 - 5	-3.1	+19.0
5 - 6	-1.8	+25.8
6 - 7	-1.8	+21.6
7 - 8	+8.9	+15.7
8 - 9	+21.0	+28.4
9 - 10	+13.4	+8.9
10 - 10.67	0	-5.4

TABLE IV-3

Species occurrence and succession. The dominant species for each station and date is in large type. The subdominant species are in smaller type and are preceeded by an arrow. Codominant species are indicated by equal type size and are not separated by an arrow.

	TR 1	TR 2	TR 3	TR 4	TR 5	TR 6	TR 7	TR 8
DEC K7235	S. costatum → P. sulcata → T decipiens	T. nitzschioides → S. costatum → T. decipiens	P. sulcata → T. nitzschioides → T. decipiens	P. sulcata → N closterium → T nitzschioides	T nitzschioides → N. closterium → P. sulcata	P sulcata → S. costatum → N closterium	P. sulcata → S. costatum → T. subtilis	S. costatum → T. nitzschioides → P sulcata
JAN K7302	S. costatum	T. nitzschioides → N. closterium → P sulcata	S costatum → T nitzschioides → N. closterium	N. closterium → T nitzschioides → S costatum	T. nitzschioides → N. closterium → P. sulcata	S. costatum → N. closterium → P sulcata	S. costatum → P. sulcata → T subtilis	S. costatum → T nitzschioides → N closterium
MAY–JUNE K 7327	T nitzschioides → S. costatum → N. closterium	L. danicus → S costatum → N closterium	Chaetoceros sp → L. danicus → N closterium	Gymnodinium sp → L danicus → Chaetoceros sp	L. danicus → Gymnodinium sp → Chaetoceros sp	L. danicus → Chaetoceros sp → Gymnodinium sp.	Chaetoceros sp. → Gymnodinium sp → L danicus	Gymnodinium sp. → C tripos → Chaetoceros sp.

	NYB 1	NYB 2	NYB 3	NYB 4	NYB 5	NYB 6	NYB 7	NYB 8	NYB 9
DEC K7235	P sulcata → T nitzschioides → T. decipiens	S. costatum → P sulcata → T decipiens	S. costatum → T. decipiens → Navicula sp	S. costatum → T subtilis → T decipiens	S. costatum → P sulcata → T nitzschioides	S costatum → T nitzschioides → P sulcata	S costatum → T subtilis → P sulcata	S. costatum → T subtilis → P sulcata	S costatum → N. closterium → T. nitzschioides
JAN K7302	S costatum → T nitzschioides → T. subtilis	S. costatum → T subtilis → T nitzschioides	S. costatum → T. subtilis → T nordenskioldii	S costatum → T. subtilis → T. nitzschioides	S. costatum → T. nordenskioldii → T subtilis	S costatum → T. nordenskioldii → T subtilis	S. costatum → T. nordenskioldii → N. closterium	S. costatum → T. nordenskioldii → T subtilis	S costatum → N. closterium → T. nitzschioides
MAY–JUNE K 7327	A. japonica → C. lineatum → Gymnodinium sp	S. costatum → A japonica → A falcatus	S. costatum → A falcatus → A japonica	S. costatum → A. japonica → Gymnodinium sp	S. costatum → A. japonica → A falcatus	Gymnodinium sp → A japonica → C. lineatum	S. costatum → A. japonica → A. falcatus	C Lineatum → S. costatum → A japonica	C. Lineatum → A japonica → Gymnodinium sp

TABLE IV-4

Phytoplankton cell counts, NYB and TR stations (cells per liter)

Station		19 - 20 Dec 1972	25 - 26 Jan 1973	30 - 31 May 1973	Average, all dates
TR	1	77,802	284,316	124,946	162,354
	2	60,815	26,017	323,927	136,919
	3	50,885	73,883	247,480	124,082
	4	46,419	44,232	216,656	102,435
	5	73,669	43,485	38,495	51,883
	6	34,617	210,233	27,064	90,638
	7	30,217	443,032	88,331	187,193
	8	31,417	457,734	79,729	189,626
Av., all stations		50,730	197,866	143,328	130,641
NYB	1	55,134	388,209	149,095	197,479
	2	100,602	424,085	1,738,497	754,394
	3	67,916	714,584	1,134,779	639,093
	4	46,017	811,283	1,997,029	951,443
	5	42,571	2,269,373	865,512	1,059,152
	6	35,684	3,222,769	726,650	1,328,367
	7	24,451	2,587,673	1,063,224	1,225,116
	8	38,184	1,347,163	1,138,085	841,144
	9	52,350	258,633	279,662	196,881
Av., all stations		51,434	1,335,974	1,010,281	799,229

TABLE IV-5

Phytoplankton cell counts, Block Island Sound stations (cells per liter)

Stations	10 Oct 72	14 Nov 72	4 Dec 72	13 Feb 73	20 Mar 73	24 Apr 73	18 Jun 73	Average, all dates
H1	4,410,497	259,748	80,781	941,923 *	2,185,331	9,862	381,462	1,181,372
H2	225,866	85,518	48,633	59,968 *	873,848	6,611	182,254	211,814
H3	119,951	1,199 *	20,749	38,811 *	264,942	2,962	1,181,625	232,891
H4	164,731	21,533	24,866	16,776 *	136,860	34,658	835,729	176,450
Av., all stations	1,230,261	91,999	43,757	264,369	865,245	13,523	645,267	450,631
Stations	16 Nov 72	8 Dec 72	20 Mar 73	21 Mar 73	24 Apr 73	26 Apr 73	18 Jun 73	Average, all dates
BR1	13,800	43,466	44,565	80,630 *	31,379	79,395	556,942	121,451
BR2	20,199	18,613	45,030	40,229 *	107,178	169,562	859,368	180,025
BR3	21,750	49,750	71,797	58,772 *	60,378	130,160	73,556	66,594
Av., all stations	18,583	37,269	53,797	59,877	66,311	126,372	496,622	122,690
Stations	10 Nov 72	6 Dec 72	14 Feb 73	20 Mar 73	24 Apr 73	25 Apr 73	19 Jun 73	Average, all dates
HB1	152,766	177,349	456,949 *	1,728,919	11,895	9,861 *	61,375	362,730
HB2	79,851	21,033	76,612 *	835,020	27,194	14,813 *	26,544	154,438
HB3	10,149	25,934	35,601 *	222,274	3,164	9,626 *	499,272	115,145
HB4	40,349	16,851	63,414 *	239,312	52,128	13,797 *	164,553	84,343
HB5	32,350	26,332	43,075 *	197,195	69,362	26,151 *	495,891	127,193
Av., all stations	63,093	41,499	135,130	644,544	32,748	14,849	249,527	168,769

* Average of more than one sample.

TABLE IV-6

Particle counts TR transect and NYB stations (particles per liter)

Station	19(TR), 20(NYB) Dec		25(NYB), 26(TR) Jan		30(TR), 31(NYB) May		1 June		Average	
	Total Particles ($\times 10^6$)	Particles >10.7μ ($\times 10^3$)	Total Particles ($\times 10^6$)	Particles >10.7μ ($\times 10^3$)	Total Particles ($\times 10^6$)	Particles >10.7μ ($\times 10^3$)	Total Particles ($\times 10^6$)	Particles >10.7μ ($\times 10^3$)		
TR 1	546	1044	143	146	228	374	205	414	281	495
2	132	400	277	292	152	526	208	510	192	432
3	264	532	207	202	204	608	174	488	212	458
4	203	344	213	146	254	-	231	380	225	290
5	211	383	265	136	132	518	153	432	190	367
6	485	470	146	362	80	494	365	742	269	517
7	337	314	219	378	264	386	238	292	265	343
8	390	332	229	464	363	498	219	422	300	429
Av., all stations	321	477	212	265	210	486	224	460	242	422
NYB 1	354	-	275	646	274	578	-	-	301	612
2	681	576	567	484	1666	1628	-	-	971	896
3	1567	464	1621	788	2677	2328	-	-	1433	1193
4	410	282	552	512	1129	1892	-	-	697	895
5	288	212	385	864	939	1180	-	-	537	752
6	240	236	219	858	609	1402	-	-	356	832
7	291	472	278	834	923	1586	-	-	497	964
8	290	410	255	570	561	1690	-	-	369	890
9	208	334	279	522	478	896	-	-	322	584
Av., all stations	481	373	492	675	1028	1464	-	-	667	837

TABLE IV-7

Particle counts (particles per liter) for Block Island Sound stations (Transects H, HB, BR)

Station	10 Nov 1972		14 Nov 1972		16 Nov 1972		4 Dec 1972		6 Dec 1972	
	Total Particles ($\times 10^6$)	Particles >10μ ($\times 10^3$)	Total Particles ($\times 10^6$)	Particles >10μ ($\times 10^3$)	Total Particles ($\times 10^6$)	Particles >10μ ($\times 10^3$)	Total Particles ($\times 10^6$)	Particles >10μ ($\times 10^3$)	Total Particles ($\times 10^6$)	Particles >10μ ($\times 10^3$)
H 1			1098 *				321 *			
2			481 *				320 *	97		
3			278 *				321 *	94		
4			253 **				371 *	133		
Average			527				333			
HB 1	281								345 **	274
2	223								246 **	137
3	201								289 **	109
4	214								367 **	107
5	208								204 **	106
Average	225								290	146
BR 1					297 ***					
2					184 ***					
3					185 ***					
Average					222					

* Average of 3 samples taken over 3 crossings of transect.
** " " 2 " " " 2 " " "
*** " " 4 " " " 4 " " "
\+ " " 5 " " " 5 " " "

TABLE IV-7 (cont'd.)

Station	8 Dec 1972		13 Feb 1973		14 Feb 1973		20 Mar 1973		21 Mar 1973	
	Total Particles ($\times 10^6$)	Particles >10μ ($\times 10^3$)	Total Particles ($\times 10^6$)	Particles >10μ ($\times 10^3$)	Total Particles ($\times 10^6$)	Particles >10μ ($\times 10^3$)	Total Particles ($\times 10^6$)	Particles >10μ ($\times 10^3$)	Total Particles ($\times 10^6$)	Particles >10μ ($\times 10^3$)
H1			314 *	1005			358	2160		
2			185 ***	556			225	468		
3			226 +	481			232	408		
4			198 *	379			200	268		
Average			231	605			254	826		
HB 1					180 *	690	306	1782		
2					165 *	418	250	462		
3					174 *	349	197	224		
4					162 *	229	213	384		
5					163 *	361	225	354		
Average					168	409	238	641		
BR 1	203 *	185					219	190	181 ***	277
2	287 *	124					568	462	194 ***	237
3	422 **	197					533	428	364 ***	334
Average	304	162					440	360	246 ***	283

TABLE IV-7 (cont'd.)

Station	24 Apr 1973		25 Apr 1973		26 Apr 1973		18 Jun 1973		19 Jun 1973		Average	
	Total Particles ($\times 10^6$)	Particles >10μ ($\times 10^3$)	Total Particles ($\times 10^6$)	Particles >10μ ($\times 10^3$)	Total Particles ($\times 10^6$)	Particles >10μ ($\times 10^3$)	Total Particles ($\times 10^6$)	Particles >10μ ($\times 10^3$)	Total Particles ($\times 10^6$)	Particles >10μ ($\times 10^3$)	Total Particles ($\times 10^6$)	Particles >10μ ($\times 10^3$)
H1	184	227					316	726			432	1030
2	241	246					308	660			293	405
3	144	150					210	1254			235	477
4	197	164					246	375			244	264
Average	191	196					270	753			301	544
HB 1	113	86	172***	185					205***	539	229	593
2	142	202	183***	211					206***	607	202	340
3	167	114	212***	102					254***	593	213	249
4	179	176	165***	128					205***	541	215	261
5	149	194	136***	109					188***	550	182	279
Average	149	154	173	147					211	566	208	344
BR 1	140	140			214	144	251*	920			215	309
2	115	163			113	154	221*	700			240	306
3	220	208			252	188	206*	317			312	279
Average	158	170			193	162	224*	645			255	297

TABLE IV-8

Phytoplankton total cells per liter ($\times 10^3$) vs particles >10.7μ per liter ($\times 10^3$) for each transect and date in Block Island Sound

Date	Station	Particles >10.7μ per liter x 10^3	Total cells per liter x 10^3	Correlation for each transect	Correlation for sampling period
12/4/72	H1-2	-	81		
	2-3	124	49	r = -0.015	r = -0.015
	3-3	102	21		
	4-2	178	25		
	Average	134	44		
12/6/72	HB1-1	196	177		
	2-3	164	21		
	3-3	98	26	r = 0.775	r = 0.775
	4-3	92	17		
	5-2	116	26		
	Average	133	41		
12/8/72	BR1-3	130	43		
	2-3	90	19	r = 0.894	r = 0.894
	3-2	200	50		
	Average	140	37		
2/13/73	H1-1	-	277		
	2-1	292	74	r = -0.624	
	3-1	272	44		
	4-1	324	12		
	3-2	602	14	r = 0.401	r = 0.929
	2-2	278	25		
	1-2	564	264	r = -0.518	
	2-3	628	81		
	4-2	338	23		
	Average	412	90		
2/14/73	HB1-1	818	218		
	2-1	390	154		
	3-1	176	24	r = 0.882	
	4-1	254	34		
	5-1	328	18		
	Average	393	90		

TABLE IV-8 (cont'd.)

Date	Station	Particles > 10.7μ per liter x 10^3	Total cells per liter x 10^3	Correlation for each transect	Correlation for sampling period
2/14/73 (cont'd.)	HB1-2	594	212		
	2-2	428	75		
	3-2	402	65	r = 0.559	r = 0.577
	4-2	306	175		
	5-2	286	37		
	Average	403	113		
	HB1-3	658	772		
	2-3	436	53		
	3-3	470	25	r = 0.674	
	4-3	128	20		
	5-3	440	36		
	Average	432	181		
3/20/73	H1	2160	2185		
	2	468	874	r = 0.961	
	3	408	265		
	4	268	137		
	Average	826	865		
	BR1	190	45		
	2	462	45	r = 0.397	r = 0.939
	3	428	72		
	Average	360	54		
	HB1	1782	1729		
	2	462	835		
	3	224	222	r = 0.945	
	4	384	239		
	5	354	197		
	Average	641	644		
3/21/73	BR1-1	226	89		
	2-1	276	63	r = 0.877	
	3-1	324	140		
	Average	288	97		

TABLE IV-8 (cont'd.)

Date	Station	Particles>10.7μ per liter x 10^3	Total cells per liter x 10^3	Correlation for each transect	Correlation for sampling period
3/21/73 (cont'd.)	BR1-2	360	123		
	2-2	222	41	r = 0.990	
	3-2	160	23		
	Average	247	62		r = 0.159
	BR1-3	314	51		
	2-3	256	26	r = 0.884	
	3-3	358	50		
	Average	309	42		
	BR1-4	168	60		
	2-4	194	30	r = -0.714	
	3-4	496	22		
	Average	286	37		
4/24/73	H1	227	10		
	2	246	7	r = -0.314	
	3	150	3		
	4	164	35		r = 0.269
	Average	196	14		
	BR1	140	31		
	2	163	107	r = 0.201	
	3	208	60		
	Average	170	66		
4/25/73	HB1-1	198	12		
	2-1	316	27		
	3-1	166	3	r = -0.496	
	4-1	131	52		
	5-1	101	69		
	Average	182	32		
	HB1-2	173	11		
	2-2	206	3	r = 0.519	
	3-2	114	3		
	4-2	138	5		
	5-2	104	37		r = -0.125
	Average	147	12		

TABLE IV-8 (cont'd.)

Date	Station	Particles >10.7μ per liter x 10^3	Total cells per liter x 10^3	Correlation for each transect	Correlation for sampling period
4/25/73 (cont'd.)	HB1-3	194	6		
	2-3	196	4		
	3-3	124	30	r = -0.917	
	4-3	156	37		
	5-3	108	56		
	Average	155	26		
	HB1-4	178	6		
	2-4	128	10		
	3-4	4	1	r = 0.579	
	4-4	90	9		
	5-4	124	5		
	Average	105	6		
4/26/73	BR1-1	144	79	r = 1.0 *n = 2	r = 1.0 *n = 2
	3-1	188	130		
	Average	166	104		
6/18/73	H1	726	381		
	2	660	182	r = 0.498	
	3	1254	1182		
	4	375	836		
	Average	753	645		r = 0.663
	BR1-1	876	557		
	2-1	894	859	r = 0.933	
	3-1	260	74		
	Average	676	496		
6/19/73	HB1-1	626	61		
	2-1	638	27		
	3-1	788	499	r = 0.509	r = 0.509
	4-1	348	165		
	5-1	692	496		
	Average	618	249		

Total correlation for all samples and all dates

r = 0.858

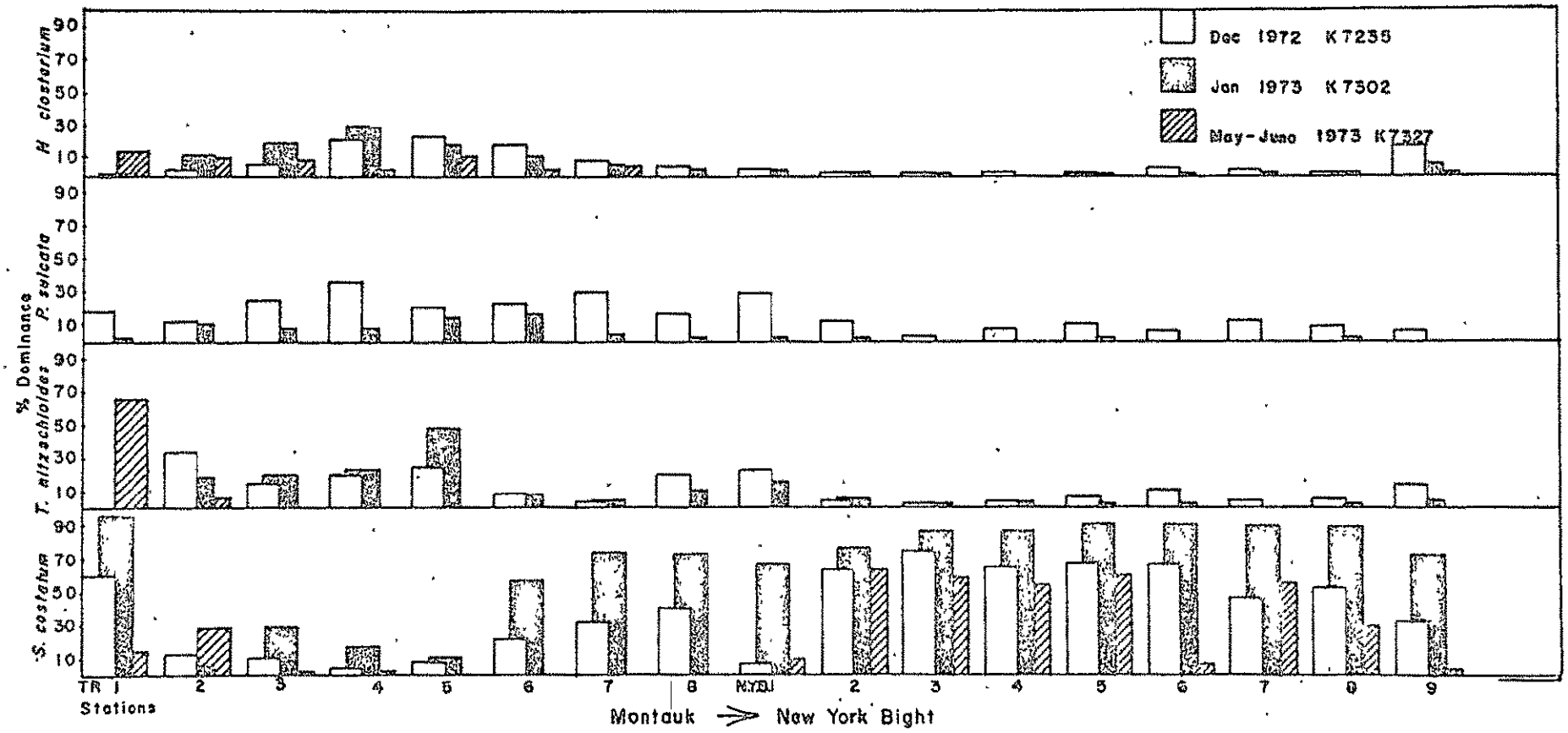

FIGURE IV-1.

Variation of dominant phytoplankton species for each sampling period at the TR and NYB station

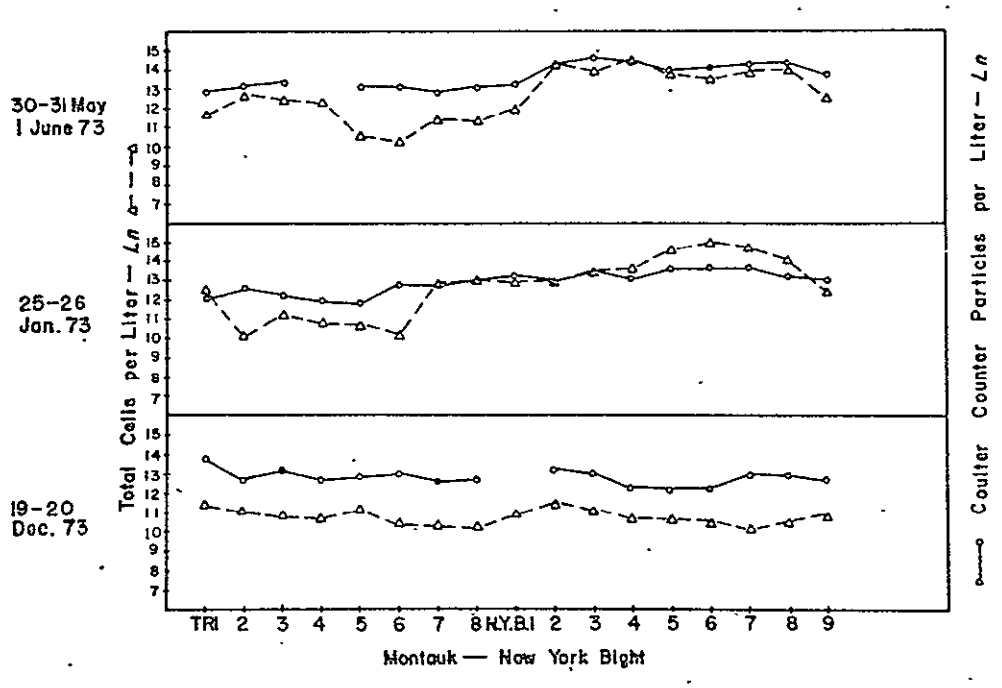

FIGURE IV-2

Total phytoplankton cell count and particles
>10.7μ for each sampling period at the TR and NYB stations

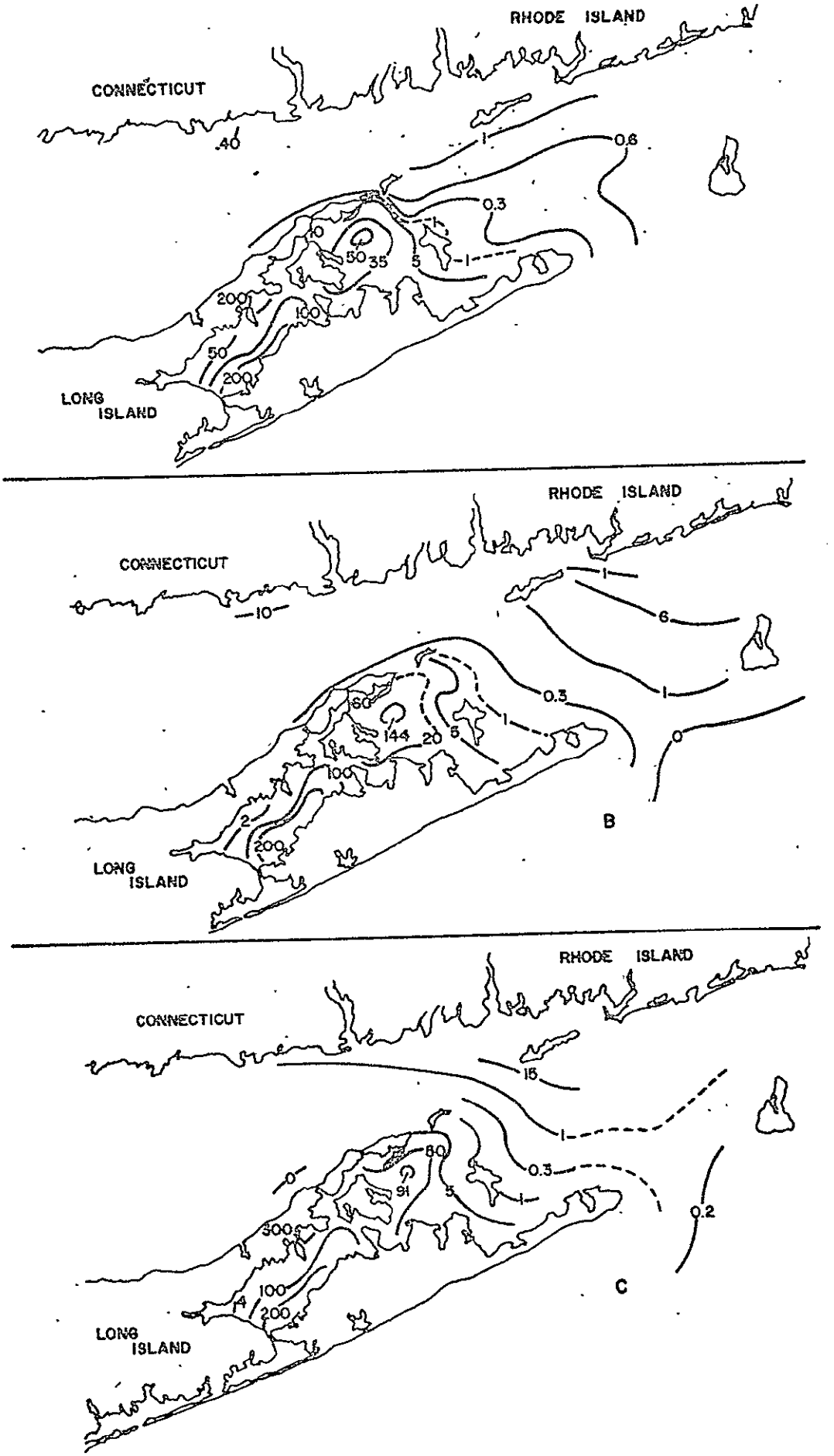

FIGURE IV-3

Surface contours *Thalassionema nitzschioides* (cells per liter x 10^3)


MAY 1975